

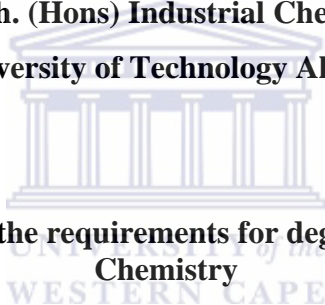
**ION TRACK MODIFICATION OF POLYIMIDE  
FILM FOR DEVELOPMENT OF PALLADIUM  
COMPOSITE MEMBRANE FOR HYDROGEN  
SEPARATION AND PURIFICATION**

**By:**

**OLUSHOLA ROTIMI ADENIYI**

**B Tech. (Hons) Industrial Chemistry**

**Federal University of Technology Akure, Nigeria**



**Submitted in fulfillment of the requirements for degree of Magister Scientiae in  
Chemistry**

**Department of Chemistry**

**University of the Western Cape, UWC**

**Supervisor: Professor L.F. Petrik**

**Co-Supervisors: Dr. Alexander Neachev**

**Dr. Patrick Ndungu**

**May 2011**

# TABLE OF CONTENTS

---

TITLE PAGE	i
TABLE OF CONTENTS	ii-viii
LIST OF FIGURES	xix-xi
LIST OF TABLES	xii
DECLARATION	xiii
ABSTRACTS	xiv-xv
PUBLICATIONS	xvi
DEDICATION	xvii
ACKNOWLEDGEMENT	xviii-xix
LIST OF ABBREVIATION	xx
KEYWORDS	xxi

CHAPTER 1 .....	1
1.0 INTRODUCTION .....	1
1.1 BACKGROUND.....	1
1.2 AVAILABLE TECHNOLOGIES FOR HYDROGEN GAS SEPARATION	6
1.3 MOTIVATION .....	7
1.4 PROBLEM STATEMENT .....	8
1.5 RESEARCH QUESTIONS.....	9
1.6 HYPOTHESIS .....	10
1.7 AIMS AND OBJECTIVES.....	10
1.8 SCOPE .....	11
1.9 DELIMITATION.....	11
1.10 RESEARCH APPROACH.....	12
1.11 THESIS STRUCTURE.....	13
CHAPTER 2 .....	16

## TABLE OF CONTENTS

---

2.0	LITERATURE REVIEW .....	16
2.1	INTRODUCTION.....	16
2.2	HYDROGEN AS FEEDSTOCK FOR INDUSTRIAL PROCESSES .....	16
2.3	SOURCES OF HYDROGEN .....	19
2.4	HYDROGEN PRODUCTION.....	19
2.4.1	Hydrogen production by coal gasification.....	20
2.4.2	Hydrogen production by methane steam reforming .....	22
2.5	CHARACTERISTICS OF HYDROGEN.....	23
2.6	USES OF HYDROGEN.....	24
2.7	HYDROGEN STORAGE AND TRANSPORTATION.....	24
2.8	HYDROGEN PURIFICATION AND SEPARATION METHODS.....	26
2.8.1	Pressure swing adsorption.....	26
2.8.2	Cryogenic distillation.....	27
2.8.3	Membrane separation.....	28
2.9	TYPES OF MEMBRANES .....	30
2.9.1	Polymeric membranes.....	31
2.9.2	Metallic membranes.....	34
2.9.3	Composite membranes.....	34
2.10	MECHANISMS OF HYDROGEN PERMEATION THROUGH MEMBRANE .....	40
2.10.1	Surface diffusion.....	41
2.10.2	Molecular sieve.....	41
2.10.3	Solution-diffusion .....	41
2.11	HYDROGEN DIFFUSION.....	42

## TABLE OF CONTENTS

---

2.12	HYDROGEN PERMEABILITY .....	43
2.13	POLYIMIDE.....	44
2.13.1	Synthesis of polyimide.....	44
2.13.2	Properties of polyimide.....	46
2.14	METHODS OF POLYIMIDE SURFACE PRE-TREATMENT.....	46
2.14.1	Heavy ion irradiation technology in polyimide surface treatment.....	48
2.14.2	Etching processes in non and irradiated polyimide .....	49
2.15	POLYIMIDE AS GAS SEPARATION MEMBRANE.....	49
2.15.1	Polyimide for gas permeability applications.....	51
2.16	LIMITATIONS OF POLYIMIDE .....	52
2.17	GLOBAL STATUS OF PALLADIUM.....	53
2.18	PALLADIUM STRUCTURAL CONFIGURATION .....	54
2.19	APPLICATION AND BENEFITS OF PALLADIUM MEMBRANE FOR HYDROGEN ECONOMY .....	55
2.20	PALLADIUM COMPOSITE MEMBRANES .....	56
2.21	DEFECTS OF PALLADIUM MEMBRANE.....	58
2.22	LIMITATIONS OF Pd MEMBRANES .....	58
2.23	METHODS OF DEPOSITION OF PALLADIUM ON SUBSTRATES .....	62
2.23.1	Electroless deposition method of palladium on substrates .....	63
2.23.2	Conditions for electroless plating .....	64
2.24	CHARACTERISATION TECHNIQUES AND SAMPLE PREPARATION 69	
2.24.1	Scanning Electron Microscope/ x-ray energy dispersion (SEM/EDX) .	69
2.24.2	X-ray diffraction (XRD) .....	70

## TABLE OF CONTENTS

---

2.24.3	Transmission electron microscopy (TEM) .....	71
2.24.4	Fourier transformed infra-red (FTIR) .....	72
2.24.5	Thermo-gravimetric analysis (TGA) .....	72
2.24.6	Peel test analysis .....	72
2.25	CONCLUSION .....	73
2.26	RESEARCH AIMS .....	73
2.27	EXPERIMENTAL TASK .....	74
2.28	DELIMITATION OF STUDY .....	75
CHAPTER 3	.....	76
3.0	EXPERIMENTAL .....	76
3.1	MATERIALS .....	76
3.2	SCHEMATIC OF METHODOLOGY .....	77
3.3	METHODOLOGY .....	79
3.3.1	Pre-plating procedure .....	79
3.4	PLATING PROCEDURE .....	82
3.4.1	Preparation of palladium-based electroless plating bath .....	82
3.5	SAMPLE PREPARATION FOR CHARACTERIZATION .....	86
3.5.1	Sample preparation (SEM) .....	86
3.5.2	Sample preparation (TEM) .....	86
3.5.3	Sample preparation (XRD) .....	87
3.5.4	Sample preparation (FT-IR) .....	88
3.5.5	Sample preparation (TGA) .....	88
3.5.6	Sample preparation (Peel test) .....	89
3.6	HYDROGEN DIFFUSION REACTOR UNIT .....	89

## TABLE OF CONTENTS

---

3.6.1	Sample preparation (hydrogen diffusion test).....	90
3.7	HYDROGEN DIFFUSION TEST .....	90
3.8	OPERATION PROCEDURE OF HYDROGEN DIFFUSION REACTOR	92
CHAPTER 4	.....	93
4.0	RESULTS AND DISCUSSIONS.....	93
4.1	INTRODUCTION.....	93
4.2	CHARACTERISATION OF UNIRRADIATED POLYIMIDE SAMPLE..	93
4.2.1	Fourier transformed infrared transmission spectroscopy.....	93
4.2.2	X-ray diffraction study of unirradiated polyimide.....	97
4.2.3	Hydrogen diffusion measurement of unirradiated polyimide.....	98
4.2.4	Thermo-gravimetric study of unirradiated polyimide.....	100
4.3	SURFACE TREATMENT OF UNIRRADIATED POLYIMIDE FILM...	102
4.4	CHARACTERISATION OF ETCHED UNIRRADIATED/IRRADIATED POLYIMIDE SAMPLES.....	102
4.4.1	FTIR of unirradiated polyimide etched with 13 % NaOCl solution....	103
4.4.2	FTIR of unirradiated polyimide etched with 0.4M NaOH solution....	111
4.4.3	FTIR of unirradiated polyimide etched with 0.4M NaOH dissolved in 13 % NaOCl solution.....	120
4.5	SURFACE TREATMENT OF IRRADIATED POLYIMIDE FILM.....	123
4.5.1	Introduction.....	123
4.5.2	Characterisation of track etched polyimide .....	123
4.6	MORPHOLOGICAL STUDY BY SCANNING ELECTRON MICROSCOPY (SEM) OF IRRADIATED POLYIMIDE ETCHED WITH 13 % NaOCl AND 0.4M NaOH/13 % NaOCl SOLUTIONS.....	124

## TABLE OF CONTENTS

---

4.6.1	The pore size distribution of track etched polyimide using 0.4 M NaOH/13 % NaOCl mixture and 13 % NaOCl solutions.....	128
4.7	SCANNING ELECTRON MORPHOLOGICAL STUDY FOR NaOCl TRACK ETCHED POLYIMIDE SAMPLES .....	129
4.7.1	Hydrogen diffusion measurement of 0.4 M NaOH/13 % NaOCl track etched polyimide sample.....	132
4.7.2	FTIR spectra of irradiated polyimide etched with 0.4M NaOH dissolved in 13 % NaOCl solution.....	135
4.7.3	FTIR spectra of irradiated polyimide etched with 13 % NaOCl solution	140
CHAPTER 5	.....	145
5.0	RESULTS AND DISCUSSION OF PALLADIUM MODIFIED POLYIMIDE	145
5.1	CHARACTERISTICS OF PALLADIUM MODIFIED UNIRRADIATED POLYIMIDE.....	145
5.2	MORPHOLOGICAL (SEM) STUDY OF UNIRRADIATED PALLADIUM MODIFIED ETCHED POLYIMIDE .....	145
5.2.1	The SEM images below represent NaOH etched polyimide film modified with palladium. ....	146
5.2.2	The SEM micrograph result images are presented for 0.4 M NaOH/13 % NaOCl etched unirradiated polyimide film modified with palladium. ....	148
5.2.3	The SEM micrograph of unirradiated polyimide film samples was etched in 13 % NaOCl and modified with palladium plating by electroless deposition.....	150

## TABLE OF CONTENTS

---

5.3	MORPHOLOGICAL STUDY: TEM MICROGRAPH OF PALLADIUM MODIFIED UNIRRADIATED POLYIMIDE.....	152
5.3.1	TEM micrograph results are presented for 0.4 M NaOH etched unirradiated polyimide film modified with palladium.....	153
5.3.2	TEM cross-section micrograph of 0.4 M NaOH/13 % NaOCl etched unirradiated polyimide film modified with palladium.....	155
5.3.3	The TEM cross-section analysis of 13 % NaOCl etched unirradiated polyimide film modified with palladium.....	157
5.4	PEEL STRENGTH MEASUREMENT ON PALLADIUM-POLYIMIDE LAMINATES .....	158
5.5	XRD RESULTS OF PALLADIUM MODIFIED POLYIMIDE AFTER ETCHING IN 13 % NaOCl SOLUTION .....	159
5.6	XRD RESULTS OF POLYIMIDE PLATED WITH PALLADIUM AFTER ETCHING WITH 0.4 M NaOH SOLUTION.....	161
5.7	XRD RESULTS OF POLYIMIDE PLATED WITH PALLADIUM AFTER ETCHING WITH 0.4 M NaOH SOLUTION.....	163
	CHAPTER 6 .....	165
6.0	CONCLUSIONS AND RECOMMENDATIONS .....	165
	CHAPTER 7 .....	171
7.0	REFERENCES .....	171
	<b>APPENDIX 1 1: LIST OF COMPONENTS FOR THE HOME-GROWN HYDROGEN DIFFUSION REACTOR UNIT .....</b>	<b>190</b>



## LIST OF FIGURES

---

Figure 2-1: Schematic of membrane structure showing mechanism of separation	29
Figure 2-2: Polymer structures (Powell <i>et al.</i> , 2006).....	33
Figure 2-3: Reaction scheme for the synthesis of polyimide.....	45
Figure 2-4: Experimental set-up for electroless plating technique .....	68
Figure 2-5: Experimental approach .....	75
Figure 3-1: Experimental protocol.....	78
Figure 3-2: Schematic diagram of home-grown hydrogen reactor unit.....	91
Figure 4-1: Selected FTIR spectra of unirradiated polyimide .....	96
Figure 4-2: XRD analysis of unirradiated polyimide .....	97
Figure 4-3: Hydrogen diffusion measurement of unirradiated polyimide film at 25°C, 250°C and 325°C.....	99
Figure 4-4: Thermo-gravimetric study of unirradiated polyimide.....	101
Figure 4-5: FTIR of unirradiated polyimide and 5 minutes 13 % NaOCl etched unirradiated polyimide.....	104
Figure 4-6: FTIR of unirradiated polyimide and 10 minutes 13 % NaOCl etched unirradiated polyimide.....	106
Figure 4-7: FTIR of unirradiated polyimide and 20 minutes 13% NaOCl etched unirradiated polyimide.....	108
Figure 4-8: FTIR of unirradiated polyimide and 30 minutes 13 % NaOCl etched unirradiated polyimide.....	110
Figure 4-9: FTIR of unirradiated polyimide and 5 minutes 0.4 M NaOH etched unirradiated polyimide.....	112
Figure 4-10: FTIR of unirradiated polyimide and 10 minutes 0.4 M NaOH etched unirradiated polyimide.....	114
Figure 4-11: FTIR of unirradiated polyimide and 20 minutes 0.4 M NaOH etched unirradiated polyimide.....	116
Figure 4-12: FTIR of unirradiated polyimide and 30 minutes 0.4 M NaOH etched unirradiated polyimide.....	118
Figure 4-13: FTIR of unirradiated polyimide and 20 minutes 0.4 M NaOH/13 % NaOCl etched unirradiated polyimide .....	121

## LIST OF FIGURES

---

Figure 4-14: SEM images of 0.4 M NaOH/13 % NaOCl track etched irradiated polyimide .....	126
Figure 4-15: Compared pore size of track etched polyimide with (a) 13 % NaOCl and (b) 0.4M NaOH/13 % NaOCl .....	128
Figure 4-16: SEM images of 13 % NaOCl track etched polyimide .....	130
Figure 4-17: Hydrogen diffusion test for 0.4 M NaOH/13 % NaOCl track etched polyimide .....	132
Figure 4-18: Hydrogen diffusion test for 13 % NaOCl track etched polyimide.....	134
Figure 4-19: Compared FTIR (800-600cm <sup>-1</sup> ) spectra of irradiated polyimide etched with 0.4M NaOH/13 % NaOCl solution (a) Unirradiated polyimide, (b) 10 minutes etched, (c) 20 minutes etched, (d) 30 minutes etched, (e) 40 minutes etched and (f) 60 minutes etched. ....	136
Figure 4-20: Compared FTIR (2000-1200cm <sup>-1</sup> ) spectra of irradiated polyimide etched with 0.4M NaOH/13 % NaOCl solution (a) Unirradiated polyimide, (b) 10 minutes etched, (c) 20 minutes etched, (d) 30 minutes etched, (e) 40 minutes etched and (f) 60 minutes etched. ....	138
Figure 5-1: SEM micrograph of palladium modified unirradiated polyimide etched with 0.4 M NaOH (a) 5 minutes, (b) 10 minutes, (c) 20 minutes, (d) 30 minutes.....	146
Figure 5-2: SEM micrograph of palladium modified unirradiated polyimide etched with 0.4 M NaOH/ 13 % NaOCl (ai) 5 minutes, (bi) 10 minutes, (ci) 20 minutes, (di) 30 minutes.....	148
Figure 5-3: SEM micrograph of palladium modified unirradiated polyimide etched with 13 % NaOCl (aii) 5 minutes, (bii) 10 minutes, (cii) 20 minutes, (dii) 30 minutes .....	150
Figure 5-4: Cross-section of TEM micrograph of palladium modified unirradiated polyimide etched with 0.4 M NaOH (a) 5minutes, (b) 10 minutes, (c) 20 minutes, (d) 30 minutes.....	153
Figure 5-5: Cross-section of TEM micrograph of palladium modified unirradiated polyimide etched with 0.4 M NaOH dissolved in 13 % NaOCl (aii) 5 minutes, (bii) 10 minutes, (cii) 20 minutes, (dii) 30 minutes.....	155

## LIST OF FIGURES

---

Figure 5-6: Cross-section of TEM micrograph of palladium modified unirradiated polyimide etched with 13 % NaOCl (aiii) 5 minutes, (biii) 10 minutes, (ciii) 20 minutes, (diii) 30 minutes .....	157
Figure 5-7: Schematic of Peel test measurement technique. ....	158
Figure 5-8: XRD of palladium plated polyimide etched with 13 % NaOCl solution (a) 5 minutes, (b) 10 minutes, (c) 20 minutes and (d) 30minutes. ....	160
Figure 5-9: XRD of palladium modified polyimide after etching with 0.4 M NaOH solution for (a) 5 minutes, (b) 10 minutes, (c) 20 minutes and (d) 30 minutes .....	161
Figure 5-10: XRD of palladium modified polyimide after etching with 0.4 M NaOH solution for (a) 5 minutes, (b) 10 minutes, (c) 20 minutes and (d) 30 minutes .....	163



## LIST OF TABLES

---

Table 1-1: List of PGM metal global resources.....	3
Table 1-2: Feedstock contribution (%) of hydrogen production .....	5
Table 2-1: Comparison of energy density of different fuels.....	18
Table 3-1: Materials and chemicals .....	76
Table 3-2: Composition of palladium electroless plating bath .....	83
Table 3-3: Sample matrix for etching and plating time of unirradiated polyimide .....	84
Table 3-4: Sample matrix of etching time for irradiated polyimide .....	85
Table 4-1: Fourier transformed infra-red of commercial polyimide .....	95



## LIST OF EQUATIONS

---

Equation 1: Hydrogen production by water gas shift reaction .....	21
Equation 2: Hydrogen production by steam reforming reaction .....	23
Equation 3: Boudouard reaction .....	23
Equation 4: Gas permeability equation.....	32
Equation 5: Fick's law .....	41
Equation 6: Permeance rate equation.....	42
Equation 7: Gas selectivity equation.....	43
Equation 8: Reaction scheme of electroless deposition.....	63



## DECLARATION

---

I declare that *ION TRACK MODIFICATION OF POLYIMIDE FILM FOR DEVELOPMENT OF PALLADIUM COMPOSITE MEMBRANE FOR HYDROGEN SEPARATION AND PURIFICATION* is my own work, that it has not been submitted for any degree or examination in any other university, and that all the sources I have used or quoted have been indicated and acknowledged by complete references.

**Full name**..... **Date**.....

**Signed**.....



## ABSTRACT

---

South Africa's coal and platinum mineral resources are crucial resources towards creating an alternative and environmentally sustainable energy system. The beneficiation of these natural resources can help to enhance a sustainable and effective clean energy base infrastructure and further promote their exploration and exportation for economic gains. By diversification of these resources, coal and the platinum group metals (PGMs) especially palladium market can be further harnessed in the foreseeable future hence SA energy security can be guaranteed from the technological point of view.

The South Africa power industry is a critical sector, and has served as a major platform in the SA's socio-economic development. This sector has also been identified as a route towards an independent energy base, with global relevance through the development of membrane technologies to effectively and economically separate and purify hydrogen from the gas mixtures released during coal gasification. Coal gasification is considered as a source of hydrogen gas and the effluent gases released during this process include hydrogen sulphide, oxides of carbon and nitrogen, hydrogen and other particulates. In developing an alternative hydrogen gas separating method, composite membrane based on organic-inorganic system is being considered since the other available methods of hydrogen separation are relatively expensive.

The scientific approach of this study involves the use of palladium modified polyimide composite membrane. Palladium metal serves as hydrogen sorption material, deposited on polyimide substrates (composite film) by electroless technique. Polyimide is a class of polymer with excellent physico-chemical properties such as good mechanical strength, superior thermal stability and high resistance to chemical attack. In this study, a composite polymer-palladium membrane was developed and investigated to determine the prospect of using this membrane as a cheap, accessible, reliable and efficient system to separate and purify hydrogen gas. Prior to the palladium metal plating, the challenge of metal adhesion on glassy polymer such as polyimide film was addressed by chemical etching and unirradiated and irradiated polyimide film surface using NaOH, NaOCl and a mixture of NaOH/NaOCl

## ABSTRACT

---

solutions. The time of etching was varied and the overall effect of this surface treatment was deeply investigated using Fourier transform infrared (FTIR) spectroscopy. The FTIR study focused on the structural deformation of the polyimide functional group units and the emergence of 'active sites' along the polyimide backbone structures that have been identified to allow the Pd metal exchange on the functionalised polyimide film. The detailed use of FTIR spectroscopic technique in this study on the etched unirradiated and irradiated polyimide film was to understand the chemical interaction between the polyimide functional group units and the chemical etchants. The surface morphology of unirradiated and irradiated polyimide samples was studied using SEM, the depth profile (penetration) of palladium particles after electroless deposition on the polyimide matrix was investigated by SEM and TEM analysis. As for the alkaline etched irradiated polyimide, pore distribution, shape and size depended on the etching time and solution. In the XRD analysis, the palladium modified unirradiated polyimide film indicated the diffraction peaks of palladium metal in the (1,1,1), (2,2,0) and (2,0,0) planes present in the polyimide surface, and the peel test showed that the strength of adhesion of palladium on unirradiated surface was low compared to the palladium modified irradiated polyimide. The NaOH solution showed the best etchant at 20 minutes for the unirradiated palladium modified polyimide.

The hallmark of this study was the design, fabrication and assemblage of home-built hydrogen diffusion reactor unit used to measure rate of hydrogen diffusion property of unirradiated and irradiated polyimide films from 25 °C to 325 °C. The rate of hydrogen diffusion was observed to depend on the etching time of polyimide surface before and after the polyimide surface irradiation treatment.



## PUBLICATIONS

---

### CONFERENCE CONTRIBUTION

Accepted Abstract: “**NANO – COMPOSITE PALLADIUM POLYIMIDE POLYMER MEMBRANES: SYNTHESIS AND PROPERTIES**” *International Conference on Clean Energy (ICCI-2010), Gazimagusa – N. Cyprus, 2010*

Accepted Abstract: “**PHYSICAL CHEMICAL PROPERTIES OF POLYIMIDE PALLADIUM NANO - COMPOSITE MEMBRANES**” *2011 IEEE Nanotechnology Conference*



## DEDICATION

---

**THIS WORK IS DEDICATED TO GOD ALMIGHTY IN WHOM I HAVE  
FOUND GRACE AND MERCY**



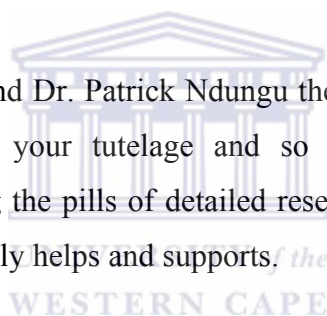
## ACKNOWLEDGEMENT

---

Indeed, it has been a painstaking journey so far with challenges for me on every side. This project would not have seen the light of the day without the help, support and understanding of some ‘exceptional personalities’ around me here in University of the Western Cape as well as other places.

A special, unreserved and profound gratitude to a personality with a large heart; Professor Leslie Felicia Petrik (Group Leader, ENS Research Group) for the financial support, constant advice and immeasurable encouragement throughout the duration of this project. I will perpetually hold your words to me in those ‘disturbing’ moments of my life in high esteem. I am sincerely grateful for the rare opportunity of being part of the Environmental and Nano-Sciences Research Group (ENS). It has been home-away-from home experience for me.

To Dr. Alexander Necheav and Dr. Patrick Ndungu the two doyen of Nanoscience, I am privileged to be under your tutelage and so grateful for your assistance, mentorship and administering the pills of detailed research skills to me. This project survived because of your timely helps and supports.



To my parents, Mr and Mrs Adeniyi, the call logs say it all. Those words of assurance will forever be in my heart. Olusesan, Olusheyi Adeniyi and Amos Moore my brothers, thank you for your faith in me. We will get there in His name. Justina, Ayomide and Pelumi Adeniyi, Damilola, T-boy (Bagwell) and Imole Adebowale you are joy to your generation.

To Mrs Funmilola Foluke Adeniyi, my lovely wife and friend, you are my rare gem, always my treasure of pleasure and ‘my tag-team partner’.

Prof. Akinwunmi, Chief Stephen Olanrewaju Ifarinde, Chief and Mrs Festus Adebowale and Sehide Ogunbeku, God bless you and your families. Femi Olaofe, Seun Olaofe, Dr. Seun Oyekola, Alfred Onaneye, Seun Fadipe, Gbenga Arotiba, Demilade (LeDiva), Dayo Adedeji and Tobi Moody you are all ‘mouthed’. Deacon

## ACKNOWLEDGEMENT

---

Adeshina and Adewumi, I will forever remain grateful. Others too numerous to mention, your labour of love will be rewarded.

All members of RCCG Household of God Parish may your oil never run dry. Thank you all.

To all ENS guys, it was an opportunity to be with you all. Averill and Vanessa, thank you for your understanding.

This work could not have been successful without the technical inputs and assistance from some personalities. Adrian Joseph (EMU, UWC.) for SEM analysis, Mohamed Jaffer (EMU, UCT) for the microtome and TEM analysis, Dr. Remy (ithemba Lab Cape Town). My interactive sessions with you all were of tremendous help and I say thank you very much.

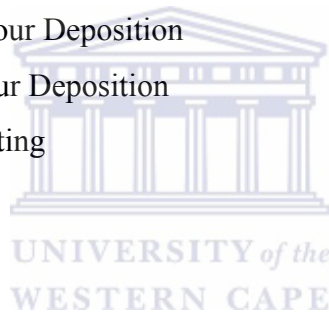
Finally, special thanks to National Research Foundation (NRF) PGM-Nano flagship for funding this project.



## LIST OF ABBREVIATIONS

---

<b>PGMs</b>	Platinum Group Metals
<b>IGCC</b>	Integrated Gasification of Clean Coal
<b>UCG</b>	Underground Coal Gasification
<b>GDP</b>	Gross Domestic Product
<b>TGA</b>	Thermo-gravimetric Analysis
<b>FTIR/ATR</b>	Fourier Transformed Infra-red Spectroscopy/Attenuated total reflection
<b>SEM</b>	Scanning Electron Microscopy
<b>TEM</b>	Transmission Electron Microscopy
<b>XRD</b>	X-ray Diffraction
<b>ATM</b>	Atmosphere
<b>PSA</b>	Pressure Swing Adsorption
<b>CD</b>	Cryogenic Distillation
<b>CVD</b>	Chemical Vapour Deposition
<b>PVD</b>	Physical Vapour Deposition
<b>EP</b>	Electroless plating
<b>PI</b>	Polyimide



## KEYWORDS

---

Composite

Membrane

Hydrogen Separation/Purification

Ion track

Electroless Plating

Palladium

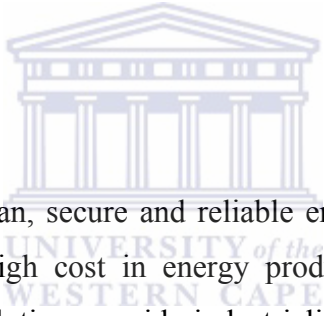
Polyimide

Functionalization



**CHAPTER 1****1.0 INTRODUCTION**

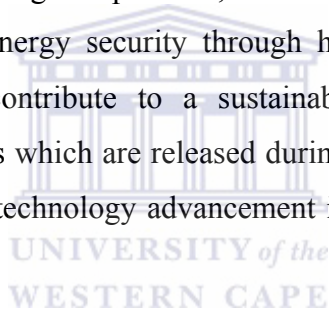
Chapter 1 of this study provides brief background information on the global perspective on the hydrogen energy status and the available technologies associated with hydrogen gas separation. It gives a brief summary of the beneficiation of platinum group metals (PGMs). The approach adopted for this work is discussed in the motivation, problem statement and research questions. This chapter also highlights the aims and objectives, scope, the research methodology and delimitation of this project. The concluding part of this chapter describes the thesis structure.

**1.1 BACKGROUND**

The availability of cheap, clean, secure and reliable energy continues to be a major global concern due to the high cost in energy production and increasing energy demand, environmental pollution, rapid industrialization and growing human population. Fossil fuel still remains the single largest source of energy and accounts for more than 80 % of the world energy need with 40 % of this energy generated from coal combustion process (Shoko *et al.*, 2006; Gray *et al.*, 2001; Gary *et al.*, 2006). The energy generated from coal is used for domestic, agricultural and industrial purposes especially in South Africa.

South Africa (SA) is a major world producer of platinum group metals (PGMs) and also with large deposit of coal. The PGMs and coal are strategic to the economy of SA. The SA Department of Trade and Industry (DTI) reported that the PGMs precious metals account for about 25 % of the country's gross domestic product (GDP). Both Coal and PGMs resources continue to serve as a source of foreign exchange earnings for SA according to DTI report (2004). In recent years, there has been a renewed focus on the need for the diversification of SA energy resources in an effort to

beneficiate coal so as to serve as a source of hydrogen gas (Shoko *et al.*, 2006). Pursuant to this national mandate towards SA hydrogen energy technology, the PGMs especially palladium metal has been identified to play a pivotal role in the PGMs beneficiation, and act as the purifier of hydrogen gas from impurities associated with effluent gases produced from the coal gasification process. For this process, PGMs such as palladium metal are required as a component in composite polymer-PGM membranes for separation and purification of hydrogen. Such polymer-PGM composite membranes can offer cheap and alternative means of hydrogen separation technology. Most significantly, the beneficiation of coal and PGMs for hydrogen production and separation promises to promote environmental remediation and sustainable development (Shoko *et al.*, 2006). By employing polymer-PGM composite membranes for hydrogen separation, PGMs may provide future alternative, affordable and dependable energy security through hydrogen processes. Also, the composite membrane can contribute to a sustainable environment through the reduction of greenhouse gases which are released during coal combustion. Moreover, this route would provide for technology advancement in energy security in SA (DTI report 2004).





The table below shows the list of PGM metal resources global reserve base and demand (Robinson *et al.*, 2006).

Table 1-1: List of PGM metal global resources

COUNTRY	RESERVE BASE			SUPPLY/ DEMAND		
	Tonnage	%	Rank	Kg	%	Rank
South Africa	70, 000	87.7	1	302,979	56.7	1
Russia	6,600	8.3	2	174,180	32.6	2
USA	2000	2.5	3	18,400	3.4	4
Canada	390	0.5	4	21,568	4	3
Other	850	1.1		17,480	3.3	-
Total	79,840	100		534,607	100	-

The table above indicates the commercial and economically recoverable PGMs. South Africa leads the pack with the highest reserve base of over 80 % and distantly followed by Russia with 8.3 %. From the supply-demand section in the table, South Africa and Russia are both responsible for the global supply of PGMs to other countries with USA being the major destination country with over 93 % as at 2002. The exploration and exportation of PGMs remain pivotal to the economy of these countries. PGMs deposits in SA are located in Merensky Reef of the Bushveld Complex, Noril'sk-Talnakh District in Russia, and the Stillwater Complex in the United States.

Hydrogen gas is a high value product with unique energy properties hence used as an energy carrier gas. It is often referred to as “A Clean and Secure Energy Future”. This

is because of its non-polluting nature when applied as a source of energy (Nathan *et al.*, 2007). During combustion of hydrogen for energy purposes, H<sub>2</sub>O is the final product. This therefore implies that environmental sustainability is feasible with hydrogen energy application. Some of the industrial processes such as petroleum refining and methane gas reforming have been used to produce hydrogen and they account for about 80 % of global hydrogen production (Nenoff *et al.*, 2006; Stiegel *et al.*, 2006).

Hydrogen as an energy carrier is expected to replace non-renewable energy sources such as coal, natural gas and petroleum which are dwindling resources due to environmental concerns and price instability. The continuous depletion of these fossil fuel resources and the need to create a sustainable environment makes hydrogen (H<sub>2</sub>) an attractive alternative (Shao *et al.*, 2009). The conceptualization of the hydrogen economy has increased in recent decades with resources channelled towards research and development (R&D) to investigate and advance hydrogen utilization for energy application (US DOE, 2006). There are several factors that have been identified to limit the success of hydrogen economy technology. These include; cost associated with hydrogen production, separation and purification technologies, storage, distribution networks and conversion of pre-existing technologies to hydrogen based infrastructure (Gary *et al.*, 2006; Stiegel *et al.*, 2006; Moore *et al.*, 2006; Shoko *et al.*, 2006).

The table below highlights the available sources of hydrogen production and their percentage composition.

Table 1-2: Feedstock contribution (%) of hydrogen production

<b>Sources</b>	<b>Composition (%)</b>
Coal	19
Natural gas	47
Electrolysis	46
Oil	30

Several advantages of hydrogen based energy include; ability to generate from a wide range of natural resources such as water, coal, natural gas and petroleum. Hydrogen has low or zero emission thereby making it environmentally friendly with relatively high energy density. Hydrogen serves as raw material or intermediate in the manufacture of numerous products such as metals, microelectronics, semi-conductors and various chemical products (Edlund *et al.*, 2000; Edwards *et al.*, 2008; Robinson *et al.*, 2006; Hurley and McCollor.1997). The production of pure hydrogen gas from fossil fuel for energy application continues to pose enormous challenges due to economic cost of the available technologies for hydrogen separation and purification processes such as pressure swing adsorption (PSA), cryogenic distillation (CD), absorption and membranes (Shao *et al.*, 2009; Sircar *et al.*, 2000).

**1.2 AVAILABLE TECHNOLOGIES FOR HYDROGEN GAS SEPARATION**

The traditional hydrogen separation and purification technologies are; Pressure Swing Adsorption (PSA), cryogenics distillation (CD) and membrane systems. Each of these technologies has limitations that hinder wide – scale production of hydrogen which is considered to limit the prospective large scale hydrogen production to meet future demands of hydrogen as an energy carrier. PSA recovers less hydrogen and it is limited to modest temperatures (Sircar, 2002). The cryogenics technology is only used in large-scale facilities with liquid hydrocarbon recovery because of its high capital cost (Shao *et al.*, 2009). Membrane systems are suggested to offer promising potentials in hydrogen separation and purification. The use of membranes in hydrogen separation is more economical than traditional separation technologies such as PSA, provided that suitable membranes are commercially available (Shao *et al.*, 2009). Membrane separation devices are potentially much simpler, more compact and use less energy. Moreover, membranes do not suffer from efficiency losses and high operational costs for heat exchangers associated with the cooling of the synthesis gas (Powell *et al.*, 2006; Koros *et al.*, 1993; Shao *et al.*, 2009).

Membranes for gas separation processes have shown great promise with respect to output and cost efficiency (Gary J.S., 2006). This method of gas separation has been fully incorporated into the hydrogen from coal programme of the United States Department of Energy (US DOE, 2006; Report, 2005). Membranes can be used in the concentration, purification or separation of gases (Nenoff *et al.*, 2006). They serve as barriers or permeable interfaces capable of selectively permitting preferred molecules to permeate across. For hydrogen permeable membrane, the thinner the membrane, the higher the permeability and such membrane must be defect-free (Naotsugu *et al.*, 2005). Some of the advantages of this technology in hydrogen processes include; continuity of operation and simplicity of application. Membrane technology is considered to be economically beneficial with relatively high separation and purification efficiency. Other advantages are; ease of application, versatility and availability of membranes

Generally, hydrogen production processes from coal gasification or methane steam reforming occurs at high temperatures and pressures along with the release of gases such as oxides of nitrogen, sulphur, carbon and heavy particulate matters (Gray *et al.*, 2001). These gases act as surface poison in hydrogen separation and purification systems such as PSA, thereby limiting the regeneration of absorbents used in the PSA technology for reuse (Escand'on *et al.*, 2008). The use of membranes in hydrogen separation requires thermally stable inorganic materials (Checchetto *et al.*, 2004), while membrane performance depends on the physico-chemical interaction of the gaseous components (Ramachandranraghu *et al.*, 1998). The selectivity properties of a membrane to transport individual component from the feed-gas mixtures more readily than the other components is another major boost to their acceptability and wide range application.

For high-purity hydrogen, Pd membranes are considered to have shown promising results being highly selective for hydrogen flux (Paglieri *et al.*, 2002). The limitation of this technology includes; the high cost of palladium, palladium embrittlement due to phase change in hydrogen atmosphere, poor thermal stability especially at elevated temperature and poisoning by hostile surface adsorbates (i.e. H<sub>2</sub>S, CO, CO<sub>2</sub>, O<sub>2</sub>, H<sub>2</sub>O) over prolonged operation ( Paglieri *et al.*, 2002; Escand'on *et al.*, 2008; Kilicarslan *et al.*, 2008).

### **1.3 MOTIVATION**

In recent time, there has been a growing need for the identification and implementation of relevant technologies aimed at harnessing South Africa platinum group metals (PGMs) resources. These resources can be diversified through the beneficiation of SA PGMs resources for sustainable economic development. The PGMs natural resources exist in large deposit in the North and Eastern province of SA with about 70 % recoverable reserve (Robinson *et al.*, 2006). In this project, the focus is to enhance the beneficiation of PGM resources in SA which is found in abundance

in the country. The exploration of SA abundant PGMs resources towards energy security can be beneficial through the production of hydrogen using cheap, reliable, efficient and affordable hydrogen gas separation and purification method by means of a polymer-PGM composite membrane system (Uemiya *et al.*, 2001). The polymer-PGM composite membrane being developed in this study should be economical, easy to use and should not require complex synthetic processes compared with other known hydrogen separation and purification technologies such as PSA, CD and absorption (Robinson *et al.*, 2006). In the utilization of South African PGMs, hydrogen gas can be generated from gasified coal and separated or purified using polymer-PGM composite membrane. Therefore availability of resources and national drive towards environmentally sustainable energy sources are among the factors responsible for undertaking this study through resources beneficiation towards energy application.

#### **1.4 PROBLEM STATEMENT**

Hydrogen is not available in its free molecular form on earth but is bound up in compounds such as water and valuable hydrocarbon deposits such as coal, natural gas among others. In order to obtain molecular hydrogen from these resources for energy purposes, it is imperative to use a cost-effective method of hydrogen separation from the other elements such as carbon, oxygen and nitrogen to which it is chemically bound. Conventional methods used for separating hydrogen from gas mixtures include; PSA, cryogenic distillation, absorption and membrane filtration (Nenoff *et al.*, 2006). These techniques do not achieve the expected separation and purification level of hydrogen needed for energy application (Shao *et al.*, 2009). Therefore, the amount of hydrogen recovery in the presence of impurities determines the choice of separation techniques. The task of producing hydrogen on an industrial scale is tremendous so also the techniques involved in its purification. Hydrogen separation and purification operations such as cryogenic distillation, adsorption and pressure swing absorption (PSA) account for high capital investment in large-scale chemical plants (Lu *et al.*, 2007). This has therefore made membrane separation technology a

preferred path in-term of cost and efficiency. This study will focus on composite polymer metal membrane as a medium for hydrogen separation and purification technique.

Polymer such as polyimide has been reported with poor surface adhesion with metals (Yi *et al.*, 2004). As a result of this, the use of surface treatment techniques to functionalise the polyimide structure and increase polyimide-metal adhesion becomes imperative. The surface treatment required for depth profiling of the polyimide surface must be carefully controlled so as to create the roughness and ‘catalytic active sites’ that can act as chemical bonding site for the metal (Mitrofanov *et al.*, 2006). A composite polyimide-metal membrane is predicted to. For an effective composite polyimide-metal membrane application in hydrogen gas separation and purification, such metal must show promising surface adhesion structures with polyimide (Dazinger and Voitus, 2003). Metals such as palladium (Pd) have been proven to show infinite affinity for hydrogen, hence Pd metal has been in use for hydrogen gas separation and purification in a composite membrane arrangement (Nam and Lee, 2000; Paglieri *et al.*, 2002). The problem associated with Pd is the hydrogen embrittlement phenomenon which occurs due to phase change of Pd at low (below 300 °C) temperature environment (Nam and Lee, 2000). This therefore implies that the operation of such composite membrane must be in a high temperature environment. Due to the high temperature environment in which hydrogen gas can be obtained, the composite membrane structure must exhibit considerable tolerance with high thermally stability.

## **1.5 RESEARCH QUESTIONS**

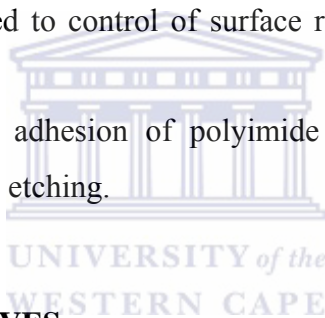
- i. How can surface modification of polyimide by etching enhance metal adhesion to the polyimide surface?
- ii. What is the suitable surface functionalization condition for polyimide film to promote metal adhesion to the polymer surface?

- iii. What is the influence of conditions such as temperature and pressure on the rate of diffusion of hydrogen gas across modified polyimide membrane?

## **1.6 HYPOTHESIS**

In order to answer these key questions, a number of hypotheses based on the literature review will be developed and presented in this thesis. These include:

- i. Prove that depth profile of polyimide by chemical etching can enhance palladium adhesion on the polyimide surface after electroless plating.
- ii. Prove that etching at low temperature and low concentration of etching solution can be used to control of surface roughness of polyimide during etching.
- iii. Prove that surface adhesion of polyimide can be enhanced by simple method of chemical etching.



## **1.7 AIMS AND OBJECTIVES**

The aims of this work are as follows;

- i. To determine the effect of surface functionalisation on polyimide as a function of time and temperature stability.
- ii. To determine whether the effect of conditions such as etching time and the type of etchant of polyimide will improve adhesion property of composite polymer-PGM membrane
- iii. To study the thermal stability of polyimide film in hydrogen atmosphere at high temperature
- iv. To investigate surface depth profile of etched polyimide by hydrogen diffusion.
- v. To determine the rate of hydrogen diffusion through the functionalized polyimide and polyimide-PGM composite membrane



- vi. To develop home built hydrogen diffusion reactor for hydrogen diffusion measurement.

## **1.8 SCOPE**

Polyimide is a unique polymer structure with excellent chemical, thermal, electrical and physical properties. In developing the composite polyimide-metal membrane for this study, the polyimide will serve as support. The scope of this study is to determine the use of commercial polyimide as a possible substrate in a composite membrane structure. Polyimide properties such as adhesion strength, thermal stability and hydrogen diffusion measurement will be examined after surface functionalisation methods. The surface modification of the polyimide film will be performed by etching in NaOH and NaOCl solutions to form porous (depth profile) polyimide surface and to improve the polymer-metal adhesion properties (Mitrofanov *et al.*, 2006). This surface treatment is followed by sensitisation/activation procedure to create active sites in the polyimide bonds for metal exchange, and acceleration in Na<sub>2</sub>EDTA and the polyimide surface is plated with palladium metal using the electroless plating technique (Shuxiang *et al.*, 2010; Edlung *et al.*, 2000).

## **1.9 DELIMITATION**

For this study, the polymer of choice is Kapton® type of polyimide. The polyimide samples used are the unirradiated and irradiated as-received polyimide film. The chemical etching was carried out at low concentrations of 0.4 M NaOH while the 13 % NaOCl solution was used as received. For the PGMs, only palladium (Pd) metal is used for this study. The Pd is not alloyed with any other metal during electroless plating on the polyimide substrate. The polyimide-palladium composite membrane is used to test for hydrogen diffusion measurement using a home-designed, fabricated and installed hydrogen diffusion reactor unit from ambient to 350 °C. Hydrogen

selectivity and purity properties of the polyimide-palladium composite membranes were not considered in this study. This is because only hydrogen gas was fed tested.

### **1.10 RESEARCH APPROACH**

The improvement of polyimide metal adhesion properties by surface functionalization of the polymer film using irradiation with heavy ion prior to chemical etching will be investigated. Chemical etchants such as NaOH and NaOCl at known concentration will be used at constant temperature and as a function of time. The measurement of hydrogen diffusion through the as-received, etched unirradiated and irradiated polyimide samples will be studied from room temperature to 350 °C to determine the thermal stability of the polyimide film.

In order to achieve the objectives of this study, the research approach is outlined;

- a. Characterization of as-received commercial polyimide. SEM, FTIR, TGA and XRD analysis were conducted to determine the physico-chemical properties of the commercial polyimide and establish a baseline data set.
- b. Etching of the as-received unirradiated and irradiated polyimide in known concentration of sodium hypochlorite and sodium hydroxide solutions. The duration of etching for the unirradiated samples was 5, 10, 20 or 30 minutes. The irradiated films were etched for 10, 20, 30, 40 or 60 minutes. All samples were etched in fresh solution for the different time and at constant temperature of 50 °C. Surface morphology was studied using SEM. The presence or absence of functional groups in the polymer structure was investigated using FTIR. This surface treatment is expected to create surface roughness of the polyimide film and also introduce a functional regime that will serve as anchor for palladium adhesion to the polymer surface in a polyimide-palladium interface (Schiedt, 2007; Mitrofanov *et al.*, 2006; Charbonnier *et al.*, 2003).

c. Electroless plating of palladium on functionalised polyimide surface was carried out after successive activation and sensitization steps. Acceleration the sensitized polyimide was investigated in acidic, basic and complexing agents such as Na<sub>2</sub>EDTA.

The characterisation techniques used are; X-ray diffraction (XRD), Fourier-transformed infrared spectroscopy/attenuated total reflection (FT-IR/ATR), transmission electron microscopy (TEM), thermo gravimetric analysis (TGA), scanning electron microscopy (SEM). A home-grown hydrogen reactor was designed, built and used to investigate the hydrogen gas diffusion of the fabricated Pd/polyimide composite membrane.

## **1.11 THESIS STRUCTURE**

### **Chapter 2: Literature review**



This chapter provides a comprehensive review of the background status of hydrogen as a future energy carrier; the conventional hydrogen separation and purification technologies as well as polyimide as a polymer support for gas separation application. The various polyimide surface treatments such as etching, heavy ion irradiation and ion implantation to improve adhesion of metals are discussed. Other sections of this chapter focus on palladium, palladium membranes, and limitations of such membranes such as the effect of surface poisons on purity and gas recovery. A review on the application of palladium membrane for gas purification and separation is discussed. The use of composites such as polymer-metal structure and the various transport mechanisms for gas permeation across membrane structure is examined. The concept of electroless plating method for metal layer deposition on polymer surfaces is explained based on the available literatures. The different characterisation techniques were discussed.

**Chapter 3: Experimental approach and methodology**

In order to address and answer the outlined objectives and questions of this study, chapter three of this study explains the systematic experimental methodology applied for the surface functionalisation of polyimide using the NaOH and NaOCl etchants. It also covers materials and experimental protocols. It details the design, fabrication and assemblage of hydrogen separation reactor unit to measure the rate of hydrogen diffusion across commercial, etched unirradiated and irradiated polyimide film. Samples preparation and each of the instrument set-up conditions for the different characterisation techniques were also included in this chapter.

**Chapter 4: Result and discussion of as-received, unirradiated and irradiated polyimide**

This chapter presents the results obtained from the experimental steps carried out on polyimide membrane before and after chemical etching of the samples. The results are discussed and compared with the literature.

**Chapter 5: Palladium plated polyimide**

In this chapter, the etched unirradiated polyimide is plated with palladium metal via electroless deposition. The palladium plated samples were characterised with SEM, TEM and FTIR techniques and their results are presented in this chapter.

The veracity of the hypothesis of this research is assessed based on the results obtained and discussions in chapter 4.

**Chapter 6: Conclusion and recommendation**

This chapter discuss the findings of the study and draw up a conclusion based on the results and recommendations for future work were highlighted.

**Chapter 7: References**

This chapter gives detail information of the materials consulted in this study.



## CHAPTER 2

### 2.0 LITERATURE REVIEW

#### 2.1 INTRODUCTION

Hydrogen as an energy carrier gas has been identified to possess some advantages such as its availability from a variety of sources such as fossil fuels and non-fossil fuels, and its high energy density properties. These properties, if harnessed, are expected to create a reliable global clean energy base with zero pollution and minimal negative environmental impacts. The major limitation to the hydrogen fuel application is the availability of infrastructure for large scale application, hydrogen distribution and storage facilities (Shoko *et al.*, 2006).

The ‘Hydrogen economy’ has been considered a future energy choice and proponents of this agenda consider it to hold great promise in addressing some of the aforementioned environmental and energy security problems. Although building an alternative economic base using hydrogen as an energy carrier has great potential to overcome several environmental and socio – economic problems when compared to the current hydrocarbon based (fossil fuel) energy carriers, fundamental problems such as safety (both in storage and transportation) and efficient method towards hydrogen economy remain a huge challenge (Nathan *et al.*, 2007; Shoko *et al.*, 2006; Nenoff *et al.*, 2006).

#### 2.2 HYDROGEN AS FEEDSTOCK FOR INDUSTRIAL PROCESSES

Pure hydrogen constitutes an important industrial feedstock material with a global annual consumption in hundreds of millions cubic meters (Paglieri *et al.*, 2002). In recent decades, there has been a steady increase in the demand for hydrogen for various industrial applications and also as an alternative energy carrier. As a replacement for fossil fuels, hydrogen as an energy carrier has the potential to promote energy sustainability with positive impacts on climate change abatement; energy safety and security, reduce dependence on

fossil fuel resources such as oil and create a robust platform for environmentally benign technology (Lu *et al.*, 2006; Amor *et al.*, 1999; Nenoff *et al.*, 2006). Technical challenges to developing cost effective hydrogen technologies include cost-effective hydrogen production, delivery and storage techniques for a commercially viable application such as in fuel cells. For industrial application, hydrogen purification systems such as pressure swing adsorption (PSA), cryogenic distillation, can be used to obtain pure hydrogen (Amor *et al.*, 1999), and this purity percentage is directly related to the industrial applications and separation techniques. Hydrogen is used as feedstock in the chemical, petrochemical and metallurgical industrial processes. Some, if not all of these industrial processes require pure hydrogen to serve as feedstock or intermediate species (Ramachandranraghu *et al.*, 1998; Lu *et al.*, 2007). In hydrogen fuel cell applications, the purity level of hydrogen is critical hence removal of impurities is an important condition for any preferred separation and purification method adopted for hydrogen production. To obtain pure hydrogen, factors like economics of infrastructure, durability of process and simplicity of technique must be considered (Hart *et al.*, 2003; Nenoff *et al.*, 2006). Hydrogen gas has been identified as a future alternative energy source thus preferred to fluid fuels and non-renewable energy sources due to its desirable qualities such as high energy density and efficiency.

Table 2.1 below outlines the different fuels and their corresponding energy density values

Table 2-1: Comparison of energy density of different fuels

Fuel	Specific energy (kW/kg)	Energy density (kWh/dm <sup>3</sup> )
Liquid hydrogen	33.3	2.37
Hydrogen (200 bar)	33.3	0.53
Liquid natural gas	13.9	5.6
Natural gas (200 bar)	13.9	2.3
Petrol	12.8	9.5
Diesel	12.6	10.6
Coal	8.2	7.6
NH <sub>3</sub> BH <sub>3</sub>	6.5	5.5
Methanol	5.5	4.4
Wood	4.2	3.0
Electricity (Li-ion battery)	0.55	1.69

Hydrogen on combustion with O<sub>2</sub> yields water with zero or near zero emission of gas pollutants (Lu *et al.*, 2007). However, the challenge to achieve a competitive and alternative hydrogen energy infrastructure which can compete favourably with other sources of energy will require an effective approach which is cheap, simple, reliable and sustainable for the purpose of separation, purification, storage and transportation of hydrogen gas (Amor *et al.*, 1999). Traditionally, methods used for hydrogen purification and separation are pressure swing absorption, cryogenic distillation and membranes. Based on economic implications as well as other factors, membrane technology is considered a cheap and affordable pathway approach to achieving hydrogen separation and purification from different sources. Several studies in thin film metal composites have been carried out to improve on the separation of



hydrogen in gas mixture using membrane technology. This will be discussed in subsequent section.

### **2.3 SOURCES OF HYDROGEN**

Hydrogen gas is present in different renewable or non-renewable resources such as mineral deposits and this has been a major boost towards hydrogen energy feasibility and utilization. The non-renewable sources are carbonaceous based i.e. fossil fuels, petroleum and natural gas while the renewable sources of hydrogen are wind, solar and water electrolysis (Johanna *et al.*, 2007). Hydrocarbons such as natural gas, oil and coal are the primary known sources of hydrogen (Hart *et al.*, 2003; Paglieri *et al.*, 2002).

### **2.4 HYDROGEN PRODUCTION**

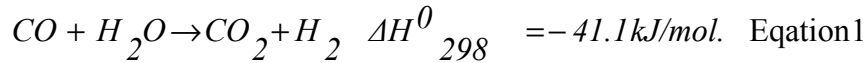
The choice of hydrogen production techniques is determined largely by the availability of resources and economic costs of the hydrogen gas from these resources. There are several techniques employed to produce hydrogen and these techniques depend on the source of hydrogen. Hydrogen can be produced from coal by gasification technology, while the hydrogen from natural gas can be produced by water gas shift reaction or steam reforming process. Other sources of hydrogen include the non-fossil fuels such as water biomass, wind and nuclear sources (Amor *et al.*, 1999). Metal hydrides such as sodium and lithium borohydrides have been reported to serve as storage material for hydrogen due to their high hydrogen storage capacity (Umegaki *et al.*, 2009). These metals hydride are known to be a safe and low-cost practical route to produce hydrogen via electrochemical mechanisms such as electrolysis. Hydrogen can be produced from coal by coal gasification and the hydrogen produced can be separated using membrane technology at high temperatures with low economic cost (Gray *et al.*, 2001). In considering the existing resources for hydrogen production, coal remains a viable resource because it offer the lowest production cost for hydrogen compared with other sources (Amor *et al.*, 1999).. Hydrogen production method such as coal gasification is a mature technology compared with other methods such as water electrolysis. Unfortunately, water electrolysis method of hydrogen production is not

appealing in terms of economics and technology blueprint to a level that could compete effectively with coal as a source of hydrogen at this stage (Shoko *et al.*, 2006). It is anticipated that if coal resources are properly harnessed by developing simple and cost effective methods, coal can serve as a source of hydrogen for energy and other hydrogen industrial application processes to meet the local energy needs as well as creating a clean and safe environment (Turner *et al.*, 2004). The preference for fossil fuel is largely due to its availability and existence of infrastructure for hydrogen production. Although fossil fuel remains a major source of greenhouse gas with several consequences resulting in ecological imbalance, the production of hydrogen gas alongside carbon sequestration technique can help mitigate environmental concerns by reducing carbon dioxide emission (Lu *et al.*, 2007).

#### **2.4.1 Hydrogen production by coal gasification**

Coal is found in large deposit in many countries including South Africa and has served as a source of energy to produce electricity (Shoko *et al.*, 2006). The coal reserve in South Africa is estimated at about fifty three (53) billion tonnes ([www.eskom.co.za](http://www.eskom.co.za)). Due to the large reserve of coal and its potential as a source of hydrogen through gasification technology, coal is expected to compete with other fossil fuels resources in the foreseeable future in the production of hydrogen gas. This is due to cost of the processes involved in producing hydrogen gas from coal and the abundance of coal resources which is predicted to last for several decades (Cleeton *et al.*, 2009). The gasification of carbonaceous and hydrogen-containing fuels such as coal has been proven to be one of the more effective methods of hydrogen production and is critical to the transition to a hydrogen economy (Stiegel *et al.*, 2006). Coal gasification technology is a high temperature reaction which is used to generate gas mixtures such as H<sub>2</sub>, CO<sub>2</sub>, CH<sub>4</sub>, H<sub>2</sub>S, H<sub>2</sub>O, CO and other trace elements and particulates (Shoko *et al.*, 2006). The process is carried out in the presence of O<sub>2</sub> or steam by partial oxidation of coal feedstock. To increase hydrogen content in coal gasification system, the water gas shift reaction (carbon monoxide and steam) is used to collect and catalyze the syngas produced from the gasified coal.

This reaction can be represented as:



Equation 1: Hydrogen production by water gas shift reaction

In general, coal gasification technology is classified based on the process of coal feed preparation and state on delivery. Other basis of coal gasification classification is the method of ash removal and the configuration of gas effluents after gasification. There are various available methods of coal gasification techniques and these are determined by factors such as intended use of product gases, coal morphology and availability and environmental regulations. These coal gasification methods can be the underground coal gasification (UCG) which is an in-situ coal processing technique to produce gas mixtures, the integrated gasification combined cycle (IGCC), Winkler process and fluid bed systems (FBS) (Shoko *et al.*, 2006).

Coal gasification (CG) has been in use for decades and hydrogen production from the gasification processes is suggested to show significant economic benefit by using membrane technology. By using the CG and membrane technology, hydrogen gas can be produced in a coal gasification and membrane technology process integration. Although CG is a commercial technology, it is not a widely practiced technology except in countries such as SA and China where natural gas or oil is less abundant and expensive (Shoko *et al.*, 2006). The economic cost of this method is high plus the negative environmental impact due to other wastes i.e. ash generated. The disposal of coal wastes has been reported to pollute soil and underground water due to some geological phenomenon. Hence, an alternative and available option for coal gasification is the use of underground coal gasification (UCG) process to replace the conventional mining method where coal is first mined before gasification.

In applying UCG, it is suggested that more hydrogen can be produced by employing an in-situ membrane technology through the separation of hydrogen gas produced along with other gas mixtures in gasification processes (Gray *et al.*, 2001). The increase in greenhouse gases

(GHGs) such as oxides of carbon, nitrogen, sulphur emission has prompted the need for an environmentally benign technology to reduce these gases and UCG technique addresses these problems considerably by reducing the atmospheric air pollution (DTI 2004). Gases released during UCG can be captured hence this technique can serve as an environmental remedial measure even though it can be on a short term approach. Although coal has a considerably low hydrogen to carbon ration, coal gasification technology has been suggested to address the continuous and unabated emission of GHGs by integration of processes to sequester carbon capture, reduce nitrogen oxides (NO<sub>x</sub>) and serve as a source of hydrogen (Shoko *et al.*, 2006). Some of the advantages of UCG process include the potential to put hydrogen production within realistic economic benefits, high coal utilization and also ensure the extraction of unmineable coal at depths or geologically difficult terrains. Another benefit of UCG method is that waste water can be used as feedstock alongside a decent waste handling mechanism through an underground ash dump technique.

The integrated gasification combined cycle (IGCC) is an advanced system process with different unit integrations. This technology is not cost effective because of the high maintenance requirement. Unlike IGCC, the Winkler method is an economical technique but energy intensive since it operates at high temperature. The fluidized beds used in Winkler method have good heat and material transfer between the gas and solid phases with the excellent temperature distribution, high specific heat capacity among other factors. The disadvantage of the fluidized beds used in Winkler method include the high dust content in the gas phase and the inconsistency between high reaction temperatures with good conversion efficiency (Shoko *et al.*, 2006; Warnecke *et al.*, 2000).

#### **2.4.2 Hydrogen production by methane steam reforming**

The methane steam reforming of fossil fuel accounts for about 80 % of the global hydrogen production (Nenoff *et al.*, 2006). This method of hydrogen production is a relatively less expensive practice but largely dependent on fuel cost due to the unstable cost of natural gas (methane) (Gray *et al.*, 2001). In this method, methane is converted to hydrogen, carbon

dioxide and carbon monoxide in the presence of steam. Steam reforming is an endothermic reaction with nickel catalyst and occurs at high temperature (700 °C - 1000 °C) and pressure (30 atm).

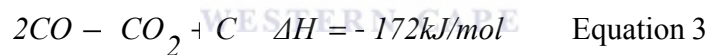
The reaction is represented below:



Equation 2: Hydrogen production by steam reforming reaction

The methane is fed through multiple beds of zinc oxide or activated carbon to prevent deactivation of the nickel catalyst used and also for the removal of sulphur impurities. To increase the conversion of methane to hydrogen, excess steam is added which also prevents thermal cracking and coking. This reaction has been reported to be susceptible to accumulation of carbon soot which leads to deactivation of the catalyst particle, causes blockage of the reactor tubes and fouling in downstream system (Gray *et al.*, 2001).

This can be represented by nickel-catalyzed Boudouard reaction:



Equation 3: Boudouard reaction

## 2.5 CHARACTERISTICS OF HYDROGEN

Several characteristics of hydrogen have been utilized in various industrial applications. Hydrogen is a colourless, odourless, non-toxic but highly flammable gas. The flammability and detonability limits of hydrogen are determined by the ratio of hydrogen/air mixture (Amor *et al.*, 1999; Sakintuna *et al.*, 2007). It has low boiling point (-252.87 °C) and its density in the gaseous state is 0.08988 g/L at low temperature 0 °C and pressure 1atm (Sakintuna *et al.*, 2007). Hydrogen can exist in different state such as solid, liquid and gaseous phase. These states depend on temperature and density (Zuttel *et al.*, 2003).

Chemically, hydrogen is a reactive element and has been employed in organic synthesis of hydrocarbon in the hydrogenation reaction process (Ramachandranraghu *et al.*, 1998).

## **2.6 USES OF HYDROGEN**

Hydrogen has been used as raw material feedstock in several industrial processes such as synthesis of ammonia, methanol and higher alcohols. It is also used in catalytic hydrogenation of unsaturated aromatic and aliphatic organic compounds, and removal of sulphur and nitrogen atoms from these organic compounds. The need to develop environmentally friendly energy fuel has resulted in intensive research on the application of hydrogen as energy carrier for automobile industries and generation of heat and power systems for households. Hydrogen energy is used in fuel cells which is an effective and efficient energy conversion system with significant reduction in the emission of air pollutants (Ramachandranraghu *et al.*, 1998). Hydrogen is used in the semi-conductor industry; in doped silicon wafers and chemical vapour deposition techniques and applied in hydrosulfurisation process of fuels, military application, scientific balloons and rocket fuel (Paglieri *et al.*, 2002).

## **2.7 HYDROGEN STORAGE AND TRANSPORTATION**

Prior to a successful application of hydrogen for energy purposes, finding the most economical, reliable and abundant source of hydrogen is imperative (Umegaki *et al.*, 2009). Beside this, there are several hurdles such as hydrogen storage and transportation in the drive towards a realistic hydrogen energy implementation. Hydrogen can be stored as a gas, liquid or solid depending on the end use. Therefore, for a material to be considered as an effective medium of hydrogen storage and transportation, such materials must show strong interaction hydrogen in a reaction process. This interaction can be in form of the ease of uptake and release of hydrogen gas by these storage materials. Hydrogen density and molecular size are

the two properties responsible for its limitations in safe and reliable storage methods (Sakintuna *et al.*, 2007).

Conventional storage methods for hydrogen include; (i) compressed gas (ii) cryogenic liquid and (iii) solid state systems and (iv) complex metals (Sakintuna *et al.*, 2007; Zuttel *et al.*, 2003). These storage methods depend on the source, amount to be stored and application as in industrial or domestic usage (Hart *et al.*, 2003; Amor *et al.*, 1999). The hydrogen storage capacity for commercialisation status is 6.5wt% and within a temperature range of 60°C to 120 °C. Hydrogen is mostly stored as solid in metals (as hydrides) due to the safety, weight and economics, and problems associated with liquid and gaseous storage techniques. Other storage systems such as metal hydrides, complex metal hydrides and carbon materials such as carbon nanostructures have been discussed by Sakintuna *et al.*, 2007.

Metal hydrides are a solid hydrogen storage technique and have been considered as a potential system to store hydrogen due to their high hydrogen storage density, ability to release hydrogen when heated and safety advantages over the gas and liquid storage methods. Hydrogen forms hydrides with metals such as Li, Ti, Be, B, Mg, Al, Na storing hydrogen at moderate temperature and pressure (Amor *et al.*, 1999; Ramachandranraghu *et al.*, 1998; Sakintuna *et al.*, 2007). These metals can form various metal-hydride compounds such as  $\text{LiAlH}_4$ ,  $\text{NaAlH}_4$  and  $\text{Mg}_2\text{NiH}_4$  among others due to their light weight property and the high number of hydrogen-metal atom ratio. Mg hydride has the highest hydrogen energy density (9 MJ/kg Mg) and combines with hydrogen at a high capacity of 7.6 wt %. Mg is a readily available metal and forms  $\text{MgH}_2$  with low cost and processing reversibility (Sakintuna *et al.*, 2007). Its use is limited due to its high storage temperature and reactivity with oxygen or air.

Metals differ in their hydrogen dissociation strength which depends on surface structure, morphology and purity. Metal and hydrogen combine in two ways to form hydrides. The  $\alpha$ -phase is a partial metal-hydride phase due to the absorption of some hydrogen atoms by the contacting metal, or the completely metal hydride  $\beta$ -phase (Sakintuna *et al.*, 2007). This study will not focus on metal hydride for hydrogen storage thus these materials will not be further reviewed.

**2.8 HYDROGEN PURIFICATION AND SEPARATION METHODS**

In recent time, a new global focus has been on system with excellent hydrogen separation and purification capacity. Such system is required to show hydrogen separation and purification efficiency output with minimal economic cost, and unique ability to produce highly pure hydrogen gas for energy application such as in fuel cells. Pure hydrogen is important in the hydrogen energy application and the hydrogen purity requirement is closely related with the type of separation and purification techniques (Paglieri *et al.*, 2002). Hydrogen is a by-product of many industrial reactions such as coal gasification (Nenoff *et al.*, 2006; Ilias *et al.*, 1996) hence hydrogen requires an effective separation and purification methods from the effluent gas mixtures. In most cases, the separation and reaction processes are often combined to remove the desired gas products from gas mixtures. For hydrogen separation, an integration of side reaction process using a membrane reactor can be used to alter equilibrium so as to increase hydrogen conversion and removal from the gas mixtures (Quicker *et al.*, 2000).

In reactions such as methane steam reforming, coal gasification and other industrial processes, there is a need to employ an efficient H<sub>2</sub> recovery technique. Such a technique when optimized can increase production and improve hydrogen purity yield. There are several traditional methods used to separate and purify hydrogen from the various industrial processes, and these methods have been considered as matured technology except for membranes techniques. Processes such as pressure swing adsorption (PSA), cryogenic distillation and membrane technology are well known separation techniques and will be discussed in the subsequent sections (Ilias *et al.*, 1996; Shao *et al.*, 2009).

**2.8.1 Pressure swing adsorption**

Pressure swing adsorption (PSA) is a conventional and advanced separation technique for hydrogen recovery from gas mixtures (Sircar *et al.*, 2000). PSA process of hydrogen separation can reduce impurities to a low level and increase the purity of hydrogen up to



99.9999% (Adhikari *et al.*, 2006). In PSA technique, hydrogen recovery depends on inlet pressure, level of impurities, purge gas pressure and hydrogen concentration (Adhikari *et al.*, 2006). PSA is an expensive method to operate and requires understanding of the gas-solid interaction and chemical compositions of adsorbents.

This method has been used for recovery of a wide range of gases in chemical industries. Some important applications of PSA are; steam-methane reformer off-gas (SMROG) for gas drying and solvent vapour recovery, fractionation of air and the refinery off-gas (ROG) for petroleum refinery of gases, separation of carbon dioxide and methane from landfill gas, carbon monoxide-hydrogen separation, n-isoparaffin separation, and alcohol dehydration (Sircar *et al.*, 2000). PSA is a high pressure system where the feed gas contacts with the solid in a packed column of the adsorbents such as activated carbon and zeolites. Purification of hydrogen from impurities can be enhanced depending on the adsorbent type (Sircar *et al.*, 2000). PSA process steps for hydrogen production involve adsorption, co-current depressurization, countercurrent purge and countercurrent pressurization. These cycles are often modified depending on the separation columns adsorbents. The adsorbents selected determine the extent of performance in PSA. Desorption of hydrogen from the solid adsorbent occur at lowered gas phase of the feed gas (Paglieri *et al.*, 2002).

### **2.8.2 Cryogenic distillation**

Cryogenic distillation is another technique employed to separate gas mixtures. This method uses a low-temperature separation process to isolate different gas components depending on their boiling temperatures. The advantages of cryogenic distillation are their large separation factors and process flow rate (Kinoshita *et al.*, 1981). It is energy consuming and yields hydrogen purity level of about 95% or less. Cryogenic distillation does not offer very high hydrogen purity gas compared with PSA (Sircar *et al.*, 2000).

Although the different hydrogen separation and purification techniques such as PSA, cryogenic have been discussed in previous section of this literature review, the subsequent section will focus on the membrane separation and its potential applications

**2.8.3 Membrane separation**

Membrane gas-separation efficiency is often governed in terms by its selectivity and permeability potentials. Permeability is defined as the ratio of mobility of a penetrating species across a membrane due to the pressure gradient (Shao *et al.*, 2009). Selectivity can be defined as the preferential adsorption of a specific species from a mixture. The selectivity and permeability properties of a membrane depend on the properties of the contacting species and membrane structure. In effect, such species can be gas or particulates depending on the membrane type and the desired products. These two phenomena determine to a large extent the efficiency of any membrane structure and also its potential application in the separation or isolation of any species. A membrane is a thin film or sheet of natural or synthetic material that is permeable to substances in either liquid or gaseous phase and selectively transports specific species across it. Factors such as selectivity potentials i.e. ability to separate a single desired component from the feed mixture, permeability strength i.e. flux of mass through a membrane per unit of area and time at a given pressure gradient, durability and mechanical tolerance in severe conditions like high temperature are important in the choice of the membrane (Nenoff *et al.*, 2006; Hassan *et al.*, 2006). Membrane investigation and development spans over a number of decades while their industrial application for gas separation and purification has existed for years. Several gases have been enriched and separated using the membrane techniques. They include; oxygen, carbon dioxide, methane, hydrogen (Powell *et al.*, 2006). Membrane systems offer competitive economic value, simplicity, compatibility with the environment, multiple applications for other gases and reactor set-up, high energy efficiency and excellent operational capacity and good unit recovery costs compared with other established separation methods. This technique still has the following limitations; restricted industrial application, gas diffusion kinetic ambiguity, low purity level and relatively new technology (Lu *et al.*, 2007).

The separation principle in membrane systems is governed by pressure and concentration gradients across a permeable barrier with or without selectivity while film microstructure determines membrane separation efficiency. For dense microstructure without pin-holes, high permselectivity can be achieved while thin film membranes exhibit high permeation rate. Thick membranes are generally more thermally stable (Yeung *et al.*, 1999). These film

structure properties determine the performance and choice of membrane either the polymeric or non-polymeric type. Gas separation membrane was first reported by Mitchell using hydrogen and carbon dioxide mixtures (Lu *et al.*, 2007).

Several other advanced membrane materials for hydrogen separation have been discussed by (Nenoff *et al.*, 2006; Paglieri *et al.*, 2002). Some of these membranes are (i) polymer, (ii) metal, (iii) silica, (iv) zeolites and (v) carbon. In this thesis, the work focuses on polymer-metal composite membranes, thus polymer and metal membranes will be discussed, and literature on similar materials will be summarized.

The diagram below is a representation of the direction of gas permeability and selectivity flow in a membrane.

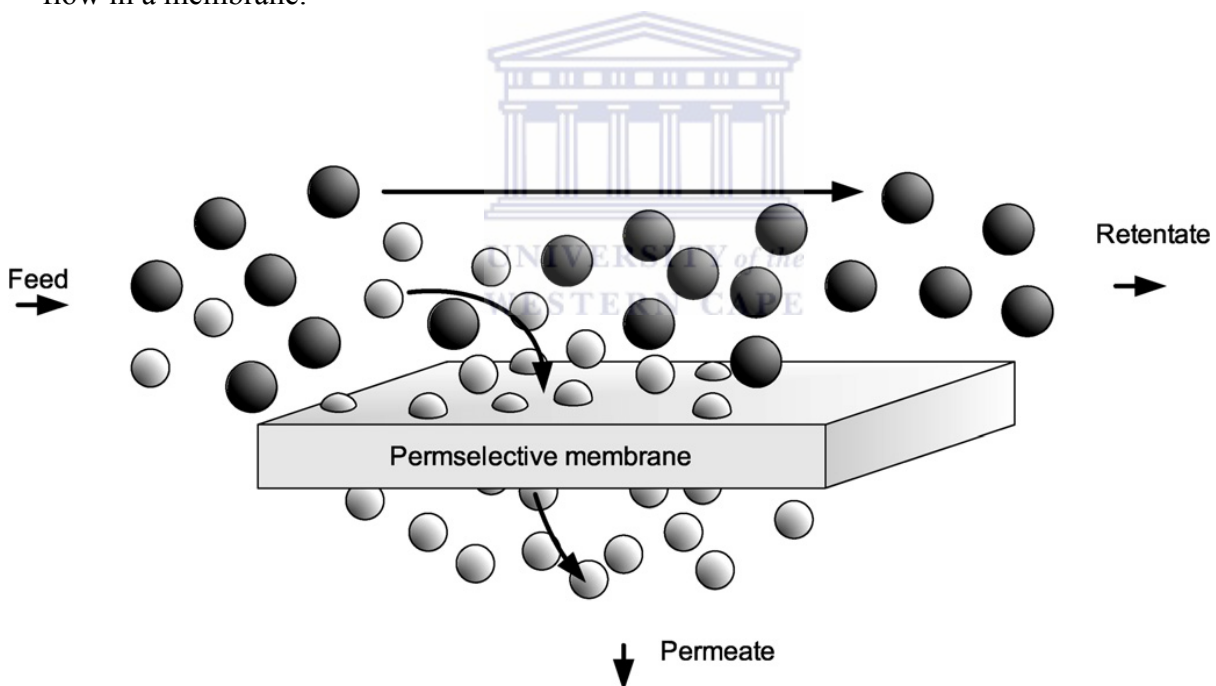


Figure 2-1: Schematic of membrane structure showing mechanism of separation

**2.9 TYPES OF MEMBRANES**

Membranes are grouped based on their chemical characteristics. They can be organic, inorganic and hybrid i.e. mixture of both organic and inorganic materials (composite). Organic membranes can be asymmetric in nature. The classification of membranes can also be based on their separation mechanisms such as Knudsen diffusion and solubility diffusion. These membrane separation mechanisms are governed by the presence of pores on the membrane surface after chemical or physical surface modification or during synthesis. Knudsen diffusion occurs due to collisions of gas molecules with the pore walls instead of intramolecular collisions. In Knudsen diffusion, gas mixture can be separated based on this difference in pore diameter of the separating barrier and the gas being separated or isolated (Sircar *et al.*, 2002; Malek *et al.*, 2003; Shao *et al.*, 2009). Solubility diffusion mechanism occurs due to the change in chemical potential gradient which is the driving force during the gas separation process. In solubility diffusion, gases are adsorbed via upstream boundary, diffused across the membrane before being desorbed in the downstream side (Shao *et al.*, 2009).

Inorganic membranes include mesoporous membranes, microporous membranes and dense membranes. These membranes are distinguished by their pore sizes and separation mechanisms. The mesoporous membranes have an average pore size of 3-5 nm range and are reported to show poor separation efficiency as their separation occur by Knudsen diffusion mechanism due to the large pore size distribution and high permeability properties (Li *et al.*, 1998). As for the microporous membranes, the pore sizes are less than 1 nm, therefore such membranes possess high selectivity due to the shape and size of the microporous structure. However, microporous membranes typically show low permeability (Li *et al.*, 1998). The dense inorganic membranes can be oxygen or hydrogen permeable depending on the properties and composition of their structures, most oxygen permeable membrane have ceramic properties while hydrogen gas is mostly permeable in metallic membranes. Examples of the metal used in the hydrogen metal permeable membrane are; palladium, vanadium, as well as alloys of these metals with transition metals.

Almost all viable hydrogen permeable membranes are PGMs based such as palladium metal. In the selection of a suitable membrane for hydrogen purification, the membrane must possess properties such as good operating temperature and pressure as these two conditions directly affect the separation performance of hydrogen gas. In addition, the composition of the feedstock gases to be separated, the material and fabrication costs of the membranes as well as the general process design, energy availability need to be taken into account (Wu *et al.*, 2005).

### **2.9.1 Polymeric membranes**

The organic membranes are generally derived from polymer materials. These types of membranes exist in different forms and usually are synthesised from organic sources. They have been under scientific investigation for gas separation application due to their unique chemical, thermal, mechanical and gas separation properties. The choice of polymeric membranes for application in industrial gas separation processes has been on the increase because they are readily available, economical, easy to process and bind in a composite configuration and can operate at low temperature (Nenoff *et al.*, 2006; Powell *et al.*, 2006). Polymeric membranes chemical functionality can be manipulated through the introduction of reactive groups along the polymer backbone structure to enhance adhesion and achieve specific gas permeability properties via surface modification (Shao *et al.*, 2009). The gas separation polymeric membranes must possess certain characteristics and the most important of the properties is to have good and preferential permeation for specific gases in gas mixtures and an ability to bind metal film layers. Several gas separating polymer membranes such as polyimides, polyamides, polycarbonates, polyanilines, polyarylates, polyacetylenes, poly (arylene ethers), poly (pyrrolones) and polysulfones have been reported in the literature (Powell *et al.*, 2006).

The two types of polymeric membranes are glassy such as polyimides or rubbery as found in poly-ethyleneterephthalate. Generally, both solubility and diffusivity factors determine the performance, selectivity and preference of polymeric membranes for different gases. The

glassy polymeric membrane is used to separate lighter gases such as hydrogen because of its small molecular size. Glassy polymers can generate high purity gas products due to their available small free-volume pores which have been suggested to allow the permeation of penetrating gases. The volume size of the polymer structure depends on synthesised polymeric material and operating temperature during gas separation. Unlike glassy polymers, rubbery polymers are used to separate heavy gases like CO<sub>2</sub> (Nenoff *et al.*, 2006). Gas separation through a polymeric membrane occurs by solution-diffusion mechanism model which can be represented by the equation below:

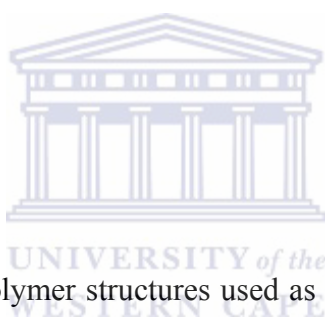
$$P = DS \quad \text{Equation 4}$$

Equation 4: Gas permeability equation

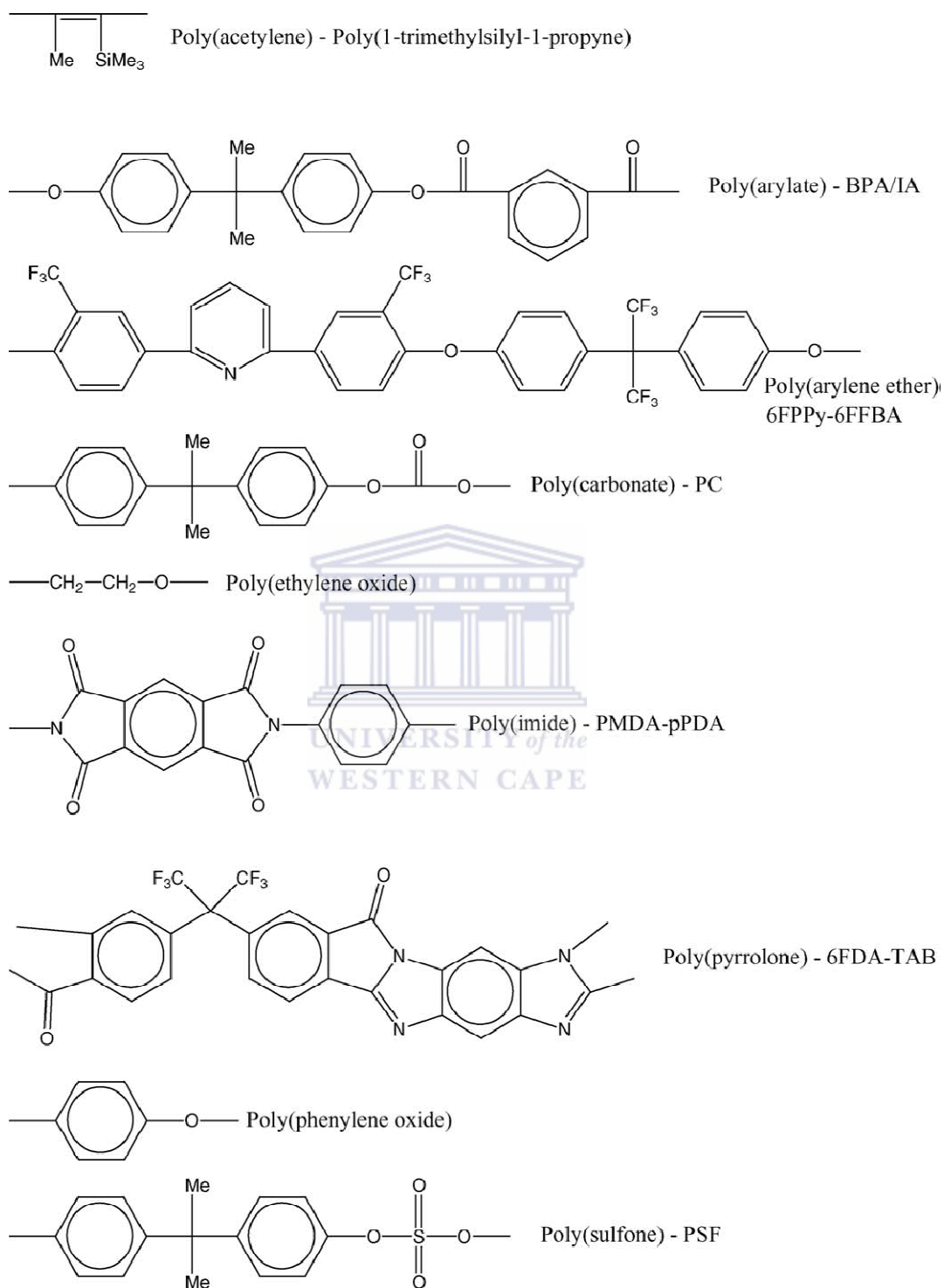
$P$  = permeability coefficient

$D$  = diffusion coefficient

$S$  = solubility coefficient



Some of the most investigated polymer structures used as organic membrane application are presented below.

Figure 2-2: Polymer structures (Powell *et al.*, 2006)

**2.9.2 Metallic membranes**

Metallic membranes have been an attractive type of membranes because they are commercially available. These membranes exist in various forms such as thin film layer in a composite structure (Lu *et al.*, 2007). The principles of gas separation by metallic membranes occur by processes of adsorption and desorption and not the pore size mechanism as in polymeric membrane structures. They can be applied in high temperature processes for gas separation (Nenoff *et al.*, 2006). In this section, the focus will be on palladium membranes since they have been proven to show unique affinity for hydrogen gas.

Among all the known metallic membranes structure, palladium (Pd) membranes remain the most effective and viable metal used to separate or purify hydrogen. This is due to their natural catalytic nature, high operating temperature and excellent permeability properties towards hydrogen gas (Nenoff *et al.*, 2006; Paglieri *et al.*, 2002). In considering palladium membranes for hydrogen separation purposes, it has been suggested that alloying palladium membrane with other metals will save cost, increase selectivity and permeability of hydrogen across the membranes structures (Nenoff *et al.*, 2006). Some of the sacrificial metals that have been alloyed with palladium metallic membrane include; Ag (Zhao *et al.*, 2000), Cu (Roa *et al.*, 2005), Ni (Nam *et al.*, 1999). Also, these alloys have been suggested to enhance the chemical stability of Pd based membranes (Paglieri *et al.*, 2002). Alloyed Pd based membranes serve to address some limitations such as cost and the hydrogen embrittlement phenomenon which will be discussed in the subsequent sections. It can also reduce the effects of surface contamination from impurities such as H<sub>2</sub>S, CO, hydrocarbon, which reduce metallic membrane efficiency and performance (Paglieri *et al.*, 2002).

**2.9.3 Composite membranes**

In view of the potentially infinite hydrogen selectivity that can be obtained from metallic membranes such as Pd based membranes, there is a continuous attempts to combine the high selectivity of Pd with the good processability of polymers in a metal-polymeric



nanocomposite membranes structure (Shao *et al.*, 2009). By depositing metallic film into a polymer matrix, it is anticipated that H<sub>2</sub> selectivity could be enhanced. Hence, fabrication of metal-polymeric nanocomposite membranes requires the polymer to possess high thermal stability since the infinite H<sub>2</sub> selectivity of the pure Pd membrane occurs at elevated temperatures (above ~300 °C). In principle, three different types of membranes have been suggested to remove hydrogen in high-temperature applications. These are microporous membranes, dense metal membranes or composite membranes. The composite membranes are considered to show high hydrogen permeability and selectivity, combined with good mechanical properties, metal composite membranes are often preferred due to their ability to undergo physico-chemical modifications (Li *et al.*, 1998). The subsequent sections of this study will focus on literature review of palladium composite in a palladium-polymer composite membrane for hydrogen separation.

Composite membranes for hydrogen gas separation and purification application have been in practice with the use of palladium-based membranes as thin walled tubes or free-standing foils (Maryam *et al.*, 2009; Yeung *et al.*, 1999). Hydrogen selective composite membranes consist of a thin metallic layer being deposited on a porous substrate. In addition, these composite membranes can exist as a combination or blend of one or more substrates of either organic-organic or organic-inorganic constituents with the desired properties and characteristics required for their application in gas separation technology (Hollein *et al.*, 2001). These supports have porous and conductive properties and exist in many forms such as stainless-steels ceramics and vycor glass are among the few supports that have been extensively alongside palladium metal (Lee *et al.*, 2002). Other reasons for the choice of these supports include economic cost and unlimited ability for hybrid materials as composite Pd based membranes supports (Paglieri *et al.*, 2002; Nam *et al.*, 2000). Metals such as nickel, vanadium and silver have been alloyed with palladium for hydrogen permeation tests as reported by Paglieri *et al.*, (2002). Composite membranes for hydrogen gas processes offer several advantages in the form of cost reduction, improved gas separation and permeation characteristics of membrane layers and provide the mechanical strength required for palladium based membranes (Quicker *et al.*, 2000).

Composite membrane applications have been used in catalytic reactor by chemical and petrochemical industries for purification purposes (Quicker *et al.*, 2000; Hsiung *et al.*, 1999). There are several parameters such as high temperature, which must be considered during gas separation processes for composite palladium membranes. During the synthesis of the palladium composite membranes, metals film must be thin, defect-free and thermally stable on the supports (Li *et al.*, 1999a).

Polymeric composite membranes have been adopted for gas separations as well although with little success due to the purity level required for the separated gases. Another issue is the need to understand the compatibility of hybrid materials, transport mechanism and adsorption-desorption properties of species across membrane structure are among the drawbacks of polymer/ metal composite material potentials (Paglieri, 2002). In developing composite polymer-metal membranes, it is important not to compromise the bulk-structural properties of the polymer structure and the metal film integrity during metal plating on the polymer surface. Other factors such as Pd thin film deposition with good high gas flux must be considered during the development of these polymer-metal composite membranes. Another challenge with thin film metal deposit is the fabrication of defect-free films for application under extreme conditions such as high temperatures and the presence of contaminants, which could result in metal lattice expansion (Li *et al.*, 2000). Polymeric-metal composite membranes must have good separation factors, highly stable in different operating environments and cost effective. Inorganic palladium composite membranes have been used by numerous researchers especially in hydrogen related reactions or gas permeability measurements (Paglieri *et al.*, 2002). Other form of membranes being studied for gas permeability and selectivity properties include composite metal-polymer matrix with modified electronegative specie such as fluorinated polyimide (Xu *et al.*, 2007; Rezac *et al.*, 1997).

Several studies have been reported on Pd composite membranes and their hydrogen separation or purification characteristics. Quicker *et al.*, (2000) prepared a Pd-alumina composite membrane and palladium-stainless steel for high temperature catalytic conversion of ethylbenzene to styrene and propane to propylene through dehydrogenation reaction. The

porous stainless-steel support membranes were coated by palladium using different coating techniques such as electroless, electroplating, and high velocity oxy-fuel spraying (HVOF), as well as the physical vapour deposition (PVD). The electroless plating of Pd on porous stainless-steel tubes resulted in uniform palladium layers deposition on the alumina and stainless supports and reported to yield the highest hydrogen permeance at temperature representative of hydrocarbon reaction (400 °C - 600 °C). The composite membrane also showed a good separation factor of hydrogen in a mixture of nitrogen and hydrogen gases.

A comparison of gas mixtures of hydrogen, helium and nitrogen gas for permeability measurement was investigated by Collins *et al.*, (1993). In their study, they developed a composite Pd-ceramic membrane by electroless plating technique. The palladium film thickness ranged from 11.4 µm to 20 µm. This composite membrane was subjected to temperature treatment between 450 °C to 640 °C and feed pressures from 160 to 2445 kPa. Hydrogen flux rate tested shows an increase from 20 % to 40 % at temperature up to 600 °C while hydrogen permeability measurement for the composite membrane was given as 3.23 x mol.m/ (m<sup>2</sup>.s.Pa) at 550 °C for a 11.4 µm Pd film thickness. The permeability test for helium and nitrogen gases indicated a poor flux rate under the same condition. Their work suggested that the increase in flux rate of hydrogen is influenced by elimination of surface contamination from the composite membrane structure at high temperature thus leading enhanced hydrogen gas permeation.

Shamsuddin *et al.*, (1996), developed composite Pd-ceramic membrane suitable for high temperature hydrogen separation performance by depositing Pd thin film on the microporous ceramic support. The deposited Pd film was observed to cover the pores of the support and the hydrogen gas permeability was monitored at elevated temperature and pressure. Under these conditions of high temperature and pressure, hydrogen gas permeability was reportedly high with no significant defect in membrane structure and the Pd-ceramic membrane thermal property showed good stability at high temperature as well.

Peachey *et al.*, (1996) in their work used groups (IV) b and (V) b metals as core central layer for palladium film deposition in a layer-by-layer sandwiched structure. The catalytic Pd metal

is deposited by electron evaporation in a vacuum chamber and ion beam sputtering techniques on the substrate. The result showed high hydrogen flux at elevated temperature (700 °C). There was no report of hydrogen separation from gas mixtures given except for argon gas which was used as a sweep gas for hydrogen across the composite membrane.

Li *et al.*, (1999b) used a mesoporous  $\alpha$ -alumina membrane as a support to deposit a 10  $\mu\text{m}$  thick Pd thin film by modified electroless plating combined with osmotic technique to enhance a defect-free Pd film. The hydrogen permeability performance of this membrane in pure hydrogen and nitrogen/hydrogen mixtures at different temperature was investigated. In their study, nitrogen was used as the sweep gas and found to have a proportional effect on hydrogen permeation rate. Although most hydrogen catalytic reactions occur at a temperature range between 300 °C to 600 °C, the composite membrane was tested for hydrogen permeability at 467 °C. Hydrogen permeability was found to increase with an increase in flow feed rate as well as at increasing sweep gas feed, in this case nitrogen gas.

Yeung *et al.*, (1999) prepared and examined Pd/vycor glass composites for kinetic, micro film growth and membrane performance for hydrogen permeation. Pd film thickness was manipulated by controlling the concentrations of Pd, hydrazine and ammonia solution as plating parameters and grain growths of the Pd seeds were obtained on the vycor glass support. A palladium film thickness of 1.6  $\mu\text{m}$  was obtained on the vycor glass while the membrane was annealed at high temperature (350 °C, 450 °C and 550 °C) in a flowing hydrogen gas. Their work reported high hydrogen permeability of the membrane which was observed at 550 °C with defects on the Pd surface film microstructure due to structural transformation and hydride phase formation of Pd membrane.

In the work of Jun *et al.*, (2000), palladium and palladium alloyed composite membranes on porous  $\gamma$ - alumina and stainless steel supports with metal film were synthesised. Pd was alloyed with nickel and niobium by modified chemical vapour deposition. Metal-organic chemical vapour deposition was used to decompose metals of interest from their organo-metallic substrates at a relatively low temperature. Hydrogen permeation was examined at 350 °C and 450 °C for the synthesised membrane. The Pd on  $\gamma$ -alumina support synthesised

membrane was observed to show low hydrogen permeation as compared with the palladium alloyed stainless steel support at 450 °C.

Bryden *et al.*, (2002) used a composite nanocrystalline Pd-Fe membrane deposited on porous stainless steel by pulsed electrodeposition to determine the effect of crystal size Pd-Fe on hydrogen permeability. Their work postulated a faster diffusion of hydrogen across nanocrystalline palladium membrane due to the presence of available free volume of grain boundaries in the composite membrane. The crystal size of the composite membrane was investigated for variation in hydrogen selectivity, flux rate and surface poison effects of the as-prepared membrane and hydrogen permeated membrane. The composite Pd-porous stainless steel was also evaluated for its conversion rate in hydrogenation of ethene to ethane. Hydrogen flux, selectivity and surface poison resistance was increased with the nanocrystalline Pd-Fe alloy. A stable reaction for ethene hydrogenation was achieved with the Pd-Fe nanocrystalline Pd-Fe alloy membrane compared with Pd-Fe alloy polycrystalline membrane.

Theon *et al.*, (2006) examined hydrogen purity, flux rate and resistance to sulphur contaminants in the hydrocarbon feedstock using Pd-Cu alloy. In their study, a composite membrane of Pd/Cu alloy deposited on zirconia coated  $\alpha$ -alumina support is developed with film thickness of 1.3  $\mu\text{m}$  Pd/Cu deposited via electroless plating with defect-free surface. The single gas permeability test was carried out at high temperature (365 °C) using hydrogen and nitrogen gases in a separate measurement and hydrogen gas permeation is reported to increase with increase in temperature upto an approximately flux rate value of 190 scfh/ft<sup>2</sup> which is close to the United States department of energy (USDOE) target value of 200 scfh/ft<sup>2</sup>.

Singh *et al.*, (2006) synthesised palladium-porous alumina composite membrane by laser surface treatment technique. This method was compared with other traditional methods like electroplating and physical vapour deposition to determine the most effective composite membrane for separation of hydrogen from gasified product gas. Pd/ $\gamma$ -alumina composite showed an increased separation of hydrogen in a high-temperature reactor system when a

mixture of hydrogen and different percentages of CO, CO<sub>2</sub> and CH<sub>4</sub> were tested by nitrogen sweeping across the membrane.

Okazaki *et al.*, (2009) demonstrated the influence of temperature on hydrogen permeability due to variation of grain size of Pd deposited on a porous alumina composite membrane. The phase change in the crystallinity of palladium on porous  $\alpha$ - alumina support at high temperature is suggested to have been due to the difference in structural and morphological arrangement of the thin film composite Pd/alumina, with a strong peak intensity observed at  $2\theta = 40^\circ$  while other diffracted but weak peaks emerged at  $48^\circ$  and  $68^\circ$ . These intensities indicated the crystal arrangement of deposited palladium and their lattice constant was changed. The grain size of palladium particles were reportedly increased from 44 nm to 150 nm at elevated temperature.



## 2.10 MECHANISMS OF HYDROGEN PERMEATION THROUGH MEMBRANE

Hydrogen permeation across a composite membrane can occur in two directions. It could be from metal film to support or vice versa and the route of diffusion can affect permeation rate of hydrogen gas across a dense or porous substrates (Liang *et al.*, 2005). Materials with improved gas separation and purification properties can be synthesised alongside membranes structures capable of achieving excellent gas selectivity and permeability. These materials can be fabricated by one or combination of techniques such as chemical vapour deposition (CVD), physical vapour deposition (PVD), magnetron sputtering, electroplating and electroless plating (Paglieri *et al.*, 2002).

Gas transport mechanism through metals membrane can occur by one or combination of these separation mechanisms: (i) Knudsen diffusion, (ii) surface diffusion, (iii) molecular sieving and (iv) solution diffusion. The type of membrane structure determines the separation mechanism for the species (Adhikari *et al.*, 2006). Diffusion of hydrogen across dense membrane materials depends on the chemical potential or concentration gradients of the feed gas. The difference in gases permeabilities determines gas separation across a membrane

(Meyer, 2006). There are several mechanisms that govern gases separation across membrane structures and each of these mechanisms will be discussed as follows:

### **2.10.1 Surface diffusion**

Surface diffusion occurs in parallel with Knudsen diffusion mechanism in which gas molecules are adsorbed on the pore walls and drift along the membrane surface due to the interactions between the membrane surface and gas molecules (Sircar *et al.*, 2002; Jaguste *et al.*, 1995).

### **2.10.2 Molecular sieve**

In molecular sieving, separation is governed by the size- exclusion principle. The mean free path of the gas molecules is relatively short compared to the pore size of the membrane and is described by Fick's law as follows:


$$j = D_t (c) \bar{v} \quad \text{Equation 5}$$

Equation 5: Fick's law

$j$  = mass flux.

$D_t$  = transport diffusion coefficient

$\bar{v}$  = concentration gradient.

$c$  = constant

### **2.10.3 Solution-diffusion**

The solution-diffusion separation is determined by solubility and mobility of the participating gas species in a membrane system and this depend on the free mean path of the separating species.

## 2.11 HYDROGEN DIFFUSION

The performance of a membrane is a function of flux or permeance and selectivity. The flux property of a membrane is defined as the cumulative transport of species such as liquid or gas across the membrane structures. Flux can be expressed as mass or mole per unit time per unit area. Permeance is defined as the flux per unit pressure of the difference between the upstream which is the retentate side and downstream also called the permeate side. The linear dependence of the hydrogen flux with the square root of pressure indicates that hydrogen flux obeys Sievert's law. The selectivity of membranes is expressed as their ratio of penetrating gas preference.

Thus the permeance rate of hydrogen gas across a membrane is represented by:

$$J = \frac{Q}{\delta} \left( P_f^{0.5} - P_p^{0.5} \right) \quad \text{Equation 6}$$

Equation 6: Permeance rate equation

Q= permeability at any given temperature

$\delta$  = metal film thickness

$P_f$  = hydrogen partial pressure in the feed streams

$P_p$  = hydrogen partial pressure in the permeate streams

The crystalline structure of a material can influence the rate of diffusion due to the presence of grain boundary components which act as diffusion pathways for hydrogen. In the case of crystalline membranes, hydrogen diffusion is determined by the atomic structure and the chemical nature of the membrane material and when compared to lattice diffusion, grain boundary diffusion is significantly faster due to the excess free volume in the grain boundaries (Bryden *et al.*, 2002).



**2.12 HYDROGEN PERMEABILITY**

Permeability can be expressed as the product of the diffusion coefficient and the solubility constant of the contacting species with membrane structure. Permeability is an important property of any membrane structure. Permeability is temperature dependent but varies inversely with the membrane thickness (Adhikari *et al.*, 2006). The hydrogen permeability follows the same phenomenon according to equation (4).

Hydrogen selective membranes have been grouped based on their preferential selectivity, flux rate, transport phenomenon and diffusion coefficient (Checchetto *et al.*, 2004). These selective membranes can occur as dense metallic, ceramics or thin films. Hydrogen is transported through the membrane in dissociated form hence dense metallic and ceramic membranes have been reported to show high selectivity for hydrogen gas (Ramachandranraghu *et al.*, 1998). Dense ceramic membranes have found numerous applications for hydrogen separation from mixed gas streams. Some advantages of dense ceramics membranes include ability to operate at high temperature, mechanical stability, and high hydrogen selectivity. However, these membrane show low hydrogen flux rates at gasified effluent and gas clean-up technology operating conditions (Hydrogen from coal programme, *external review 2005*). The selectivity of a membrane is defined by the product of ratio of diffusivity and solubility of gases across it and can be represented as:

$$\alpha_{A/B} = P_A/P_B = D_A S_A/D_B S_B \quad \text{Equation 7}$$

Equation 7: Gas selectivity equation

$P_A$  = Pressure gradient of A

$P_B$  = Pressure gradient of B

$D_A$  = Diffusivity gradient of A

$S_A$  = Solubility gradient of A

$D_B$  = Diffusivity gradient of B

$S_B$  = Solubility gradient of B

**2.13 POLYIMIDE**

Polyimides (PI) are nitrogen-carrying, condensed aromatic rings in a polymeric structure with high glass transition ( $T_g$ ) temperature and tight chain packing. They have functional groups such as phenyl, ether linkages (C-O-C), carbonyl groups (C=O) and C-N which act as electron donors and acceptors, and these properties are responsible for their excellent physico-chemical characteristics (Ramos *et al.*, 2003). PI being high-performing polymeric material possess important properties of inorganic materials such as rigidity, excellent thermal stability and chemical properties, high heat resistance and mechanical strength (Li *et al.*, 2004; Koros and Fleming 1993). The organic characteristics of PI include flexibility, ductility and ease of processability. These properties have been attributed to the wide range of studies on polyimides and also responsible for polyimides application in material science and for gas separation purposes (Nenoff *et al.*, 2006; Mishra *et al.*, 2003).

**2.13.1 Synthesis of polyimide**

The synthesis of PI occurs by condensation polymerisation reaction of the aromatic monomers of dianhydride and diamine components to yield polyamic acid in a two-step reaction process. This is followed by spin coating and thermal curing to obtain an insoluble polyimide film which varies in thickness and comes under different trade names (Lieberman *et al.*, 1996).

The synthesis of polyimide reaction schematics is presented below.

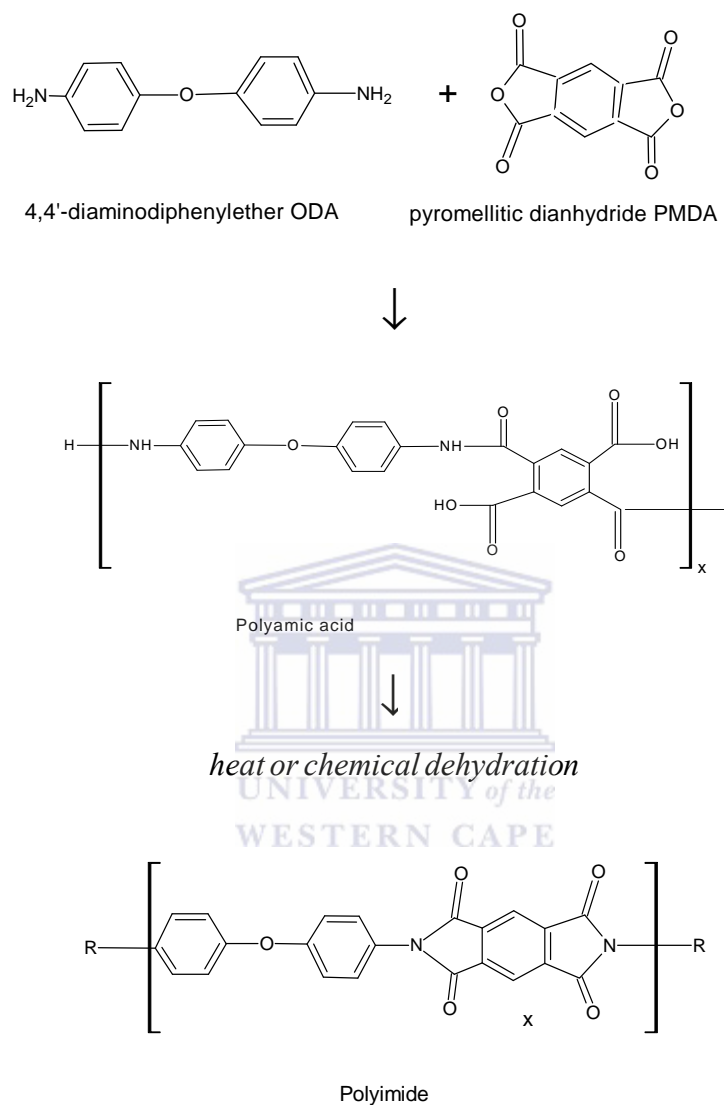


Figure 2-3: Reaction scheme for the synthesis of polyimide

In the synthesis of PI, the variation of the dianhydride and diamine monomers determines the final physico-chemical properties of PI. The synthesised PI can be linear or branched chain structures with amine or anhydride termination ends depending on starting materials (Park *et al.*, 2008a).

**2.13.2 Properties of polyimide**

PI compounds show unique thermal stability within temperature range of -296°C to +400°C (Trautmann *et al.*, 1996a), mostly amber in colour, they exhibit excellent stability against radiation compared with other investigated polymers (Trautmann *et al.*, 1996a). Polyimides are widely used as membranes for gas separation, and also in the microelectronics, photonics and optics industries due to their unique properties as polymers (Lieberman *et al.*, 1996; Stephens *et al.*, 2000; Kawakami *et al.*, 2003; Tran *et al.*, 2008; Mathakari *et al.*, 2009).

**2.14 METHODS OF POLYIMIDE SURFACE PRE-TREATMENT**

The use of polyimide as a support for metal deposition or dispersion of metals into its polymer matrix requires surface treatment to create vacant or active sites in the polyimide structure and to enhance metal film adhesion to the polyimide surface (Charbonnier *et al.*, 2003). Such sites can be hydrophilic or hydrophobic depending on the method of the surface treatment used. The surface modifiers enhance chemical interaction between the polyimide and metal species by interlocking processes, enhance polyimide-metal surface adhesion strength and increase surface roughness. Adhesion of metals to the polymer surface also determines the type of surface treatment chosen. The improvements of polymer surface wettability increase the adhesion properties while ion irradiation can lead to the exposure of the polyimide surface to improve adhesion due to the alteration of the polymer backbone structures (Park *et al.*, 2008b).

The choice of polyimide surface treatment depends on the purpose of application of the polyimide hence multiple surface treatments can be used simultaneously (Esinger *et al.*, 2007; Ramos *et al.*, 2003). Such surface modification techniques can be done by dry or wet approach. The dry methods such as plasma treatment, ion implantation and irradiation have been used as surface treatment of polyimide, whereas wet surface treatment approach such as chemical etching using NaOH and NaOCl solutions is one of the most used surface modification method for polyimide (Esinger *et al.*, 2007; Tran *et al.*, 2008). These surface

treatments techniques can be used to introduce desirable functionalities such as polar groups (Liang *et al.*, 2005) into PI structure, chemical fusion of more than one polyimide as in copolyimidization through cross-linking reactions (Wang *et al.*, 2008) and chloromethylation (Li *et al.*, 2008a; Xu *et al.*, 2007). Depending on the type of functional group being introduced into the polyimide structure, alkyl groups can inhibit the backbone chain packing and increase the free volume available for molecular transport which was observed to increase gas permeability (Nenoff *et al.*, 2006). The newly introduced functional groups in the PI are carefully manipulated to ensure that the bulk physico-chemical properties of the polyimide structure are maintained (Rezac *et al.*, 1997). Surface treatment of PI by wet or dry methods are important in the use of polyimide as a support in a composite membrane system especially for gas separation purposes (Ramos *et al.*, 2003). In the study of Wang *et al.*, (2008), a blend of polyimides with the addition of alkyl were synthesised to study their gas permeability and selectivity ratio. This study showed that gas permeability decreased with increase in addition of alkyl aniline substituent in the co-polymer blend during the reaction process.

For the gases investigated, it was reported that the permeabilities decreased due to the difference in the kinetic diameter of the gas molecules in the order of  $H_2 > CO_2 > O_2 > N_2 > CH_4$ . The effect of irradiation (2 MeV) was reported by Mishra *et al.*, (2003) to cause surface modification of PI leading to decrease in thermal stability and an increased intensity of absorbance of the existing bonds of the PI. Other properties affected by ion bombardment include chain scission, generation of free radicals and cross-linking (Park *et al.*, 2008b; Mathakari *et al.*, 2009; Bhansali *et al.*, 1995).

The overall objective of this study is to functionalise polyimide surface by using a simple and effective surface treatment such as alkaline etching method. This is expected to modify the polymer backbone compositions by molecular rearrangements, cross linking or chain scission across polymer structures. By using etching method, surface roughness is expected to enhance the adhesion of palladium thin film on the polyimide surface.

**2.14.1 Heavy ion irradiation technology in polyimide surface treatment**

Heavy ion bombardment on polymer films such as polyimide is a successful method of surface treatment and has been reported to promote structural changes in the physical and chemical properties of this material (Esinger *et al.*, 2007). Both bulk and surface properties of polyimide can significantly change under different fluence rate of ion (Mathakari *et al.*, 2009). Their work showed the characteristic overall effect of heavy ion irradiation on the polyimide back-bone structure by chain scission and carbonisation, cross linking and amorphisation with reduced intensities of functional groups. Among the importance of heavy ion surface treatment include creation of defined pores with various diameters after etching of heavy ion treated polymer films in alkaline solutions (Sciedt, 2007). Ion track etched polyimide can be applied for various applications such as aerosol collection, particle filtration in liquids and gas separation purposes. The surface of the polyimide was observed to be roughened after ion bombardment as observed by SEM studies (Esinger *et al.*, 2007).

Tian-Xiang *et al.*, (2009) studied the surface resistivity of polyimide by using Si ion to irradiate polyimide at 2 MeV. The spectral analysis after irradiation indicated a decrease in the intensity of functional groups of the irradiated species as the irradiation was increased. The irradiation was reported to change the crystalline property of the polyimide and reduced the lattice spacing from 4.37 Å to 3.93 Å. After irradiation, weakened poorly defined peaks were observed suggesting a partial destruction of the crystallinity property of the irradiated polyimide film.

The structural and surface morphology of heavy ion irradiated polyimide film was investigated by Mathakari *et al.*, (2009). The study indicated significant alteration of the surface properties in polyimide after heavy ion irradiation on the polyimide film and they concluded that processes of cross linking, molecular rearrangement and chain scissions occurred along the polyimide backbone structure which resulted in the physico-chemical modification of the polyimide film with characteristic properties due to the heavy ion bombardment.

**2.14.2 Etching processes in non and irradiated polyimide**

Etching of the irradiated polyimide film using sodium hypochlorite and sodium hydroxide for improved surface adhesion properties is considered promising due to several advantages such as simplicity of the procedure. During etching process, the imide rings of polyimide are attacked and opened up for incorporation of metal ions via ion exchange reaction in carboxyl groups and the formation of amide and sodium polyamate (Nurdan *et al.*, 2008; Shuxiang *et al.*, 2010). The etching of irradiated polyimide in alkaline solution requires extra caution because polyimide dissolves in strong alkaline solution such as high concentration Li *et al.*, (2004). The pH of the etching solution is an important parameter for controlling the degree of etching along the polyimide surface (Trautmann *et al.*, 1996b; Ferain *et al.*, 2003). The rate of polyimide etching increases as the pH and temperature of the etchant is increased. In effect, the pH values and the type of etching determine the shape and size of pores formed on the polyimide surface which can be cylindrical or conical in shape.

Nurdan *et al.*, (2008) used NaOH solution as a surface modification technique to enhance the deposition of silver metal on flexible polyimide membrane. This approach resulted in the metallisation of polyimide surface by the silver metal ion which was deposited after the polyimide was treated with NaOH solution. It was suggested that the NaOH solution to open the imide rings cleavage active sites exposing the imide ring for Ag ion exchange.

**2.15 POLYIMIDE AS GAS SEPARATION MEMBRANE**

Polyimide as a material for gas separation can be symmetric and asymmetric type of membranes. These two types of membranes can be composite (i.e. contain more than one blend of material) in nature but differ due to the presence of non-homogenous porous channels in the asymmetric types. In asymmetric membranes, the pore gradients at the top layer vary in size to the pore at the bottom layers. The symmetrical membranes can be non-porous, porous of channels or spongy structure depending on the method of preparation and applicability.

Marin *et al.*, (1995), studied diffusion of Cu and Ti into the polyimide after irradiation and annealing of the polyimide surface. The annealing temperature and irradiation were used as surface treatment techniques to alter the polyimide surface properties, and incorporate Cu and Ti metals into the polyimide structure. It was observed that Cu formed clusters near the annealed polyimide surface at temperature below the polyimide glass transition temperature. Cu cluster was observed to diffuse into polymer film at temperature above the polyimide glass transition temperature hence the study concluded that increase in annealing temperature can be responsible for metal impregnation into polyimide film. The irradiation of polyimide was observed to create depth profile of 500 nm on the polymer surface which resulted in the penetration of Cu cluster into the polyimide matrix. The Ti did not show good dispersion in the metal-polyimide after annealing and irradiation. This was suggested to be due to Ti high reactivity with oxygen which has been made surplus by the annealing and irradiation of the polymer surface. The non-diffusion of Ti was explained to be due to the strong bond between the Ti and carbonyl oxygen that was made available after annealing and irradiation of the polyimide. Mei-Hui *et al.*, (2009) demonstrated that the modification of surface functionality of polyimide membrane using silane and metal oxide can alter the surface composition thereby increasing polyimide adhesive strength. The study was to determine copper adhesion to the polyimide surface which showed an excellent adhesion of metal-polymer matrix and improved thermal stability.

A blend of polyimide structures studied by Lau *et al.*, (2003) for surface modification showed an effective use of alkaline etchant to promote Cu film adhesion on polyimide. The adhesion of Cu layer on the polyimide was attributed to the ease of surface modification of the BPDA-PDA polyimide, while 4,4'-(hexafluoroisopropylidene)diphthalic anhydride-4,4'-oxydianiline 6FDA-ODA polyimide type showed poor adhesion to Cu. (Park, 2008b), also studied the adhesion of Cu metal after oxygen ion bombardment on polyimide surface. They concluded that the surface modification of polyimide as a function of oxygen ion dose bombardment increased metal adhesion to the polyimide surface.



**2.15.1 Polyimide for gas permeability applications**

Several surface modification processes have been used to modify polyimide characteristics and test for their gas permeability capacity. Some of the polyimide gases permeability have been investigated using various approaches (Tsutomu *et al.*, 1996; Janes *et al.*, 1997; Matsui *et al.*, 1998; Mathakari *et al.*, 2009). In cases where poor gas permeability was observed, the densification of polyimide and low cross-linking of the polymer backbone structure have been suggested as the factors responsible for polyimide poor gas permeability.

Kawakami *et al.*, (2003) investigated the gas selectivity properties of asymmetric polyimide by induced shear stress. The molecular orientation of the synthesised asymmetric polyimide was used to assess its gas permeance efficiency. Comparisons between dense and asymmetric membranes show that the gas selectivities of the asymmetric polyimide membranes were similar to or greater than those of the dense composite membrane. Structural arrangement such as chain packing and thin surface skin layer of polyimide film was the two major phenomena used to describe the gas permeability of asymmetric polyimide.

Reza *et al.*, (1997) studied the effect cross-linking of polyimide by blending of different polyimides to examine the density and gas permeability measurement of the blended polyimides. They reported an improved gas permselectivity measurement after cross linking and higher chemical resistance of the blended polyimide. The density of the blended polyimide was also found to increase while their gas permeability is reduced by 50%.

Tsutomu *et al.*, (19996) reported the influence of UV irradiation on gas selectivity and permeability of polyimide. A benzophenone sensitiser was used on cross linked polyimide which was treated with UV irradiation, the UV treated polyimide was reported to show a decrease in H<sub>2</sub>/N<sub>2</sub> permeation as the UV radiation time was increased. Their study also reported that the H<sub>2</sub>/N<sub>2</sub> gas separation factor of the polyimide was increased after addition of the sensitiser.

**2.16 LIMITATIONS OF POLYIMIDE**

A major challenge is the poor selectivity of polymeric membranes compared with their metallic counterparts especially for gas separation purposes. PI show poor adhesion properties with metals due to the rigid molecular structure and the dominance of high surface (aromatic ring) energy by low surface (polar) energy in the surface phase. PI which is a glassy type of polymer has smooth surface which makes deposition of metals on polyimide surface very difficult (Ree *et al.*, 2000), thus there is a limit to metal incorporation into polyimide matrix for polymer-metal composite development (Ramos *et al.*, 2003; Li *et al.*, 2004). The adhesion of metal-polyimide system depends on the physical interaction, strength of chemical bond and mechanical interlocking of the metal-polyimide composite at the polyimide surface. Such chemical or mechanical interlocking can be induced by the use of surface treatment methods such as ions bombardments or chemical etchants. The chemistry of this metal exchange into the polyimide structure is suggested to occur at the electron deficient sites of the polyimide according to Park *et al.*, (2008b). Metals deposited on polyimide surface are predicted to bond at five and six fold ring sites of polyimide structure where the amide and imide functional groups are present. The metal-polymer interaction occurs by amide-imide rings opening after the polymer has been treated in alkaline solution (Ramos *et al.*, 2003; Lau *et al.*, 2003).

Polyimide being a high performance polymer plays a unique role as a support in a polymer-metal composite system for gas separation purposes. Several steps ranging from different surface modifications to polyimide synthesis conditions have been developed to improve the structural, chemical and physical characteristics for better performance in metal adhesion and gas permeability. This is because gas transportation property of polyimide has been associated to their structures. The surface modification of polyimides tailored by novel structural architecture and molecular rearrangement cannot be trade-off if their gas separation properties must be improved. From the literatures reviewed, there seems to be a common trend of multiple surface modification of polyimide film. The adhesion of metal to polyimide surface has not been proven to show good even after surface modification hence the need to examine depth profile of polyimide surface. In this study, a single step surface treatment by

alkaline etching is used to modify the polyimide film. This is due to the chemical availability, cost and the time frame for this study.

### **2.17 GLOBAL STATUS OF PALLADIUM**

In this section, the palladium as a metal will be reviewed as well as its application as a metal for hydrogen separation and purification. This section will discuss palladium beneficiation, palladium membrane and the effects of surface poisoning on the palladium membranes.

The global demand of palladium (Pd) has risen in the last decade primarily as a result of the increase in palladium aesthetic values as well as its applications in automobile and electronic industries. In addition, the hydrogen enrichment property of palladium metal due to its ability to purify and separate hydrogen gas from gas mixtures has been identified as a future potential to influence the increase in demand of the precious metal. Palladium has been employed in several chemical processes and 'green' application in automobile (converter) industries, and as membrane electrode in fuel cells (Brodgen *et al.*, 1970). Palladium is used in medicine, ornamental (jewellery), electrical appliances and source of foreign earnings for countries rich in mineral deposit of palladium (Antler *et al.*, 1987).

Pd as a transition and rare element, is inert in nature, and occurs naturally as ores of copper and nickel. This ore is soluble in aqua-regia (a combination of nitric and hydrochloric acids in ratio 1:3 respectively) and this acid solution mixture is often used to separate palladium from the ore. In terms of solubility, palladium can be dissolved in strong acids and strong bases. Palladium acetate and chlorides are the two important compounds often applied to prepare catalysts. Pd has excellent conductive properties and serves as a replacement for microcircuit components when alloyed with other metals. The versatility of palladium in nano-particulate state has been employed in a wide range of applications in catalysis and material sciences (Fleischmann *et al.*, 1989). Chemically, Pd is a good catalyst for hydrogenation or dehydrogenation reaction processes especially for hydrocarbon compounds (Sakintuna *et al.*, 2007).

**2.18 PALLADIUM STRUCTURAL CONFIGURATION**

Pd metal has a face-centred cubic (fcc) structure. The phases of palladium crystal arrangement can be in (1 1 1), (1 1 0) and (1 0 0) planes. Although most studies focus on the (1 1 1) plane, which is the most densely packed, and also identified as the plane with a higher hydrogen adsorption sites. In Pd (1 1 1) surface plane, there are four different potential adsorption sites for hydrogen atoms. In the case of hydrogen absorption in a palladium crystal lattice, the absorption occurs at octahedral interstice and the rate of absorption depends on amount of palladium atoms available for hydrogen attachment. This is closely related with the (fcc) adsorption phenomenon for hydrogen. Palladium can adsorb and absorb hydrogen, stores hydrogen at high density and form a stable palladium hydride (Stevens *et al.*, 2008).

Pd has two overlapping bands of allowed electron states. These are the 's' and 'd' bands. Other naturally occurring palladium is found in isotopic forms of Pd<sup>104</sup>, Pd<sup>102</sup>, Pd<sup>106</sup>, Pd<sup>108</sup> and Pd<sup>110</sup>. Palladium like other transition elements has variable oxidation states of 0, +2, +4 oxidation states. These oxidation states determine the physico-chemical characteristics of Pd, with the most stable of the oxidation states being +2 states which are very reactive and excellent catalytic properties. Palladium is reduced from +2 oxidation state to zero oxidation state during electroless plating of palladium on support. This zero oxidation state is considered as the active catalytic state obtained during palladium electroless deposition technique (Liang *et al.*, 2005).

Palladium alloyed with other metals like Cu, Au, Ag, etc as membrane structure have been employed in separation, ultra-purification and isolation of hydrogen gas from different gas mixtures where hydrogen is present. Metals such as silver (Ag) are often alloyed with palladium metal to prevent hydrogen embrittlement phenomenon and increase gas flux (Keuler *et al.*, 1999; Huiyuan *et al.*, 2004).

## **2.19 APPLICATION AND BENEFITS OF PALLADIUM MEMBRANE FOR HYDROGEN ECONOMY**

For hydrogen energy application, the role of palladium as a source of hydrogen storage and purification metal will be of enormous importance. Palladium will continue to be relevant in the drive towards the hydrogen economy goal. However, the overall applications of palladium have been limited by its cost as a precious metal.

Pd membranes have been used for numerous applications especially in the recovery of hydrogen from industrial processes. The enrichment of hydrogen gas from the stream of effluent gas mixtures, as well as in in-situ membrane reactor hydrogenation reactions are other aspect of Pd membrane applications. Pd membranes have also been applied to produce ultra-pure hydrogen for industrial applications such as in metallurgical processes and the manufacture of semiconductors. Pd metal has been in use for hydrogen gas selectivity for several decades and is the only known metal with excellent preference and an exclusively permeable medium for hydrogen gas separation and purification. Pd is capable of hydrogen uptake of about 900 times its own volume without Pd metal lattice deformation under high temperature and pressure conditions. During permeation processes, hydrogen readily dissociates on palladium surfaces. This unique property and affinity for hydrogen by palladium has made Pd the preferred metal for hydrogen related reactions in the chemical, automobile and petrochemical industries (Stevens *et al.*, 2008).

Palladium interaction with H<sub>2</sub> has been studied in hydrogenation catalysis with promising potential for hydrogen selectivity in separation and purification applications. The process of H<sub>2</sub> permeation across palladium membranes structure is a sequential path which follows H<sub>2</sub> adsorption, dissociation, diffusion through the metal lattice, recombination and desorption of molecular H<sub>2</sub> (Buxbaum *et al.*, 1996; Paglieri *et al.*, 2002; Klienert *et al.*, 2005; Zhongliang *et al.*, 2006a; Zhongliang *et al.*, 2006b). To achieve hydrogen gas separation potentials of palladium, Naotsugu *et al.*, (2005) proposed that a thin film of palladium be deposited on supports at various thickness ranges as low as nanometer scales. The thickness of Pd based membrane that is deposited on supports is proportional to the hydrogen flux and serve as a

cost benefit measure for Pd metal. This is because Pd membrane has been fabricated at different thickness of microns range especially with alloying with other metals (Thoen *et al.*, 2006).

## **2.20 PALLADIUM COMPOSITE MEMBRANES**

The membranes used for supporting palladium metal are mainly dense structural configuration such as ceramic supports. Other supports for Pd metal layer deposition include stainless steel, vycor glass among others but mostly porous. The use of porous substrates as a support for the Pd metal layer in a membrane system is to improve the adhesion of the deposited metal layer on the support surface and also reduce Pd metal thickness to obtain a high gas flux rate (Li *et al.*, 2000b). Such porous surface can be macro porous with pore size less than 5nm, mesoporous materials have pore size range between 3-5 nm and or microporous have pore size less than 1nm (Pan *et al.*, 2003). Economic and mode of application of the fabricated palladium membrane determines the choice of these supports for any industrial usage.

Among the different metallic membrane techniques used for H<sub>2</sub> purification, the use of semi-permeable membranes has gained an increasing interest because of its low cost and eases of processability. This separation technique requires membranes that can withstand contamination and possess good thermal integrity and mechanical strength under high temperature conditions (Paglieri *et al.*, 2002). Pd membrane applications for hydrogen processes (i.e. separation, purification and possibly storage abilities) have witnessed increased interest. Pd is often alloyed with other metals e.g. silver, titanium, vanadium and niobium, copper and gold. Alloying of Pd with these metals has been found to improve the efficiency as well as the enhancement of Pd membrane set-up for hydrogen. These membranes are often employed in in-situ membrane reactor processes at high temperature for hydrogenation and dehydrogenation reactions. Palladium based membrane has remained the preferred metallic membrane for hydrogen because Pd membranes allows H<sub>2</sub> permeation and can be used to produce, separate and purify hydrogen gas for the purpose of hydrogen enrichment (Paglieri *et al.*, 2002; Zhongliang *et al.*, 2006a; Zhongliang *et al.*, 2006b). Despite

the choice of palladium to separate hydrogen, the cost of palladium being a precious metal remains a huge challenge hence the development of Pd-composite membranes. Alloying Pd with other metal will reduce the Pd thickness. Pd-based membranes have high temperature resistance due to the metallic properties of palladium metal. In a Pd-composite membrane, ultrathin layer of the Pd is deposited on supports (Nam *et al.*, 1999). Such Pd-layer must be thin and defect-free so as to enhance hydrogen permeability or permselectivity outputs. The permeation of hydrogen gas is controlled by the diffusion of atomic hydrogen through the palladium membrane and not by the dissociative adsorption of hydrogen molecules on the membrane surface (Okazakia *et al.*, 2009). This implies that hydrogen permeability and high hydrogen selectivity can be achieved with the Pd-based membranes. Also, ultrapure hydrogen can be obtained by separating hydrogen from the hydrogen-containing mixtures and equilibrium switch for dehydrogenation reactions can be realised by continuous removal of hydrogen from the reaction zone using these Pd-based membranes (Li, 1998). In such palladium membranes, the thickness of the metal on the supports determines the hydrogen flux rate (Uemiya *et al.*, 1991) and the rate determining step for hydrogen diffusion is the permeation of hydrogen gas through the bulk of the Pd film membrane (Li *et al.*, 2000a).

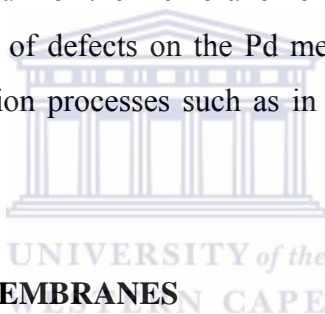
One of the advantages of Pd based membranes is their high temperature and reaction capability which make Pd membranes most suitable for hydrogen gas separation. These membranes can be used to achieve high level of hydrogen gas permeation over a prolonged time. The permeation of hydrogen across Pd composite membrane occurs with good separation factors. Other advantages include stable thermal cycling and resistance to poisoning by the common contaminants (Thoen *et al.*, 2006).

A major drawback in the application of Pd composite membrane metal is poor adhesion on polymer film surfaces. Also, Pd based membrane undergoes phase change of palladium lattice in hydrogen atmosphere at lower temperature as in hydrogen embrittlement. Other limitations which will be discussed in subsequent sections Pd susceptibility to chemical attack such as surface poisoning by other gases during gas separation (Nathan *et al.*, 2007; Paglieri *et al.*, 2002).

This study is aimed to address and examine the adhesion strength of palladium metal film layer deposited on etched polyimide surface performed by peel test.

### **2.21 DEFECTS OF PALLADIUM MEMBRANE**

One of the major defect in Pd membrane is the irregular thermal coefficient expansion between the Pd metal and the membrane substrates due to their difference in thermal properties. Another source of defects on Pd composite membranes occur when such membranes are used at high temperature for catalytic and separation reactions such that carbonaceous impurities may be deposited on the membrane surface. Such impurities can accumulate and diffuse into the bulk of the membrane hence leading to formation of defects in the membrane. A third source of defects on the Pd membrane could be from the use of impure chemicals during deposition processes such as in plating solutions as in electroless method (Li *et al.*, 1999b).



### **2.22 LIMITATIONS OF Pd MEMBRANES**

A key problem with Pd membrane for hydrogen gas separation in a gas mixture is surface poisoning or chemical damage suffered from associated gas pollutants such as H<sub>2</sub>S, CO, steam and other organic gases like methane, ethylene. This is because hydrogen is bounded up with other gases and these gases reduce the rate of permeation across palladium membrane by forming compound of palladium. Another limitation of Pd membranes is hydrogen embrittlement phenomenon due to Pd phase change from  $\alpha$ - $\beta$  phase in hydrogen atmosphere at lower temperature <300°C (Uemiya *et al.*, 1991; Sakamoto *et al.*, 1997). The presence of contaminant gases limits hydrogen permeation across Pd membranes. This results in the poor hydrogen gas selectivity due to the reduction in the free volume size of the Pd membrane after poisoning by these gases, hence the efficiency of Pd based membranes for hydrogen processes is reduced. The poisoning of palladium surface by impurities is in general related to



the chemisorption of contaminants along with the formation of compounds of the contaminants with the palladium metal.

Alloying of Pd membrane with other metals to adjust the crystal structures and lattice arrangement of Pd metal and the synthesis of nanophase or amorphous metal membranes has been used to address these limitations. The effect of the presence of trace of sulfide compound on reduction of hydrogen permeance across the Pd and Pd coated membranes was investigated. These membranes were reported to rupture in the presence of gas contaminants with palladium sulfide film formed on the surfaces of Pd membrane due to the presence of hydrogen sulfide in a gas stream and reduced the hydrogen flux rate by 25 % across the Pd membrane (Nathan *et al.*, 2007; Huiyuan *et al.*, 2004; Kawijara *et al.*, 1999).

A detailed overview presented by Unemoto *et al.*, (2007) gave a summary on the effect of various gas mixtures with hydrogen gas when tested for hydrogen permeability performance in Pd and palladium alloyed membranes. Some of these limitations associated with the selectivity and permeability of hydrogen across palladium membrane are discussed below. It is worthy of note that the effects of these gases impurities on Pd membrane hydrogen permeation and diffusion capacity are dependent on the methods of plating and the precursor of the precious metal used as discussed by (Uemiya *et al.*, 2001).

### **i. Carbon monoxide**

Carbon monoxide (CO) hinders the permeation flux rate of hydrogen gas through Pd membrane when CO is present in a gas stream. Studies by Amandusson *et al.*, 2001 and reports from Li *et al.*, 2000b indicated that the presence of CO gas at different temperatures (below 300 °C) and at increased concentration of carbon monoxide lowers the rate of hydrogen transport across palladium membrane. Their study revealed the influence of film thickness of the Pd membrane upon the structure and transport mechanism of CO and hydrogen. CO acts as an inhibitor to hydrogen permeance on Pd based membrane, but it is a reversible process thus hydrogen permeance can be reasonably restored after the removal of CO (Uemiya *et al.*, 2001).

In the work of Li *et al.*, (2000b), CO gas fed into the permeator at lower feed flux showed a decrease in hydrogen gas permeation through the Pd membrane and they concluded that when a mixture of hydrogen and CO gas were permeated through Pd membrane, a decrease in hydrogen diffusion occurred. They suggested that the decrease in hydrogen permeation was due to the adsorption of CO gas on the Pd surface thereby decreasing the available channel of hydrogen passage hence reducing the rate of diffusion of hydrogen through the bulk Pd membrane.

### **ii. Water vapour poisoning**

At increased concentration, water vapour decreases hydrogen permeability across Pd membranes. Steam is adsorbed on Pd membrane surface and unlike CO and CO<sub>2</sub> gases, hydrogen recovery is possible with Pd membrane after a gradual removal of steam as reported by Li *et al.*, (2000b), and this agreed with the result obtained by Jung *et al.*, (2000). They suggested that the reduction in hydrogen permeation may be caused by competitive adsorption between hydrogen and steam on the surface Pd active sites. This process makes steam surface poisoning of Pd membrane a reversible reaction. The concept of irreversible reaction of palladium and steam is due to the bond formation on Pd surface after exposure to steam. It was explained that the surface diffusion-dissociation of hydrogen was due to higher operational temperature was responsible for the reversible reaction of steam poisoning of palladium surface (Huiyuan *et al.*, 2004).

### **iii. Coke poisoning**

Carbonaceous matters such as hydrocarbons are the known source of carbon, which are dissolved in palladium thereby reduce hydrogen gas permeability rate. Several conditions such as reaction parameters and the compositions of the feedstock determine the amount of carbon deposited on the Pd membrane. This has been explained to result in the decline of the Pd hydrogen permeability properties. Coke retards the catalytic activities of the Pd membrane surface, decreasing hydrogen permeability and permselectivity at high temperature (Li *et al.*, 2000b).

**iv. Sulphur poisoning**

Organic chemical reactions especially those of volatile organic compounds often result in the release of sulfur and other sulfur related compounds i.e. oxides and sulfides. Sulfur from H<sub>2</sub>S gas inhibits the performance of electroless plated Pd membrane. The Pd lattice constant has been reported to expand on exposure to sulfur poison which results in the formation of cracks on the Pd membrane surface (Uemiya *et al.*, 2001) This lattice constant expansion can alter the physico-chemical properties of the Pd metal and reduce the permeability property of the Pd membrane structure (Escand'on *et al.*, 2008). As a result, there is partial or complete inhibition of the prospective active sites for catalytic reactions in the presence of sulfur. Palladium catalytic property as investigated by (Escand'on *et al.*, 2008) using different supports concluded that zirconia supported palladium performs better in methane compared with alumina, silica and titania supports.

**v. Hydrocarbon poisoning**

Pd membranes can suffer surface poisoning due to the presence of contaminant gas from different sources. Hydrocarbon sources with product gases like oxides of carbon and sulphide have been the major challenge in Pd membrane surface poisoning. This is because hydrocarbons serve as the main source of hydrogen gas, and the carbon and sulphide gases in the hydrocarbon mixture inhibits hydrogen permeation through Pd membrane which is vital for hydrogen separation and also critical for optimal performance with minimal effects of the gas poisons.

Methane is one of the known volatile organic molecules which require high temperature reaction for its oxidation to generate hydrogen and carbon. Pd-based membranes can be used for the separation of H<sub>2</sub> from refinery off-gas streams, which often contain CH<sub>4</sub> and other hydrocarbons in considerable concentrations (Li *et al.*, 2008b). The presence of methane in gas streams has been shown to reduce H<sub>2</sub> permeation through Pd-based membranes. The presence of hydrocarbons such as methane in gas streams forms layer of palladium carbide (PdC) on Pd membrane surfaces, and this inhibits H<sub>2</sub> dissociation and recombination

reactions on the Pd membrane surface through adsorption phenomenon thereby decreasing the H<sub>2</sub> permeation rate (Li *et al.*, 2008b). Li *et al.*, (2008b) focused on the use of methane gas at different concentrations to investigate the effects of CH<sub>4</sub> on hydrogen flux in Pd membrane. Their study indicated that the permeability rate of hydrogen through Pd membrane was temperature dependent as they observed a decrease in hydrogen permeation rate as temperature increases when methane gas is fed into Pd membrane system. They proposed that methane served as a source of carbonaceous deposits on Pd membrane which lowers the hydrogen transport across the membrane. Jung *et al.*, (2000) explained that heating of the Pd membrane at high temperature in air after contamination can serve as a mean of regeneration of the Pd or Pd alloyed membrane after exposure to gas contaminants.

### **2.23 METHODS OF DEPOSITION OF PALLADIUM ON SUBSTRATES**

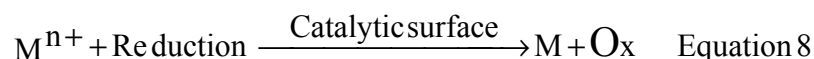
Palladium membranes have been the subject of research due to their numerous application potentials in hydrogen gas separation and purification, sensor and sorption tests, various hydrogenation reactions mainly for unsaturated hydrocarbon compounds, and Pd catalytic properties. This versatility of palladium has been the basis of scientific enquiries for the purpose of optimization especially for hydrogen separation and purification from gas mixtures. Specifically, the quest to increase hydrogen permeation has been responsible for the fabrication of Pd-composite membranes using various supports and also evaluation of the Pd alloyed membranes to analyse their gas separation properties.

The need to increase hydrogen permeation, understand hydrogen gas separation in gas mixtures, fabricate thin film Pd-metal composite membrane and study their hydrogen flux rate as well as other properties of the Pd membrane system after exposure to gas mixtures has led to the development (for comparison purposes) of different deposition techniques. These methods include; thermal deposition, sputter coating, chemical vapour deposition, electrochemical plating and electroless plating. Electroless plating (EP) technique has been the conventional and most accepted method of metal deposition on supports. EP offers better approach because of its ease of application and simplicity compared with other plating techniques (Rothenberger *et al.*, 2004).

In considering the task of achieving uniformity of palladium metal deposition on polyimide surface, this study will focus on the use of electroless plating technique. Electroless plating has several advantages which includes economic cost and easy alternative to other methods of metal deposition on supports. This section will review the electroless plating technique and discuss its principles

### **2.23.1 Electroless deposition method of palladium on substrates**

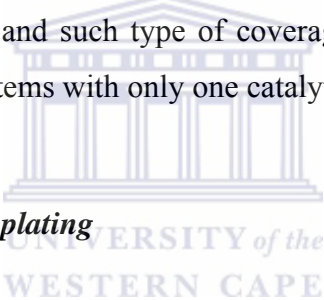
Electroless plating (EP) deposition is one of the conventional methods of metallization on different substrates. EP is an electrochemical process which involves a reduction–oxidation reaction with cathodic metal deposition and anodic oxidation of reductants due electron transfer across the metal substrates interface (Ye *et al.*, 2007). Electroless plating is a heterogeneous reaction process with metal deposition occurring at the solid–liquid interface between the plating surface and the solution. EP is an auto-catalytic procedure where the plating mechanism of metal ions by reduction occurs on the targets referred to as supports or substrates in an appropriate reducing agents i.e. hydrazine or hypophosphate. Palladium electroless plating of etched PI sample was conducted in alkaline solution in the presence of hydrazine (N<sub>2</sub>H<sub>4</sub>) as the palladium metal reductant. Hydrazine is a better reducing agent in alkaline solution rather than acidic solution. Hydrazine ensures that the high pH value reduces losses of the metal precursor, acts as stabilizer for the plating solution and facilitates high cation exchange. The stability of the metal complexes increase the Pd<sup>2+</sup> → Pd<sup>0</sup> turnover rate, and ensure the correct potential difference for the oxidation of the reducing agent (Williams, 2009). The reaction below represents the process of metal electroless deposition on a support.



Equation 8: Reaction scheme of electroless deposition

This process of metallization on substrates affords the utilization of inexpensive and simple approach for gas separation and recovery processes. Electroless deposition technique is attractive for fabricating thin film of uniform metal coatings on various types of substrates in the absence of an external electric current. EP requires a compromised balance between the plating conditions of the electroless plating solutions and the stability of the supports (Maurizio *et al.*, 2006).

For metal deposition in the electroless plating technique, the dipping of supports for Pd deposition can result in a two sided such as a sandwiched structure or one sided Pd metal plating on the substrates. The fully immersed substrate in the plating bath results in Pd metal plated on both sides of the support giving a “sandwich-like” structure. On the contrary, when the support floats in the solution of the plating bath, palladium is plated only the surface in contact with the plating solution and such type of coverage could be useful in the field of catalysis for the fabrication of systems with only one catalytic surface (Maurizio *et al.*, 2006).



### **2.23.2 Conditions for electroless plating**

For a successful electroless plating technique, parameters such as temperature, pH, plating bath composition and the type of reducing agent determine the metal grain size of deposited metal on the substrate surface and the gases evolved during the plating process (Kilicarslan *et al.*, 2008). In most electroless plating processes, gases such as nitrogen, hydrogen and ammonia can be bubbled out during plating and this may reduce the uniformity of metal plating on support and the overall completion of plating process in the bath. It is therefore imperative to understand the chemistry of the metal precursors, support to be used and the reducing agents of the electroless bath composition metal plating technique (Cheng *et al.*, 2001). There are two commonly used reducing agents during electroless plating. These are the hydrazine and the hypophosphate solutions. Hydrazine is a better metal reducing agent because it does not generate hydrogen gas, and can be used in basic medium. It is less stable and must be used when freshly prepared. Hypophosphate is more stable than hydrazine but has shown to be less attractive reducing agent during electroless plating (Maurizio *et al.*, 2006).

In EP technique, the surfaces of supports to be plated undergo surface activation which is a seeding process followed by the sensitisation or nucleation process before the metal plating. These two steps are essential during electroless deposition procedure. The activation process involves the use of acidic SnCl<sub>2</sub> solution to activate the surface of the support so as to create active sites for palladium metal exchange during electroless plating. This is followed by sensitisation of the supports where the supports are immersed in acidic PdCl<sub>2</sub> solution to seed the surface of the support and initiate the exchange of SnCl<sub>2</sub> metal by PdCl<sub>2</sub> metal present in the activation solution (Mardilovich *et al.*, 1998). The activation and sensitization step is followed by rinsing the supports in deionised water after each activation and sensitisation procedures. From literatures, other activation method that have been reported include; ion implantation (Bhansali *et al.*, 1995), laser-assisted decomposition of spin-coated metal-organic films, (Zhang *et al.*, 1997), photo-aided or immersion of supports in a Pd metal solution for ion exchange process (Li *et al.*, 2004; Shuxiang *et al.*, 2010), sol-gel method (Zhao *et al.*, 1998) and by induced osmotic technique (Li *et al.*, 1998), as well as metal organic chemical vapour deposition (MOCVD) technique (Huang *et al.*, 2007).

In the case of using a polymer substrate, it is necessary to achieve good adhesion of metals on the polymer surface. Thus pre-treatment such as surface modifications of support as in polyimide (PI) film is required before the electroless deposition of Pd metal on the polyimide surface. To this effect, alteration of the polymer surface morphology by chemical or physical etching methods is often adopted to improve adhesion of a metal film to substrate surface (Li *et al.*, 2004). Several attempts have been made to advance the adhesion property of the PI surface using electroless plating techniques but with little success. Attention is also being given to synthesis of polymer structure with unique chemical and physical properties so as to achieve functionalized material with desired compositions. Physical processes such as plasma grafting, UV laser treatment and ion-beam irradiation require somewhat expensive equipments (Naddaf *et al.*, 2004).

In the work of Maurizio *et al.*, (2006), palladium metal was deposited by electroless technique on anodic alumina support in an optimized plating bath composition. The stability and adhesion of metal on anodized alumina membrane was considered in the choice of the plating bath composition and the optimized time. The amount of Pd metal plated on the

support was determined by complexometric titration method. Their work established that the effect of plating time on membrane resulted in notable damage of membrane due to the alkalinity strength of the plating bath. It was concluded that varying alkalinity of bath affects the stability of membrane since high alkaline solution dissolved the membrane structure. Also, at low high acidic solution, Pd layer was not uniformly deposited on the membrane. This was attributed to non-stability of the plating bath under acidic condition.

Robertis *et al.*, (2008) investigated the influence of plating time and concentration of plating bath in the electroless deposition of alloyed Pd-P metal on carbon steel. They assessed the quality of Pd-P film layers formed at different plating times and reducing agent concentration. It was observed that an overall increase of hydrogen evolution reaction activity by Pd adsorption/desorption process was enhanced at low phosphorus content in the Pd-P alloy. This was attributed to that phosphorus acted as a reducing agent and allowed for hydrogen permeation. Their work showed a homogenous distribution of Pd-P metals, the use of hypophosphate as reducing agent in the electroless plating bath resulted in cracks of the of the Pd-P films due to the evolution of hydrogen gas during plating.

Ye *et al.*, (2007) used the electroless technique to deposit Pd and Ag metal layers on silicon wafer. The surface of the silicon wafer was etched in a mixture of hydrofluoric acid and ammonium fluoride and the silicon surface was activated by immersion in separate solutions of Ag and Pd which was referred to as the co-deposition method. The Pd and Ag seeding technique used in this study nucleated the surface of the silicon wafer. They observed that Pd seeded surfaces preferentially accommodate the film deposition of Ag whereas with the Ag seeded silicon support, low Ag metal film deposition was reported on the Ag silicon activated surface. The Pd/Ag bimetallic activated (seeded) surface of the silicon wafer showed positive activation potentials of the seeding mechanism as catalytic sites for ease of plating of each Pd and Ag metals.

In the work of Liang, *et al.*, (2008), copper metal was plated via the electroless technique on the polyimide surface which was activated by an atom-transfer radical polymerisation method. The atom-transfer radical polymerization (ATRP) procedure was used to induce the creation of activated sites for Cu plating on polyimide (Kapton®) surface, and a comparison



with Cu electroless deposition on the polyimide (Pristine®) showed that a good adhesion of Cu metal can be achieved on the polyimide (Kapton®) surface. They suggested that the use of the ATRP method of surface treatment improved the ease of Cu electroless plating on the polyimide surface compared to the conventional two step surface activation procedure using the acidified palladium and tin solutions.

Williams *et al.*, (2009) discussed an approach to improve palladium electroless plating on rare earth metal hydride-forming alloys by using hydrophilic  $\gamma$ -aminopropyltriethylsilane at different concentrations to activate the surface of the composite material and to determine the hydrogen sorption kinetic of the electroless Pd plated alloy.

They showed that it is possible to activate the surface of metal hydrides alloys in assembly formation of functional groups and therefore facilitate the nucleation of Pd particles for hydrogen adsorption kinetic. Their study indicated that electroless deposition of Pd film in a layer by layer pattern on the activated metal-hydride alloy showed improved adhesion after silane treatment at increased concentration.

Cheng *et al.*, (2001) studied the palladium microstructure and the palladium film reaction kinetic on glass and stainless steel supports. The palladium was deposited using the hydrazine and hypophosphate based electroless plating baths. Their work examined the Pd film quality deposited on the two different supports for the hydrazine and hypophosphate reductant solutions. These reductants were applied and varied in time and concentration. The plating efficiency of hydrazine-based solution proved excellent for Pd film deposition on the glass and stainless steel supports. The palladium film showed better adhesion to the supports in the hydrazine-based electroless bath compared with hypophosphate-based electroless solutions. Although hypophosphate gives better plating rate for a longer plating time, the release of hydrogen by oxidation of hypophosphate caused film delamination and crack formation hence poor adhesion of the Pd film on support after removal from the plating bath.

This scope of this study does not cover the industrial application of electroless plated hence further literatures will not be reviewed.

The image below represents the schematic of the electroless plating experimental set-up

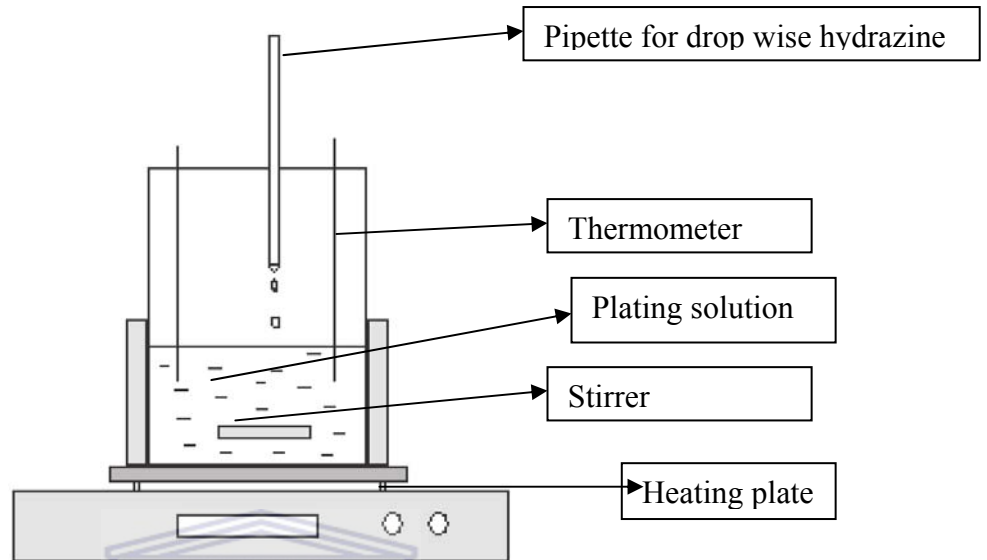


Figure 2-4: Experimental set-up for electroless plating technique

Some of the advantages of electroless deposition techniques mentioned earlier such as its simplicity of application, uniform dense coatings on both conducting and non-conducting surfaces and cost are responsible for the choice of electroless plating (Zhang *et al.*, 2007). However, EP is time consuming compared with other metal plating techniques. The generation of toxic wastes is another limitation of electroless plating technique as well as low deposition rate, metal loss, film impurities and difficulty in the control of metal film thickness on the substrates (Maurizio *et al.*, 2006). A careful selection of plating bath parameters such as metal precursors of the plating bath, concentrations of the plating components, pH of bath and temperature has been reported to help to address these limitations (Kirlicarslan *et al.*, 2008). The importance of electroless plating method has been demonstrated in industrial applications of materials with metals such as nickel, cobalt, silver and some platinum group metals (PGMs) have been commercially plated using electroless plating technique (Robertis *et al.*, 2008).

In summary, the use of palladium as a selective metal membrane for hydrogen permeability and separation from gas mixture and purification processes is highly significant in numerous

high temperature industrial applications. Consequently, the use of the electroless plating method to deposit palladium metal on various supports has been discussed and the influence of substrate type, surface morphology, plating kinetics, plating bath concentrations and time on the thickness of palladium film during electroless plating technique was reviewed. The preference for electroless plating method by many workers is indicative of the simplicity of the method, the ease of application and the wide range of substrates that can be used.

## **2.24 CHARACTERISATION TECHNIQUES AND SAMPLE PREPARATION**

This section will discuss the different characterization techniques used in this study and their relevance. The as-received unirradiated and irradiated polyimide film, the alkaline etched and palladium plated as-received unirradiated polyimide samples were characterised. Emphasis is given to the importance of each technique to understand how the samples are investigated.

### **2.24.1 Scanning Electron Microscope/ x-ray energy dispersion (SEM/EDX)**

Scanning electron microscopy (SEM) is a versatile imaging analytical technique and capable of producing three-dimensional profiles of material surfaces. SEM can be used to obtain both quantitative and qualitative information pertaining to particle size/shape and surface dispersion of sample on a template as in the case of palladium electroless plating on PI (Esinger *et al.*, 2003). The basic instrumental operation in SEM entails the interaction of an accelerated highly mono-energetic electron beam sourced from a cathode tungsten filament, with the atoms at a sample surface. The electron beam is focused into a fine probe and rastered over the sample surface. The scattered electrons are collected by a detector, modulated, and amplified to produce an exact reconstruction of the sample surface and particle profile displayed on monitor screens.

**2.24.2 X-ray diffraction (XRD)**

XRD analytical technique is a powerful and valuable tool in the research and development of advanced materials. XRD is a resourceful and a non-destructive technique in the study of crystallinity, chemical structure and phase orientation of metal arrangement in materials, and forms an integral part in a comprehensive characterization study thereof. This technique can be employed to investigate unknown materials as it is capable of identifying single and multiple phases, quantification of minerals of interest, detection of impurities, determination of the crystallographic structure of materials (i.e. space Methodology group determination; indexing; structure refinement; structure identification, orientation of crystallites), texture analysis, structure deformation, residual stress analysis, studies of lattice properties, and crystallite size determination. The benefits of this analytical technique cannot be overstated as no comprehensive materials characterization study would be complete without an XRD investigation. Information obtained from XRD analysis can be used to establish the presence of elemental phases of a given sample.

For the purpose of this study, XRD was used to investigate the presence of palladium metal planes and determine the crystallite phases of as-received polyimide film, irradiated polyimide film before and after palladium electroless plating of the PI samples (Mu *et al.*, 2010; Ke *et al.*, 2007).

In XRD analysis, solids are bombarded with a collimated x-ray beam which causes crystal planes atoms, serving as diffraction gratings, to diffract x-rays in numerous angles. Each set of crystal planes (*hkl*) with interplanar spacing (*d<sub>hkl</sub>*) can give rise to diffraction at only one angle. The diffractions are defined from Bragg's Law ( $n\lambda = 2d \sin \theta$ ), where the intensities of diffracted x-rays are measured and plotted against corresponding Bragg angles ( $2\theta$ ) to produce a diffractogram. The intensities of diffraction peaks are proportional to the densities or abundance of the corresponding crystal facets in the sample lattice. Diffractograms are unique for different materials and can therefore qualitatively be used in material identification.

**2.24.3 Transmission electron microscopy (TEM)**

The use of microcopies technique to image samples has been an important in the investigation of particle size distribution, agglomeration and surface morphology. In this study, TEM analysis is employed to probe the palladium metal into the polyimide matrix after palladium plating of the polymer as adapted from the work of Yoda *et al.*, (2004); Marin *et al.*, (1995); Yi *et al.*, (2004).

Transmission Electron Microscopy (TEM) is used in the investigation of surface morphology, average particle size and shape and particle size distribution of these particles across the surface of a material.

In TEM characterisation technique, a special sample preparation is required using the microtome method. Details of this sample preparation will be presented in the next section.

**2.24.3.1 Ultra microtome**

Reichert ultracuts (microtome machine) consists of block of metal which sits the metal tabs segment for sample holding. This sample holder has a self-locking precision drive for eucentric movement of sample during trimming and cutting of the specimen. There are two types of knives used in ultracuts, the glass or diamond knives. The knife is attached to the cutting block first to trim resin, exposing the embedded samples prior to cutting the samples and collected on a copper grid.

The knife sits on block with locking lever base and an attachment of moveable stage to adjust the knife to desired position. Glass knife is often preferred to diamond knives due to cost and availability of the glass knives. The knives which are either glass or diamond cut at cross-section thus palladium metal layer cannot be peeled from the polyimide surface. The stereo zoom microscope and knob changer, focusing knob and breath shield are used to adjust the focus of sample during trimming and cutting of sample.

**2.24.4 Fourier transformed infra-red (FTIR)**

Fourier transformed infrared (FT-IR) spectroscopy is an analytical technique used to determine the bond characteristics of a material by identifying the functional groups present in a sample. In FT-IR analysis, bonds vibrate at frequencies which are transmitted or absorbed at specific wavelengths with corresponding peaks identical to the bonds (Coates, 2000; Naddaf *et al.*, 2004; Quarmara and Garg, 2007; Mathakari *et al.*, 2009).

**2.24.5 Thermo-gravimetric analysis (TGA)**

Thermo gravimetric analysis (TGA) is an analytical technique used to determine materials thermal stability and its fraction of volatile components by monitoring the weight change that occurs as a specimen is heated at steady rate increasing temperature. TGA measurement is carried out in air or in an inert atmosphere such as helium or argon, and the weight is recorded as a function of increasing temperature. The technique can characterise materials that exhibit weight loss or gain due to decomposition, oxidation, or dehydration (Quershi *et al.*, 2007; Yi *et al.*, 2004).

**2.24.6 Peel test analysis**

The Peel Test measures the strength required to separate a bonded surface. This method of analysis has found application in material science to determine the degree of bonding between two surfaces. Peel test can be used to evaluate adhesives and adhesive tapes and in other attachment methods. This analysis is useful in the application of composite membranes systems where metal can be deposited on polymer surface hence employed in this study to investigate the adhesion of palladium on polyimide surface after etching (Dazinger and Voitus, 2003; Park *et al.*, 2008; Tsai *et al.*, 2009).

## **2.25 CONCLUSION**

In order to achieve effective gas separation and purification, the choice of membrane as a separation technology requires careful selection of materials to accomplish this task. This is because of the conditions such as the gas purity level; economic cost and availability of such techniques are needed in the membrane application. Ultimately, the overall application of this membrane separation technique at industrial level is another major consideration. Upscale of the membrane separation method could serve as an alternative to the pre-existing separation techniques that have been identified in the literature.

Palladium represents the most effective hydrogen separation metallic membrane and its availability in South Africa can enhance its beneficiation through application in a composite polymer membrane configuration. The ability of palladium to withstand surface poisoning from hydrocarbon sources during hydrogen separation application remain a challenge and this is due to the fact that coal contains mixtures of gases that affect the effective permeation property of palladium as a metallic membrane material. On the other hand, the use of polymer and choice of polyimide as a support in the composite organic-inorganic membrane for this study could project a promising potential if the problem of surface adhesion of the polyimide film is solved. The hurdle is to find the suitable surface treatment processes for the polyimide film by surface functionalisation to improve metal adhesion to the polyimide surface. These conditions must be cheap, available and easy without compromising the bulk properties of the polyimide film structures.

## **2.26 RESEARCH AIMS**

The overall aims and objective of this study is summarised as follow:

- a. To develop scientific approach for successful synthesis of composite membrane based on polyimide modified with palladium thin film layer by electroless deposition and as an attractive alternative for inorganic and organic membranes for hydrogen gas separation.

- b. To develop simple material and technologies which can effectively and economically separate hydrogen from coal gasification processes
- c. To develop composite membrane with pre-defined tolerance limits such as excellent adhesion property and stable at high temperature.
- d. To investigate the effect of surface functionalisation on polyimide film as a function of time and temperature.
- e. To investigate surface depth profile of etched polyimide by hydrogen diffusion.
- f. To design, fabricate and install a home-grown hydrogen diffusion reactor unit for hydrogen diffusion measurement of the composite membrane

## **2.27 EXPERIMENTAL TASK**



In this study, different surface functionalisation treatment will be considered to determine a cheap, available and easy method for improved metal adhesion property of the polyimide. The conditions found in literature will be modified to address some of the problems identified as stated in section 2.27. For this study, low concentration of etching solutions and temperature of etching will be used as compared with the reports from literature. The characterisation techniques that will be employed will help to investigate the physico-chemical properties and hydrogen gas diffusion polyimide film after successive treatment.

The scope of this study will be to examine polyimide film as a suitable polymer for polymer-metal composite membrane. In other to study the rate of etching with time on the polyimide surface, a simple hydrogen diffusion reactor unit will be designed, fabricated and installed for express gas diffusion test. This unit will be designed to accommodate single gas diffusion test but can be upgraded for more advanced gas diffusion analysis such as multiple gas diffusion analysis in composite membrane material.



Based on the available literature reviewed, the summary of the experimental schematic as presented below was formulated for the surface functionalisation and palladium plating of etched polyimide film. This research design will be to focus on the use of easy method of metal plating on polymer surface and the details of the step-by-step approaches are discussed in details in chapter 3 of this study.

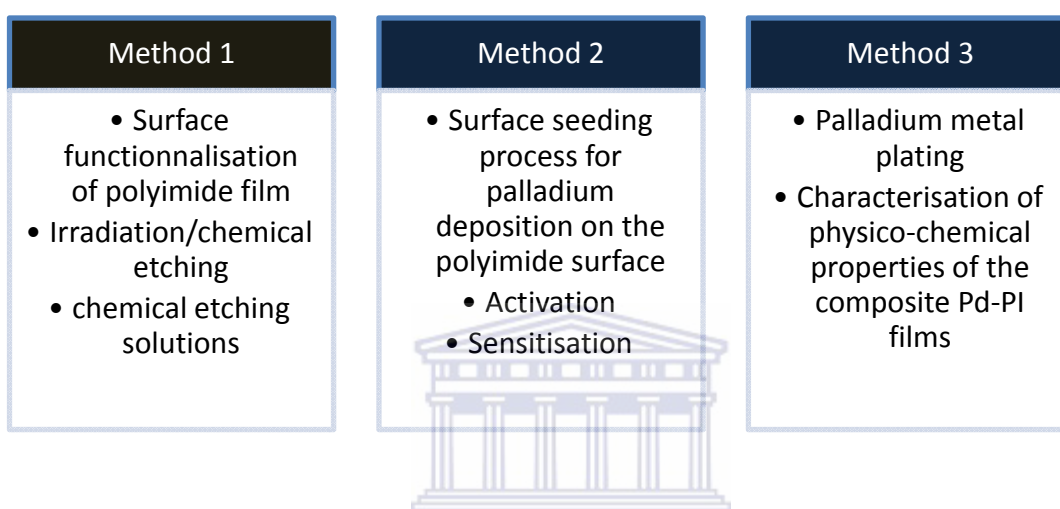


Figure 2-5: Experimental approach

## 2.28 DELIMITATION OF STUDY

This study was limited to the use of Kapton® type of polyimide. Although several other polymers can be applied for gas separation purposes as found in the literature, polyimide possesses excellent thermal and mechanical properties. Hence the study focused on chemical etching of polyimide film at low concentrations using 0.4 M NaOH and 13 % NaOCl solution. The effective etching of the polyimide samples was investigated for the non and irradiated polyimide film. In the case of palladium (Pd) metal used for this study, only the unirradiated polyimide samples were plated with palladium metal and the samples characterised. In the hydrogen diffusion analysis, only hydrogen gas is fed into the hydrogen reactor unit hence gas selectivity was not examined.

## CHAPTER 3

### 3.0 EXPERIMENTAL

This chapter will focus on the materials, methods and equipment used for this work. Also included in this section is the experimental protocol, the instrumental set-up used for sample analysis and procedures for samples preparation.

### 3.1 MATERIALS

Table 3-1: Materials and chemicals

Chemicals	Specifications	Source
Polyimide	50 $\mu\text{m}$ thickness	Goodfellows (UK)
NaOH	AR 98 %	Kimix (SA)
NaOCl	15%	Sigma Aldrich (SA)
N <sub>2</sub> H <sub>4</sub>	35%	Sigma Aldrich (SA)
PdCl <sub>2</sub>	PDS002	SA precious metals
NH <sub>4</sub> OH	2.5 % (CP)	Kimix (SA)
Na <sub>2</sub> EDTA	98.50%	Kimix (SA)
SnCl <sub>2</sub>	98%	Sigma Aldrich (SA)
HCl	37%	Sigma Aldrich (SA)

### **3.2 SCHEMATIC OF METHODOLOGY**

In this section, the various experimental procedures are presented schematically to show the sequential processing step as carefully analysed.

The as-received polyimide film (Kapton®) was first cleaned and treated to allow for comparison with the irradiated polyimide film. The procedure was thereafter as indicated in Section 3.3 for etching in alkaline solutions and Section 3.4 for sample characterisation techniques. The experimental protocol is represented schematically in Table 3.2 below;



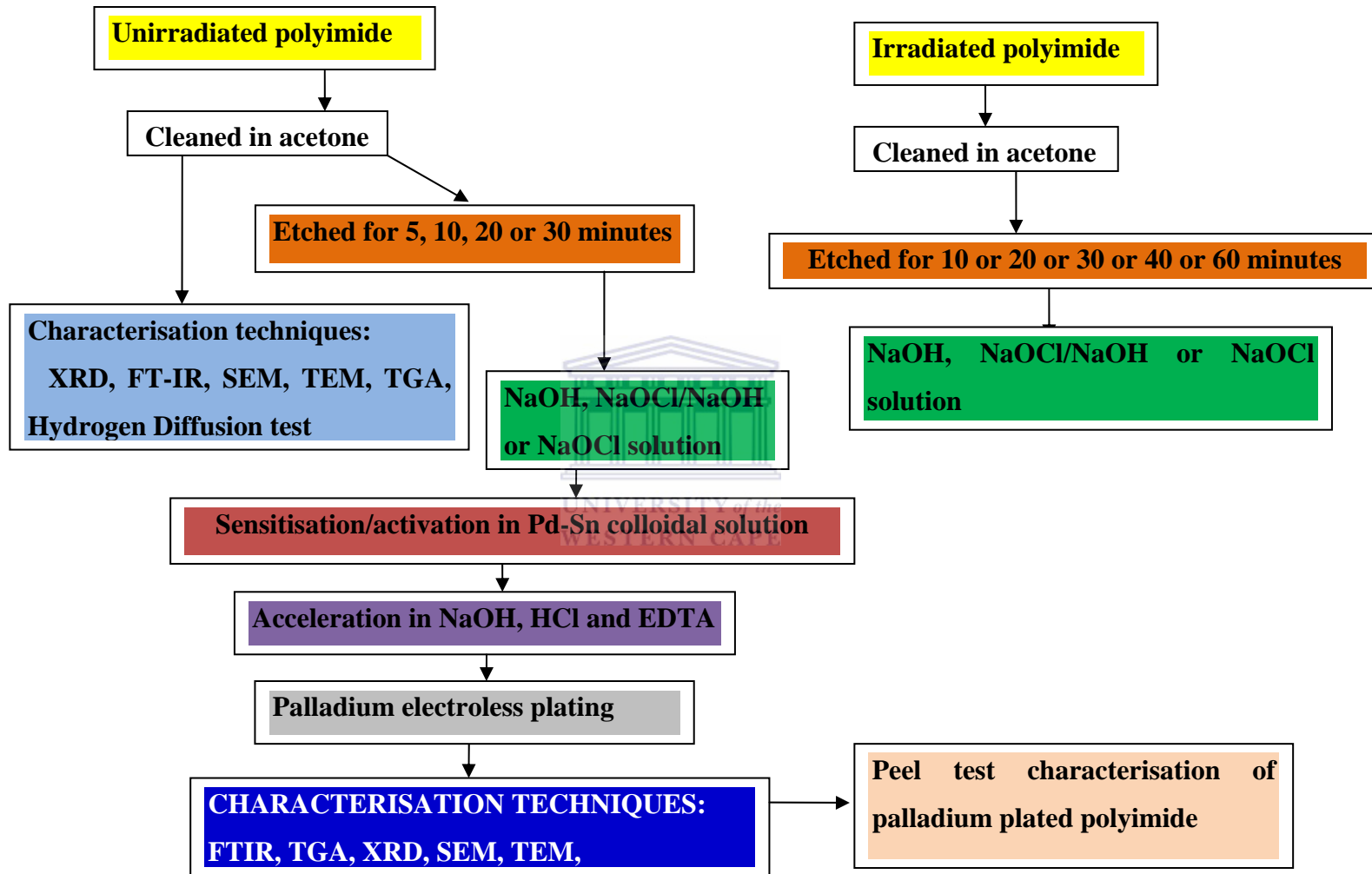


Figure 3-1: Experimental protocol

**3.3 METHODOLOGY**

This section covers the pre-plating procedures i.e. preparation of the different etching, activation and sensitization solutions, and the plating procedure i.e. preparation of electroless bath for palladium plating on surface treated polyimide samples.

**3.3.1 Pre-plating procedure****3.3.1.1 Preparation of polyimide films**

As-received unirradiated and irradiated PI films were cut into circular discs of 20 mm diameter size. In all, twelve (12) samples were prepared; six (6) samples each for etching in two separate solutions of 0.4 M NaOH and 0.4 M NaOH in 13 % NaOCl respectively for 5, 10, 20, or 30 minutes (Table 3.3) for the unirradiated polyimide samples. The irradiated polyimide samples were etched for 10, 20, 30, 40 or 60 minutes (Table 3.4). All samples were etched at 50 °C in a water-bath system in the etching set-up. Prior to etching in alkaline solution, each PI piece was cleaned in 5 mL acetone and deionised water to remove dirt and other impurities. The pieces were air dry and stored in carefully labelled vials.

**3.3.1.2 Preparation of 0.4 M NaOH solution**

8.000 g NaOH pellets were accurately weighed using a weighing boat and dissolved in deionised water, agitated using a mechanical shaker to dissolve the pellets. The solution was quantitatively transferred and made up to the mark in a 500 mL volumetric flask. For each irradiated PI sample, 20 mL of 0.4 M NaOH solution was measured using a measuring cylinder and poured into cleaned 105/95 cm petri dish. Cleaned PI film was

then immersed in the solution to etch the irradiated PI surface. Each PI sample was treated in a 10 mL fresh solution of 0.4 M NaOH, removed and carefully rinsed with deionised water to remove the excess sodium hydroxide.

### ***3.3.1.3 Preparation of 13 % NaOCl solution***

As-received NaOCl (Sigma Aldrich) contains 13 % chlorine. The solution was stored in cold (4 °C) and well shaken before each use. 10 mL of 13 % NaOCl solution was used for the surface etching of irradiated polyimide films. 10 mL of the 13 % NaOCl was measured into 105/95 cm petri dishes and PI film samples immersed for different time (Table 3.3 and 3.4) at 50 °C in a water bath system using hot plate heater and thermometer to monitor the temperature during etching. Fresh solutions of 13 % NaOCl were used for each PI samples piece, and samples were rinsed with deionised water after etching to remove excess solution from PI surface.



### ***3.3.1.4 Preparation of mixture of 0.4M NaOH in 13% NaOCl solution***

To prepare 500 mL of 0.4 M NaOH in 13 % NaOCl solution, 8.000 g NaOH pellets was dissolved in 500 mL 13 % NaOCl solution. The mixture is shaken to complete NaOH pellet dissolution in 13 % NaOCl solution, and stored in volumetric flask. Each of the cleaned irradiated PI pieces is soaked in petri dish of 10 mL fresh 0.4 M NaOH in 13 % NaOCl solution at 50 °C according to the sample matrix in Table 3.3 and 3.4 as indicated in Table 3.3 and 3.4. After etching, each sample is rinsed with deionised water and stored in rubber vial.

**3.3.1.5 Preparation of 0.1 M palladium solutions and plating etched polyimide**

For a 250 mL 0.1 M PdCl<sub>2</sub> solution, 0.445 g PdCl<sub>2</sub> (SA Precious Metal) was accurately weighed on a 4 place balance using a plastic weighing boat and dissolved in 2 mL hydrochloric acid (Sigma Aldrich). The dissolved PdCl<sub>2</sub> solution was made up to the mark with deionised water in 250 mL volumetric flask. 10 mL of the solution is collected with a measuring cylinder and transferred into 105/95 cm petri dish.

Each of the polyimide samples treated in either 0.4 M NaOH, or 13 % NaOCl or a mixture of 0.4 M NaOH in 13 % NaOCl and sensitised (section 3.3.1.6) were soaked separately in 0.1 M PdCl<sub>2</sub> solution in the ion exchange bath for 24 hours.

**3.3.1.6 Preparation of colloidal Pd<sub>x</sub>-Sn<sub>y</sub> solution for activation and sensitisation of etched polyimide film**

Prior to palladium electroless plating, surface of unirradiated polyimide films were activated using “one-step” sensitization / activation method after the samples have been separately etched in 0.4 M NaOH or 13 % NaOCl or mixture of 0.4 M NaOH/13 % NaOCl solutions according the time indicated in sections (sections 3.3.1.2 – 3.3.1.4). Fresh solution of 10 mL each of the Pd-Sn colloidal solution was used to sensitised and activate the etched unirradiated polyimide samples 30 minutes at room temperature.

The Pd-Sn colloidal solution was prepared as follows:

*Solution A:* 0.3 g PdCl<sub>2</sub> was dissolved in 2.15 g HCl solution and 5.0 mL deionised water at 70 °C with stirring (200 rpm).

*Solution B:* 25 g SnCl<sub>2</sub>·2H<sub>2</sub>O was dissolved in 14.5 g HCl solution (preheated to 50 °C). The mixture was cooled to room temperature after which 30 mL deionised H<sub>2</sub>O was added.

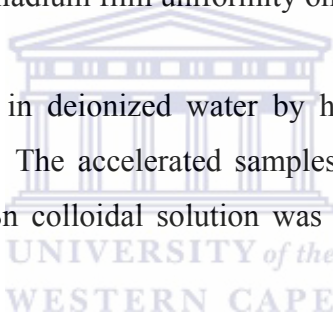
*Solution B* was added to *Solution A* and *Solution (A+B)* was heated to 90 - 100 °C for 15-20 minutes.

*Solution C*: 8.75 g KCl was dissolved in 250 mL deionised H<sub>2</sub>O. 80 mL HCl was then added to the KCl solution.

*Solution C* was then added to *Solution (A+B)* and made up to 500 mL with deionised water.

Following sensitization / activation of etched unirradiated PI samples in Pd-Sn colloidal solution for 20 minutes, samples were carefully rinsed with deionised H<sub>2</sub>O and the Sn layer was removed by ‘acceleration’ through immersion of samples in 100 mL of 100 g/L disodium ethylenediaminetetraacetic acid (Na<sub>2</sub>EDTA) or NaOH (30 g/L) or HCl (100 g/L) solutions for 10 minutes. The samples were accelerated in these solutions separately and plated afterwards. A comparison of the effect of acceleration of these different solutions was studied on the palladium film uniformity on polyimide surface.

The Na<sub>2</sub>EDTA was dissolved in deionized water by heating at 70 °C, with constant agitation, and allowed to cool. The accelerated samples were then rinsed in deionised H<sub>2</sub>O and air dried. Fresh Pd-Sn colloidal solution was used for the activation of each sample.



### **3.4 PLATING PROCEDURE**

#### ***3.4.1 Preparation of palladium-based electroless plating bath***

Each sample of etched polyimide was plated with 10 mL of electroless plating solution for 10 minutes. The table below highlights the electroless plating bath used in this study.



Table 3-2: Composition of palladium electroless plating bath

<b>Chemical</b>	<b>Amount (g/L) or (mL/L)</b>
Palladium chloride (PdCl <sub>2</sub> )	0.8 g
Na <sub>2</sub> EDTA	60 g
NH <sub>4</sub> OH	200 mL
Hydrazine	30 mL
Temperature	70 °C

Fresh palladium plating solution of 10 mL was used for each sample. After plating is completed; the samples were carefully removed, dried in air and stored in plastic vials for characterisation using the SEM/EDS, XRD, TEM, FTIR, TGA analytical techniques.



The table below represent the sample matrix of the unirradiated polyimide film for different etching time, the sensitisation/activation and electroless plating conditions. The samples for each etching solution treatment time are in triplicates.

Table 3-3: Sample matrix for etching and plating time of unirradiated polyimide


Sample Numbers	0.4 M NaOH solution	13 % NaOCl solution	0.4 M NaOH + 13 % NaOCl solution	Sensitisation/Activation	Palladium electroless plating		
<b>OA1-1</b> <b>OA1-2</b> <b>OA1-3</b>	5 minutes 10minutes 20 minutes 30 minutes			10 minutes	10 minutes		
<b>OA2-1</b> <b>OA2-2</b> <b>OA2-3</b>	5 minutes 10minutes 20 minutes 30 minutes					10 minutes	10 minutes
<b>OA3-1</b> <b>OA3-2</b> <b>OA3-3</b>	5 minutes 10minutes 20 minutes 30 minutes						

Table 3-4 below represent the sample matrix of irradiated polyimide for NaOH and mixture of NaOH/NaOCl etching solution. The irradiated polyimide samples are not prepared in triplicate because of the limited amount of irradiated polyimide sample.

Table 3-4: Sample matrix of etching time for irradiated polyimide

Sample Numbers	0.4 M NaOH solution	0.4 M NaOH + 13 % NaOCl solution
<b>OB1-1</b>	10 minutes 20minutes 30 minutes 40 minutes 60 minutes	
<b>OB2-1</b>		10 minutes 20minutes 30 minutes 40 minutes 60 minutes

**3.5 SAMPLE PREPARATION FOR CHARACTERIZATION****3.5.1 Sample preparation (SEM)**

Etched polyimide samples were air-dried for SEM analysis to determine the pore size and distribution across the surface of the irradiated polyimide film. Samples were prepared by mounting the cut pieces on a double-sided carbon conductive adhesive tape on aluminium sample stubs. The samples were then gold-coated to make them conductive with an Edward sputter coater for 5 minutes.

**3.5.1.1 Instrumental set-up condition (SEM)**

---

Model	Hitachi X-650 EM
Working distance	(15 mm)
Accelerating voltage	(25 kV)
Emission current	(75-80 A)

---

**3.5.2 Sample preparation (TEM)**

Palladium plated samples are neatly sliced and embedded in epoxy resin to cure for 24 hours at 60 °C in an oven. The Reichert ultracuts microtome machine is used to prepare (section) the samples for TEM analysis.

### 3.5.2.1 Instrumental set-up condition (TEM)

Model	Tecnai G2
Accelerating voltage (kV)	200
Current ( $\mu\text{A}$ )	20
Condenser aperture	1
Objective aperture	3
Exposure time	3

### 3.5.3 Sample preparation (XRD)

For sample preparation in XRD analysis, air-dried etched polyimide samples are mounted on aluminium stubs by adhesive tapes and the surface was flattened to promote maximum x-rays exposure. After the collection of the XRD spectra, the crystalline and plane identification was performed by matching with the JCPDS (Joint committee of powder diffraction standards) file data base software is used to investigate the qualitative and relative abundance of the palladium or other metals present in the sample.

#### 3.5.3.1 Instrumental set-up condition (XRD)

Model	Bruker AXS D8 Advance
Detector	Sodium Iodide
Monochromator	Graphite
Generator current (mA)	40
Electron Intensity (keV)	40
X-ray source	Cu-K $\alpha$
Radiation wavelength ( $\lambda$ )	1.542 Å
$\alpha_1/\alpha_2$	0.497
Scan range ( $2\theta$ °)	5-100
Scan rate	0.05 /min

### 3.5.4 Sample preparation (FT-IR)

Etched and palladium plated PI samples are cut into small pieces (~2 mm X 2 mm) size and placed in the metal disc plate for analysis. IR spectra are collected from 4000  $\text{cm}^{-1}$  - 380  $\text{cm}^{-1}$  at 4  $\text{cm}^{-1}$  scan rate and pressure gauge of 150. Spectra are auto corrected for background noise, smoothed and normalised.

#### 3.5.4.1 Instrumental set-up (FTIR)

---

Model (FT-IR/ATR)		PerkinElmer 100series
Wave number range (cm-1)		4000- 380
Scan rate (cm-1)		4
Force gauge		150

---

### 3.5.5 Sample preparation (TGA)

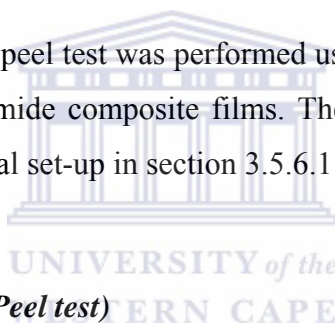
Samples of polyimide films are cut into pieces and placed into a platinum pan. The pan is supported on an analytical balance, located outside the heating furnace. The balance is calibrated to zero prior to heating of the sample. The rate of heating is adjusted to 10 °C until the maximum temperature set at 900 °C. The balance sends the weight signal to the computer for storage, along with the sample temperature and elapsed time. The TGA curve plots the TGA signal, converted to percentage weight change on the Y-axis against the reference material temperature on the X-axis

**3.5.5.1 Instrumental set-up (TGA)**

Model (TGA/DSC)	Q500 thermo-gravimetric analyzer
Atmosphere	N <sub>2</sub>
Temperature (°C)	25-900
Rate (°C/min)	10

**3.5.6 Sample preparation (Peel test)**

The sample preparation for the peel test was performed using the Cu foil as the substrates to adhere the palladium–polyimide composite films. The peel test analysis was carried out according to the instrumental set-up in section 3.5.6.1 below.

**3.5.6.1 Instrumental set-up (Peel test)**

Method	90 degree
Pressure	20 kg/cm <sup>2</sup>
Angle	190 degree
Time	5 minutes
Peel rate	50.8 mm/min

**3.6 HYDROGEN DIFFUSION REACTOR UNIT**

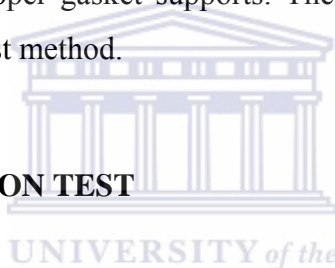
The hallmark of this project was the development of a simple, efficient and cheap hydrogen reactor unit. This unit was designed, fabricated and installed to evaluate the hydrogen diffusion across the different samples. The hydrogen diffusion unit was developed due to the economic cost of sample analysis using industrial gas diffusion

installation and to also ensure express analysis of polyimide samples. In developing this hydrogen membrane unit, basic understanding of material science in membrane application and engineering expertise is enhanced. Also included in the design of the design of the reactor unit is the upgrade of the unit by coupling with gas chromatography and computerised for future application as a multi-gas diffusion system.

### **3.6.1 Sample preparation (hydrogen diffusion test)**

Samples are prepared using a 22 mm<sup>2</sup> size circular puncher to cut into size and placed in the membrane holder with copper gasket supports. The holder is screw tight and leak tested using the soap bubble test method.

## **3.7 HYDROGEN DIFFUSION TEST**



Preliminary hydrogen diffusion measurement is carried out in the home-grown hydrogen diffusion reactor on samples of as-received, irradiated and etched polyimide samples from ambient temperature to 325 °C in hydrogen atmosphere. The home-grown hydrogen reactor is developed to measure hydrogen gas permeation across polyimide membrane samples and to investigate the effect of surface treatment and temperature on irradiated, etched and palladium plated samples. A comparison of the rate of diffusion of hydrogen gas can establish if pinholes are present in samples to allow permeation of hydrogen gas.

The apparatus for hydrogen diffusion experiments is shown below. The main components are: a gas storage and supply system (gas cylinder) a temperature regulator, membrane holder, buffer cylinders (high and low) to regulate the flow of hydrogen gas across the membrane and reduce diffusion kinetics, stainless steel block which sits the membrane



holder for temperature transmission via band heater cable. A thermocouple probe is clamped between the steel block and membrane holder to monitor the original temperature of the membrane holder.

The diagram below represents the schematic outlay of the hydrogen diffusion unit with all the unit components.

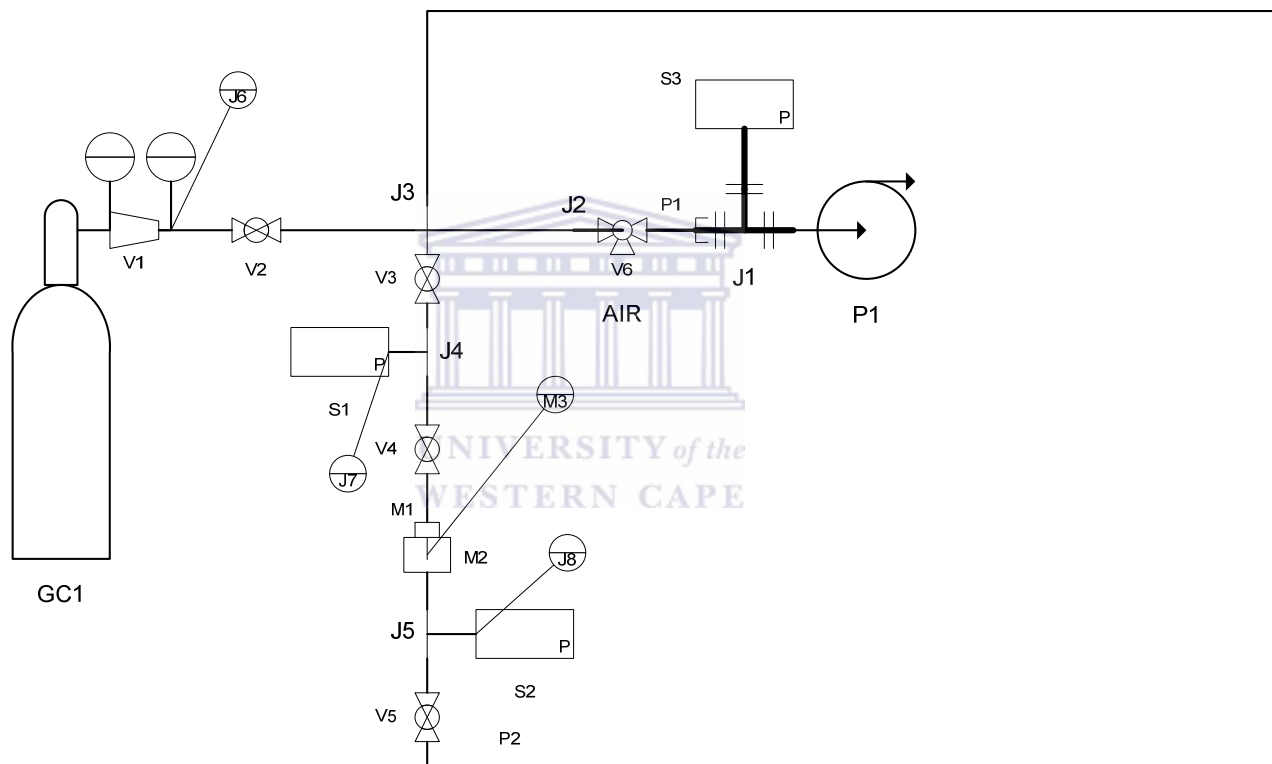


Figure 3-2: Schematic diagram of home-grown hydrogen reactor unit

### **3.8 OPERATION PROCEDURE OF HYDROGEN DIFFUSION REACTOR**

Prior to hydrogen diffusion measurement, the home-grown hydrogen diffusion reactor system is evacuated by switching on the vacuum pump and valves V3, V4, V5 and V6 of the system. The evacuation is maintained and monitored on the vacuum meter display for a minimum of 30 minutes to establish vacuum in the gas line and ensure the stability of the corresponding pressures such as the high and low pressure readings which are monitored on the pressure digital display screen. To ensure complete vacuum, calibrated pressure values for the high and low pressure digital display are -0.147 bar and 0.021 bar respectively must be displayed. To feed hydrogen gas into the system, valves V3, V4, V5 and V6 are closed. The valves V2 and V3 are turned on to introduce hydrogen into the line at the low pressure side of the membrane holder via the buffer cylinder. Valves V2 and V3 are closed after few minutes which depend on the preferred pressure volume displayed on the digital sensor for the amount of hydrogen gas fed into the system. The pressure sensor has a maximum capacity of 3 bar. To study the rate of hydrogen diffusion, valve V4 is opened to transport hydrogen gas into membrane holder which contains the sample while V2 and V3 are closed. The effective membrane area is 22 mm<sup>2</sup> and sample is sandwiched between two perforated copper gaskets in the membrane holder. Heat is conducted into the membrane holder by the stainless steel block where the membrane holder is encased. This is followed by the feeding of the primary gas to the high pressure buffer chamber of the diffusion cell.

The details of the home-built hydrogen diffusion reactor components is presented in Appendix 1

## CHAPTER 4

### 4.0 RESULTS AND DISCUSSIONS

#### 4.1 INTRODUCTION

This chapter will present results and discussions of the as-received (commercial) polyimide (section 4.2), alkaline etched unirradiated (section 4.4) and alkaline etched irradiated polyimide samples (section 4.5). The first part of this section will focus on the results and discussions of the as-received polyimide samples to serve as baseline data. In the latter section of this chapter, the results and discussions of alkaline etched unirradiated and irradiated polyimide samples will be presented.

#### 4.2 CHARACTERISATION OF AS-RECEIVED POLYIMIDE SAMPLE

The FTIR, XRD, TGA and hydrogen diffusion measurement results and analysis performed on the as-received polyimide will serve as the baseline data for the cleaned as-received polyimide samples. After the baseline characterisation of the as-received polyimide samples, freshly cleaned unirradiated and irradiated polyimide samples are etched with separate alkaline solution of 0.4 M NaOH, 13 % NaOCl and a mixture of 0.4 M NaOH/13 % NaOCl solutions. The procedure for preparation of the alkaline etching solutions has been fully described in sections 3.3.1.2 – 3.3.1.4 and detailed schematic of the pre-treatment and characterisation procedures are presented in section 3.2.

##### 4.2.1 *Fourier transformed infrared transmission spectroscopy*

In the spectroscopic study of the as-received (commercial), alkaline etched unirradiated and irradiated polyimide samples, was performed using the Fourier transformed infra-red spectroscopy (FTIR) using the Perkin Elmer® (Universal ATR)

machine as discussed in section 3.5.4 and the instrumental set-up conditions presented in section 3.5.4.1. In using the FTIR study for the different polyimide samples, absorption intensities were examined to determine the presence of specific functional groups according to Table 4.1. In effect, the presence, absence and reduction in absorption intensity of these functional groups (Table 4.1) along the polyimide structure can indicate the effect of surface treatment as function of etchant composition and time on the polyimide samples. The distortion or molecular rearrangement in the polyimide bonds, due to the effects of chemical (alkaline) or physical (irradiation) treatment of polyimide samples has been predicted to determine the ion exchange capacity during the etching of polyimide samples.

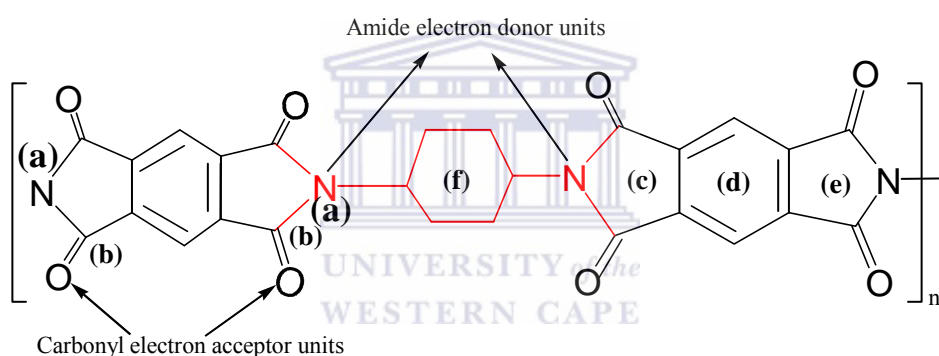


Figure 3: Polyimide structure showing the electron donor and acceptor species as indicated in the Table 4.1 below

Table 4-1: Summaries of the Fourier transformed infra-red spectra and their associated wavenumbers located in commercial polyimide. The bracket alphabets indicated in the table below represent the different functional groups identified in the polyimide structure presented above.

WAVENUMBERS (cm <sup>-1</sup> )	FUNCTIONAL GROUPS
721	deformation of imide ring (a)
1079	carbonyl stretching (b)
1164-1491	cyclic ketone and amide stretch (c)
1706	cyclic ketone and imide bending (d)
1773	cyclic imide and C=O bending (e)
2017-2159	aromatic amide stretch (f)

From table 4.1 above, a summary of the polyimide structures, their respective wavenumbers and functional groups are presented. From these selected wavenumbers of interest and their corresponding functional groups, the reaction process and choice of etchant reactivity on the polyimide structure during alkaline etching can be predicted based on the overall change in the absorption intensities. This IR study is aimed at understanding the bonds that are available along the polyimide structure and to determine how the polyimide physico-chemical properties may be affected after etching in different solutions of 0.4M NaOH, 13 % NaOCl and 0.4 M NaOH/13 % NaOCl. For the FTIR analysis, polyimide absorbance values have been classified into three (3) according to Shriner *et al.*, (2004). The first region of the polyimide absorbance value is called 'functional groups' and has wavenumbers between 1600 cm<sup>-1</sup> and 4000 cm<sup>-1</sup>. The 'finger print' region lies within 1000-1600 cm<sup>-1</sup> and the aromatic regions occur from 675 cm<sup>-1</sup> to 900 cm<sup>-1</sup>.

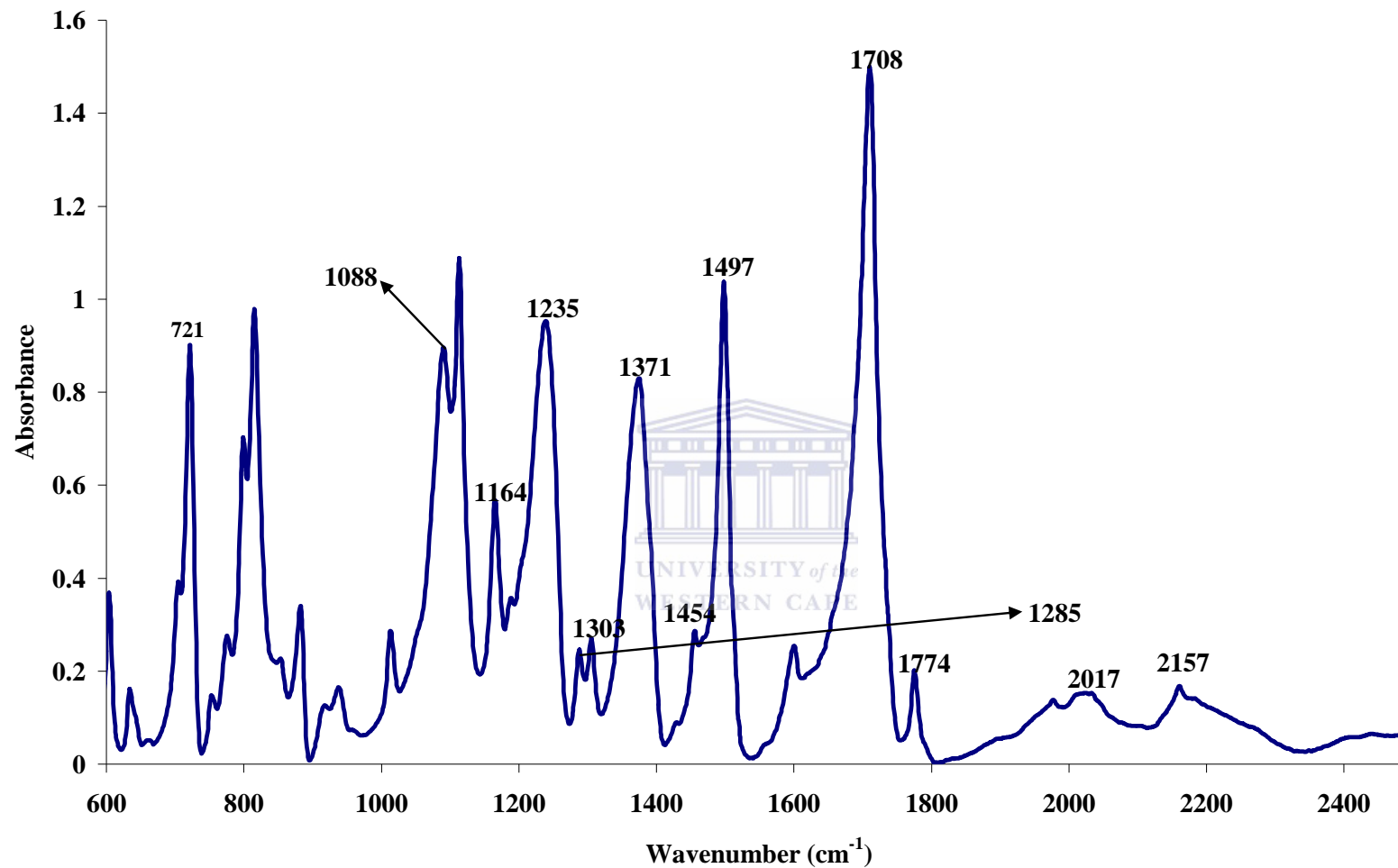


Figure 4-2: Selected FTIR spectra of unirradiated polyimide

The FTIR result of as-received polyimide (Fig. 4.1) showed the absorption intensity bands present and their functional groups as highlighted in Table 4.1. The major functional groups observed in the as-received polyimide structure are the imide-amide bonds which occurred within the spectra collected and as labelled in Fig. 4.1. These bonds constitute the main back bone of the polyimide ring structures and have been identified as the site for ion exchange (Chae *et al.*, 2002; Mathakari *et al.*, 2010).

#### 4.2.2 X-ray diffraction

X-ray diffraction (XRD) characterisation was performed on the as-received polyimide to investigate the polymer crystalline properties. Polyimides are known to be semi-crystalline polymer structure with characteristic diffraction intensity that lies between  $14^{\circ} - 26^{\circ} 2\theta$ . The XRD instrumental set-up has been described in section 3.5.2.1 and the XRD sample preparation explained in section 3.5.2.

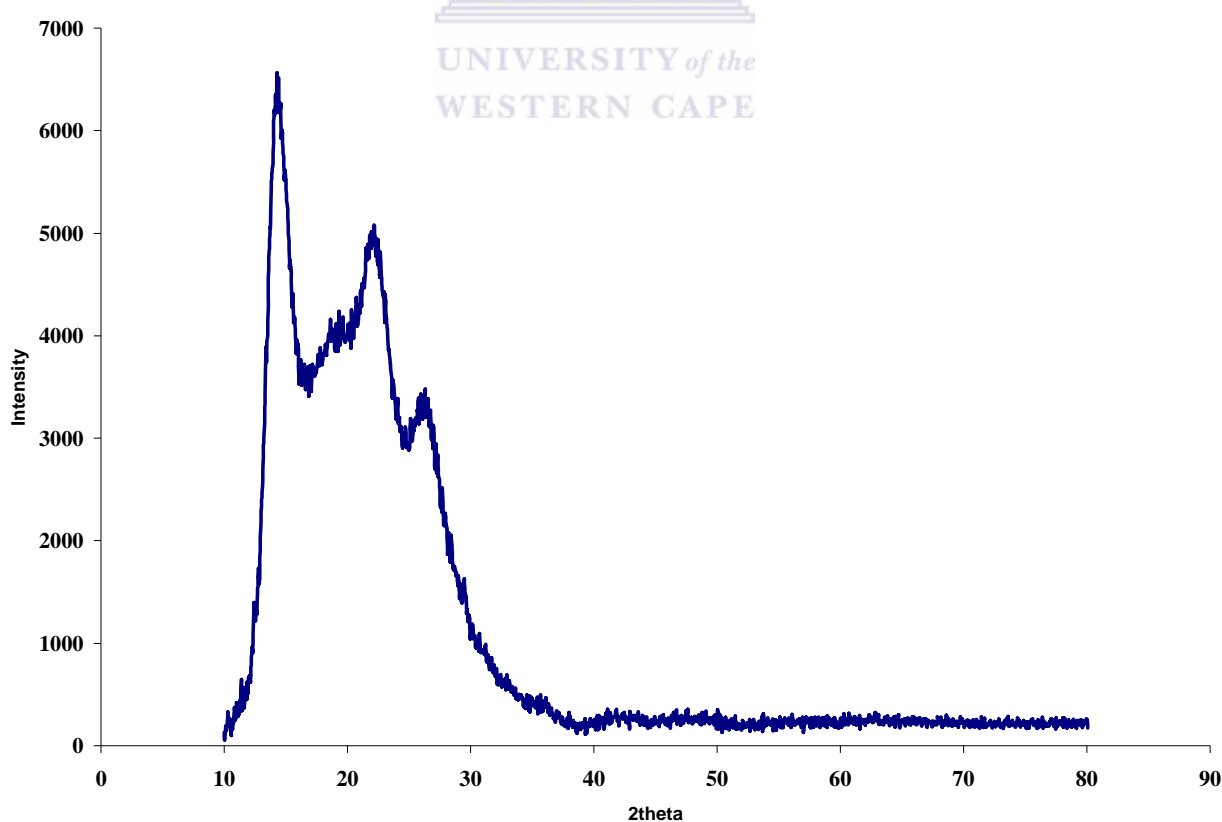


Figure 4-3: XRD analysis of as-received polyimide

Fig. 4.2 showed the XRD spectra of as-received polyimide film. The XRD diffraction peaks indicated sharp peaks at  $14^\circ$ ,  $22^\circ$  and  $26^\circ$   $2\Theta$ . These XRD peaks suggest that polyimide possesses crystalline properties even though most polymers are non-crystalline while semi-crystallinity is often ascribed to polymers such as polyimides. The presence of peaks at  $14^\circ$  and  $26^\circ$  agreed with the result of Shuxiang *et al*, (2010). According to the study of Shuxiang *et al*, (2010), Pristine® type of polyimide used compared to the Kapton® type investigated in this project. From Fig. 4.2, a new peak was observed at  $22^\circ$   $2\Theta$  for the Kapton® polyimide film. The presence of a new diffraction peak could be due to the structural configuration such as regular structure at defined d-spaces of the intermolecular arrangement and the tight chain packing of atoms in the Kapton® type of polyimide film. Also, the crystalline property of Kapton® could be higher than the Pristine® type of polyimide investigated by Shuxiang *et al*, (2010).



#### 4.2.3 Hydrogen diffusion measurement

The hydrogen diffusion measurement was performed on the as-received polyimide samples; to investigate the presence of pinholes defect on the polyimide surface and to determine its thermal stability over 10 hours at various temperatures. The temperatures for hydrogen diffusion across the polyimide sample were varied between  $25^\circ\text{C}$ ,  $250^\circ\text{C}$  and  $325^\circ\text{C}$  using the home-built hydrogen diffusion unit. The detail of the hydrogen reactor set-up has been described in section 3.6.



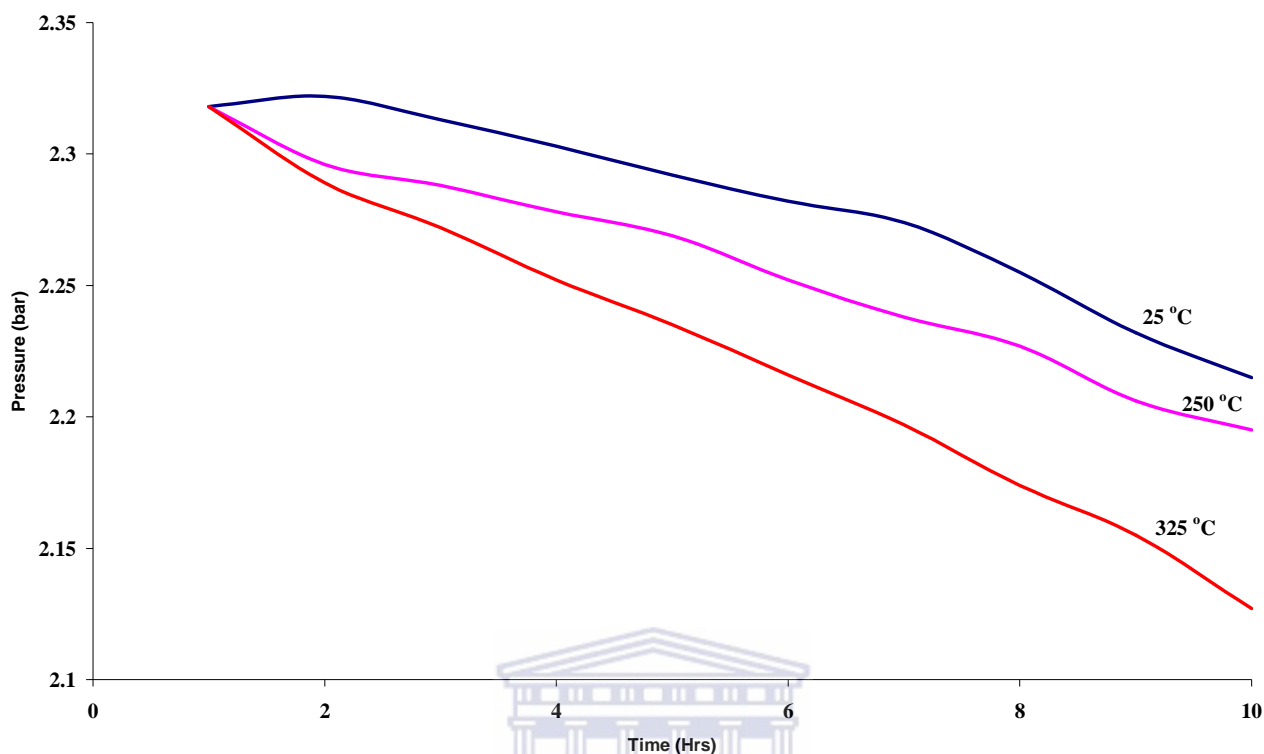


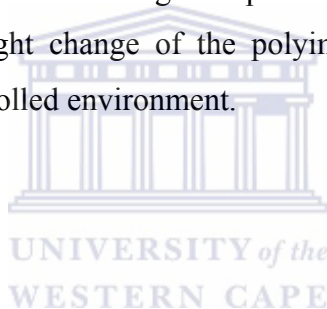
Figure 4-4: Hydrogen diffusion measurement of as-received polyimide film at 25°C, 250°C and 325°C

In Fig. 4-3 above, the pressure value was plotted against time to determine the presence of surface defects such as pinholes and thermal rigidity of the as-received polyimide samples at various temperatures. For the hydrogen diffusion measurement at 25 °C, the pressure drop across the polyimide samples was observed to show steady hydrogen gas diffusion difference of 0.07 bar after 10 hours. The slow rate of hydrogen gas diffusion could be attributed to the defect-free surface and thermal stability of the as-received polyimide at room temperature. At temperatures of 250 °C and 325 °C, the polyimide sample showed increase in flux rate of hydrogen diffusion across polyimide film and the pressure drops were 0.12 bar and 0.17 bar respectively after 10 hours. Although a comparative increase in hydrogen gas diffusion could be observed after the polyimide samples were heated at 250 °C and 325 °C, the rates of diffusion at these high temperatures were relatively stable over time. The hydrogen diffusion analysis suggests that at higher temperature, as-received polyimide samples

do not indicate any surface defects and thermal degradation of the polyimide samples. Although polyimides are known to be relatively stable at high temperature, the as-received polyimide sample showed good thermal rigidity in high temperature environment and agreed with the result of Trautmann *et al.*, (1996a).

#### 4.2.4 Thermo-gravimetric

In this section, the thermo-gravimetric analysis (TGA) of as-received polyimide samples is presented. The detail of sample preparation for TGA analysis has been described in section 3.5.5, and the instrumental set-up is presented in section 3.5.5.1. The investigated the thermal stability and degradation of as-received polyimide samples in extreme conditions such as high temperature environment, and measured the amount and rate of weight change of the polyimide sample as a function of temperature or time in a controlled environment.



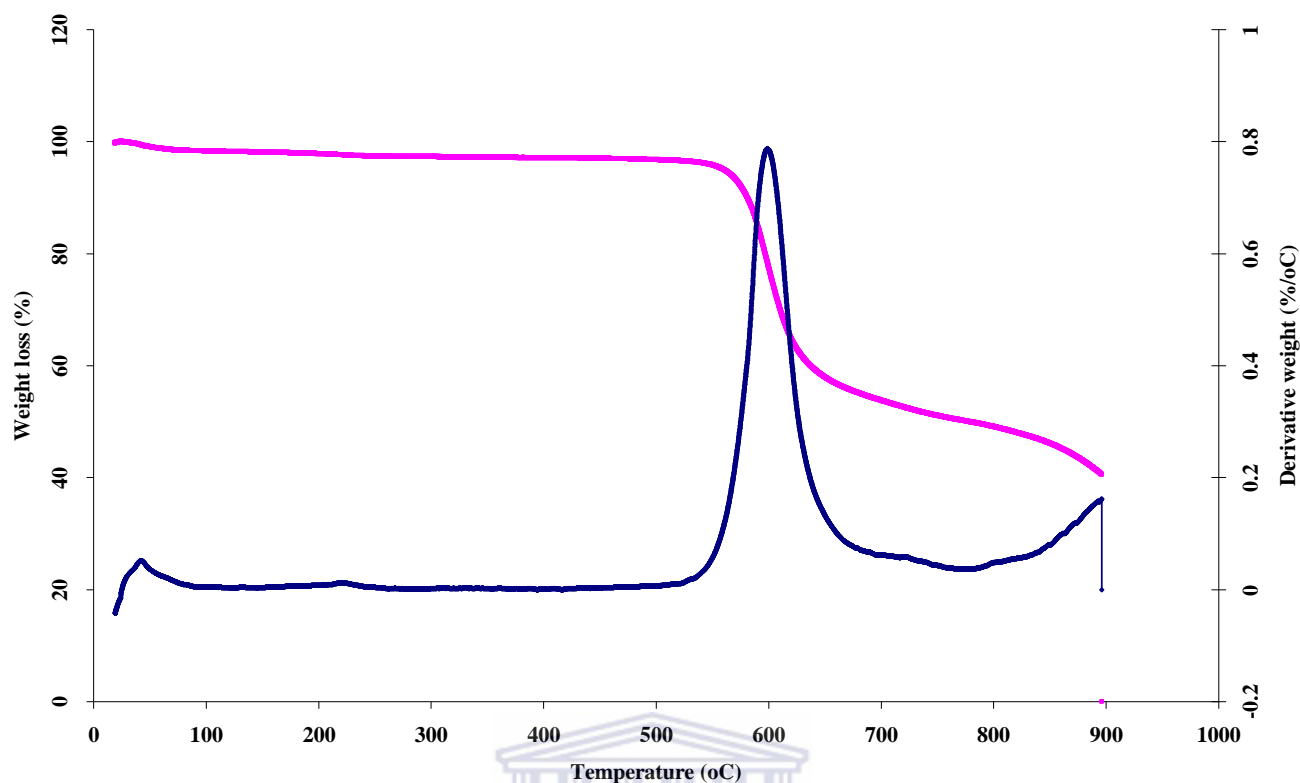


Figure 4-5: Thermo-gravimetric study of unirradiated polyimide

Fig 4.4 represents the thermal degradation of the as-received polyimide film before surface treatment by etching in alkaline or irradiation. From figure 4.4 above, it was observed that the as-received polyimide sample showed relative stability without any weight loss of polyimide film beyond 500 °C in nitrogen atmosphere. The polyimide sample thereafter decomposed with a large exotherm at 600 °C and about 60 % of the polymer was combusted. This exotherm indicated the decomposition of polyimide volatile side chains. The backbone structure could have been the residual 40 % left over. The residual polymer may be indicative of the durability of Kapton® compared to the Pristine® type of polyimide film studied by Qureshi *et al.*, (2000). In their work, Pristine® was reported to be thermally stable up to 500 °C. The DSC showed an exotherm profile of two consecutive peaks with maximum intensity at 600 °C and 800 °C. The exotherm peak at 50 °C has been suggested due to dehydration during polyimide imidization reaction (Suzuki *et al.*, 2004). The exotherm reaction observed at 600 °C is assigned to the thermal degradation of the volatile units of the polyimide sample since the peak appeared with high intensity. However, it is obvious that a

thermally initiated reaction occurred on the unirradiated polyimide samples due to the emergence of these two exotherm peaks. It was observed that beyond 800 °C, the exotherm goes up again and is accompanied by further 15 % loss which was interrupted by the termination of the experiment. This could suggest that the residue remaining after the large decomposition at 600 °C was thermally stable until 800 °C.

### **4.3 ETCHING BY ALKALINE SOLUTION OF UNIRRADIATED AND IRRADIATED POLYIMIDE FILM**

The use of a chemical etching procedure was employed to activate the polyimide surface. This surface treatment method of the unirradiated and irradiated polyimide samples was adapted from the work of Mitrofanov *et al.*, (2006). In their method, the irradiated polyimide samples were track etched at higher concentrations (0.8 M) of NaOH/NaOCl solutions mixtures and high etching temperature (80 °C). In comparison, this study employed etching of the polyimide samples at 50 °C with 0.4 M NaOH, 13 % NaOCl and mixture of 0.4 M NaOH/13 % NaOCl solutions. The use of lower temperature and concentration of etchants is to control the depth profile of the polyimide film during etching. The details of the preparation of the etchants used in this study (NaOH and NaOCl), and etching procedure have been discussed in chapter 3 (section 3.4.1). The etching solutions and variable parameter (time) used has been discussed in Table 3.3.

### **4.4 CHARACTERISATION OF ALKALINE ETCHED UNIRRADIATED AND HEAVY ION IRRADIATED POLYIMIDE SAMPLES**

This section will present the characterisation results of alkaline etched unirradiated polyimide samples with the use of separate solutions of NaOH, NaOCl and NaOH/NaOCl. Fresh etching solutions were used for each polyimide sample in a thermometer-control water bath to keep the temperature constant 50 °C for all etching time. The characterisation techniques employed to investigate the etched unirradiated

polyimide samples include; the Fourier transformed infra-red/Attenuated total reflection (FTIR/ATR) which was used to study the presence of functional groups and their respective bonds as a function of etching time. The Scanning electron microscopy (SEM) technique was used to examine the effect etching on surface morphology of the samples after each successive etching time.

#### ***4.4.1 FTIR of etched unirradiated polyimide sample using 13 % NaOCl solution***

The etched unirradiated polyimide samples were analysed by FTIR technique after etching with 5 mL of 13 % NaOCl solution. This section will present the spectra results for the various etching time at 5, 10, 20 and 30 minutes.



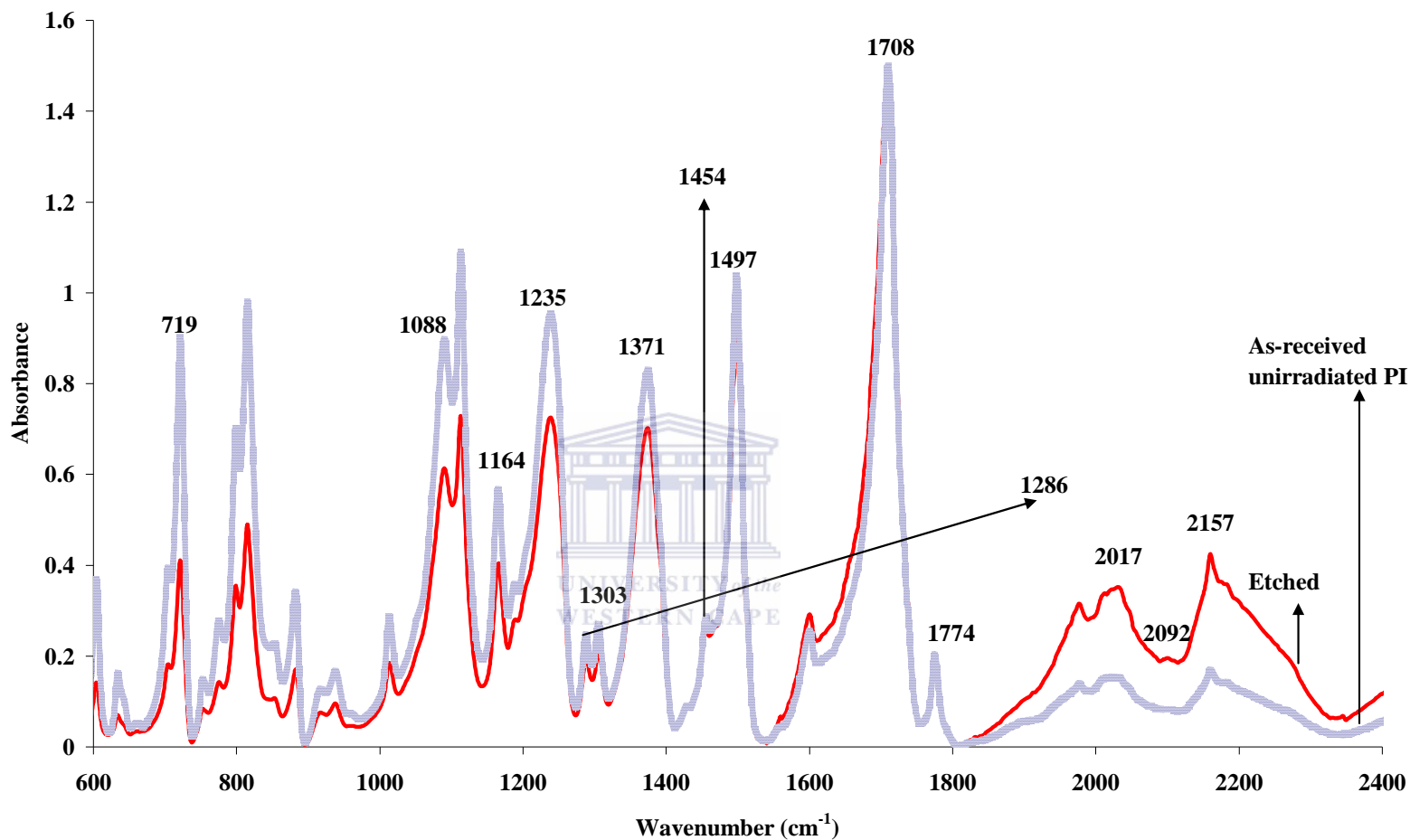


Figure 4-6: FTIR of unirradiated polyimide and 5 minutes 13 % NaOCl etched unirradiated polyimide

The IR spectra of unirradiated polyimide etched with 13 % NaOCl solution for 5 minutes (Figure 4.5) showed a reduction in absorption intensity for almost all the functional groups present in the polyimide structure except the bands at  $1497\text{ cm}^{-1}$  and  $1708\text{ cm}^{-1}$  which correspond to amide stretch and imide bending groups. The treatment after 5 minutes suggest that the less tightly packed chains with weaker bonds are attacked immediately by NaOCl etching solution whereas there has not been any literature report for etching of polyimide at such a low treatment time probably due to the less effective chemical modification of polyimide. Some broad peaks appeared at regions of  $2017\text{ cm}^{-1}$  with bumps located at  $2092\text{ cm}^{-1}$ . This region contains the aromatic amide group and the increase in the absorption band suggests ring closure after etching.



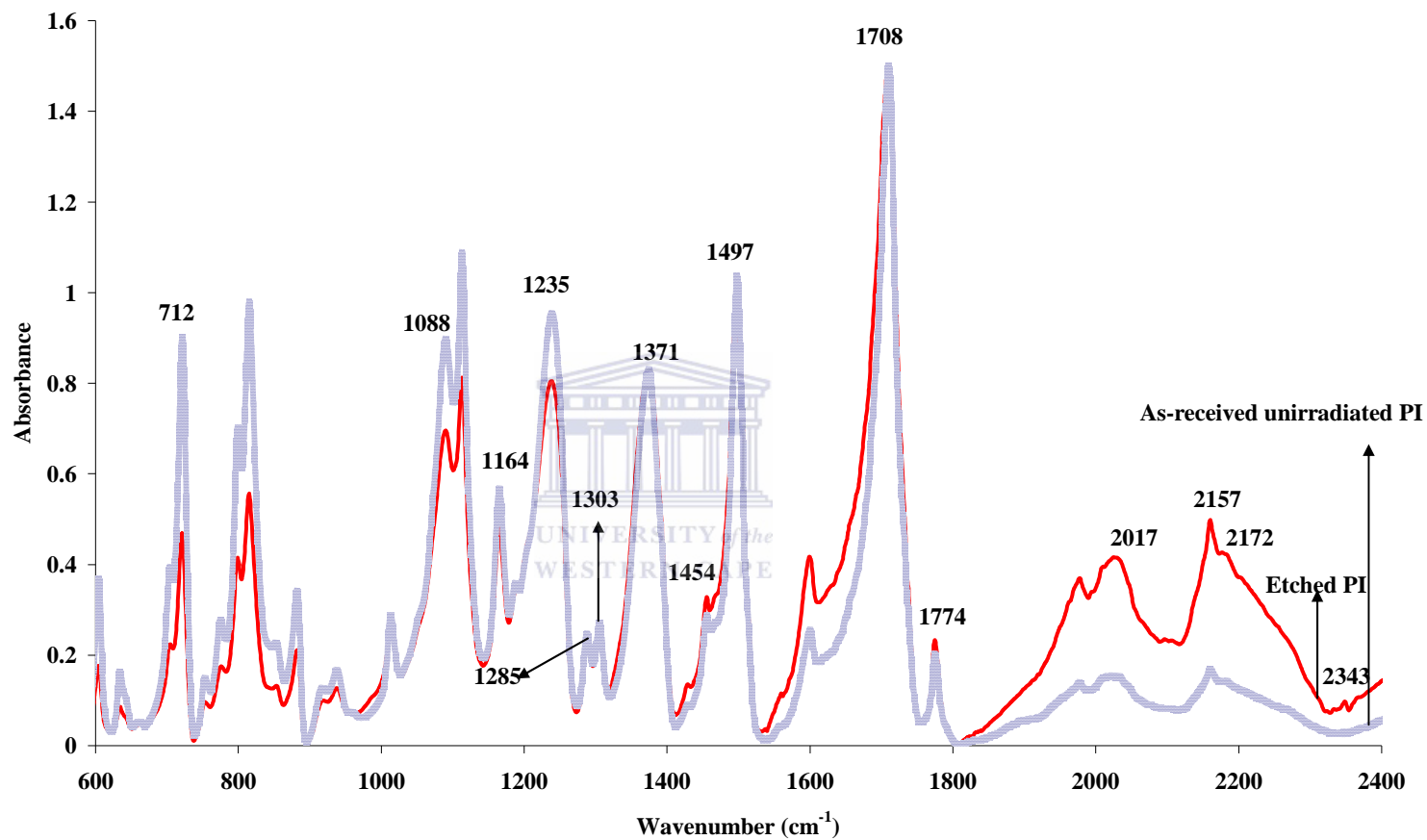


Figure 4-7: FTIR of unirradiated polyimide and 10 minutes 13 % NaOCl etched unirradiated polyimide



In Fig 4.6, the effect of etching on unirradiated polyimide with 13 % NaOCl for 10 minutes resulted in overall decrease in the absorbance intensities across the major functional groups that have been identified according to Table 4.1. A similar trend as observed in the 5 minutes of polyimide etching appears consistent in the 10 minutes treatment, with a new peak observed at  $2343\text{ cm}^{-1}$ . This peak has been identified due to a methyl group according to Zhang *et al.*, (2007). The tight chain packing of the polyimide structure could have been affected during etching time.



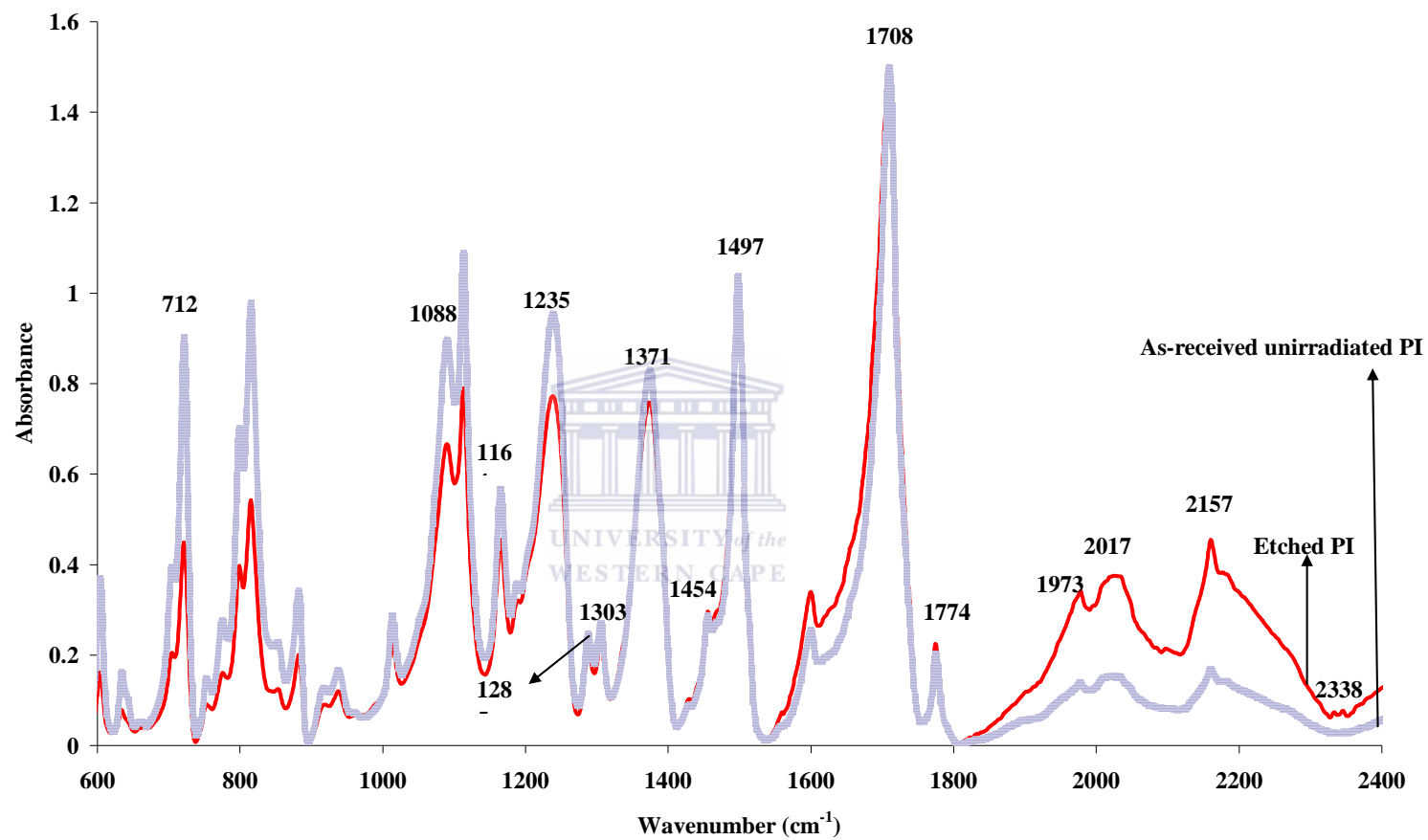


Figure 4-8: FTIR of unirradiated polyimide and 20 minutes 13% NaOCl etched unirradiated polyimide

The spectra in fig. 4.7 represent the unirradiated polyimide and the 20 minutes etched unirradiated polyimide film. The etching was performed in 13 % NaOCl solution. It could be observed that there was a continuous decrease in the absorption bands intensity across the functional groups of the etched polyimide sample compared with the untreated commercial polyimide film. The absorption bands from  $1774\text{ cm}^{-1}$  to  $1454\text{ cm}^{-1}$  remained unaffected for the etched polyimide sample. This may be attributed to the rigidity of the polyimide film, since these bonds regions make up the polyimide backbone structure hence their high resistance to chemical attack. The absorption band at  $1973\text{ cm}^{-1}$ ,  $2017\text{ cm}^{-1}$ ,  $2157\text{ cm}^{-1}$  and  $2338\text{ cm}^{-1}$  became visible for this treatment time.



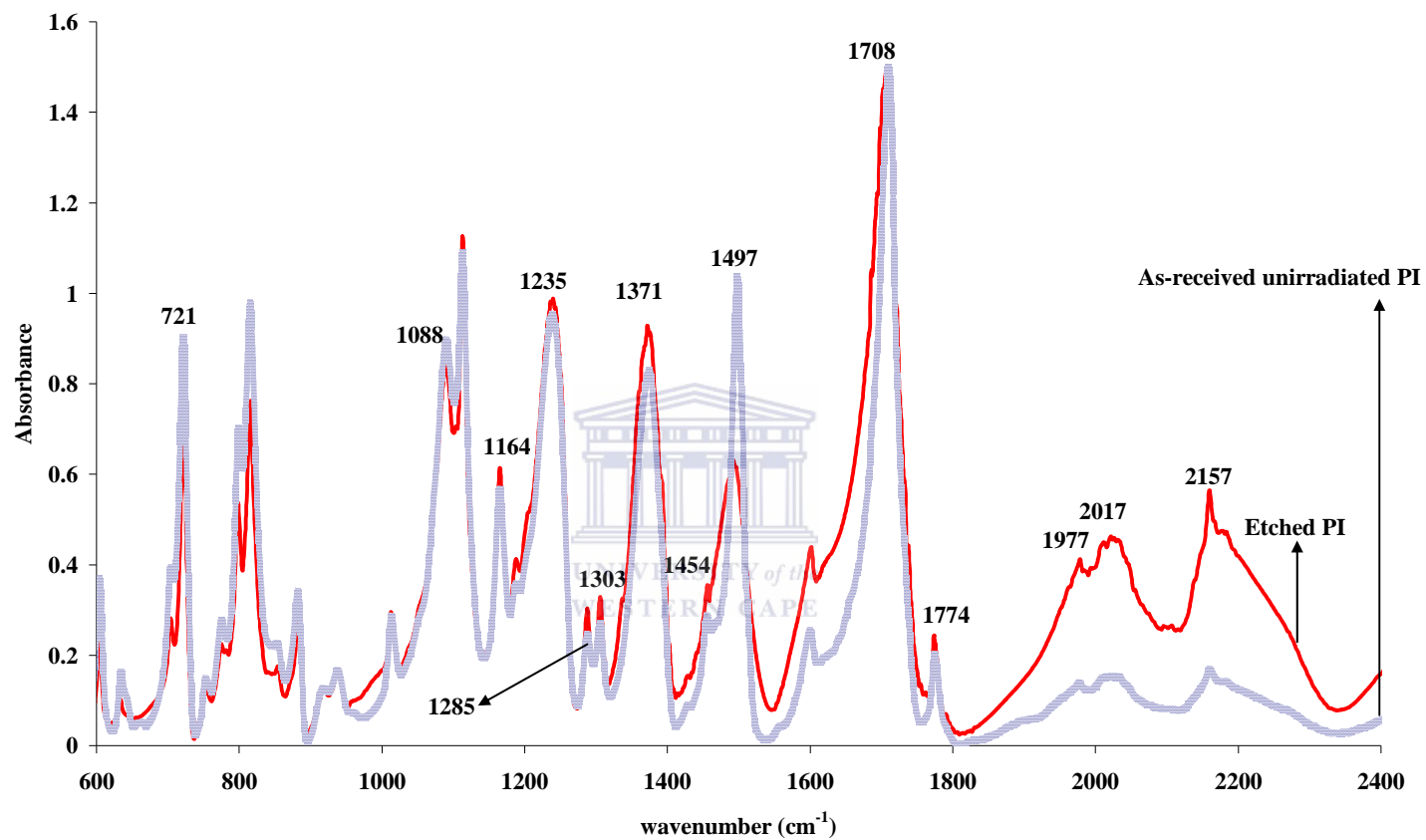
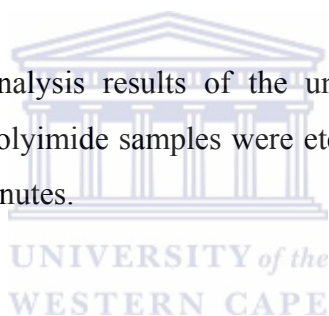


Figure 4-9: FTIR of unirradiated polyimide and 30 minutes 13 % NaOCl etched unirradiated polyimide

In figure 4.8, after the 30 minutes of etching the unirradiated polyimide film in 13 % NaOCl solution, it can be seen that the absorption band at  $1454\text{ cm}^{-1}$  and  $2343\text{ cm}^{-1}$  had disappeared and the absorption at  $1497\text{ cm}^{-1}$  showed reduced intensity. The 30 minutes etching seems to affect the selective chain structures such as the absorption band at  $1497\text{ cm}^{-1}$ ,  $1977\text{ cm}^{-1}$ ,  $2017\text{ cm}^{-1}$  and  $2157\text{ cm}^{-1}$ . The emergence of these bonds varied from other polyimide samples at lower etching time. The absorption peak at  $2338\text{ cm}^{-1}$  was absent while peaks at  $1708\text{ cm}^{-1}$  and  $1774\text{ cm}^{-1}$  did not show any significant change in absorption intensity as compared with the untreated polyimide sample.

#### **4.4.2 FTIR of unirradiated polyimide etched with 0.4M NaOH solution**

In this section, the FTIR analysis results of the unirradiated polyimide will be presented. The unirradiated polyimide samples were etched with 10 mL 0.4M NaOH solution for 5, 10, 20 Or 30 minutes.



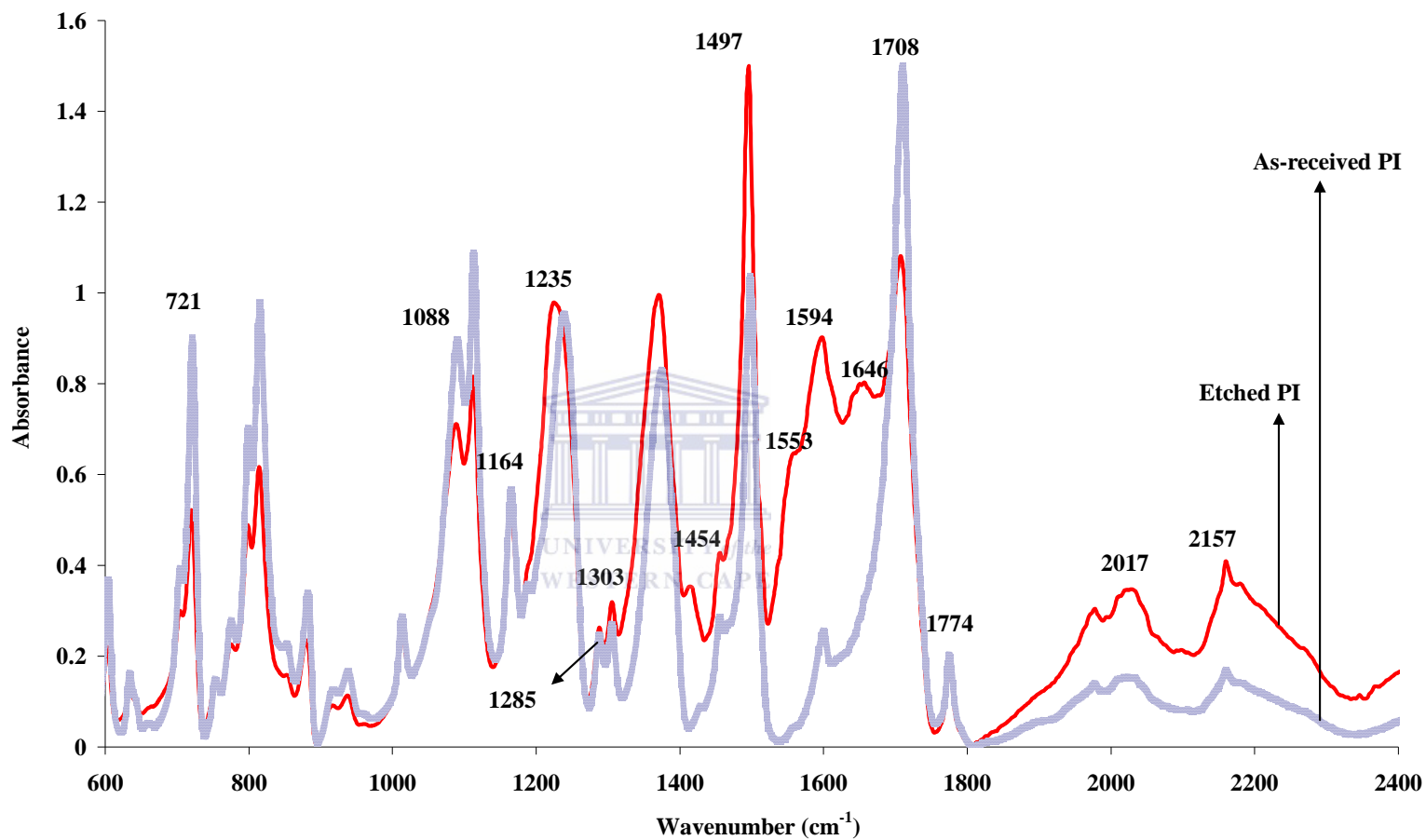


Figure 4-10: FTIR of unirradiated polyimide and 5 minutes 0.4 M NaOH etched unirradiated polyimide

Fig. 4.9 represents the FTIR spectra of etched polyimide film in 0.4 M NaOH solution for 5 minutes. The spectra showed reduced band intensity at  $721\text{ cm}^{-1}$  assigned to imide ring deformation in the polyimide structure. The amide stretch region which lies between  $1164\text{ cm}^{-1}$  and  $1491\text{ cm}^{-1}$  can be seen to show a new peak at  $1454\text{ cm}^{-1}$ , a shoulder at  $1550\text{ cm}^{-1}$  and a bump can be seen at  $1690\text{ cm}^{-1}$ . These new peaks suggest opening of amide ring and the ketone bonds associated with these absorption bands and agreed with the result of Mathakari *et al.*, (2009). This could suggest that a strong chemical reactivity between the NaOH solution and amide functional which may result in the reorientation amide/imide chain and molecular rearrangement after etching.



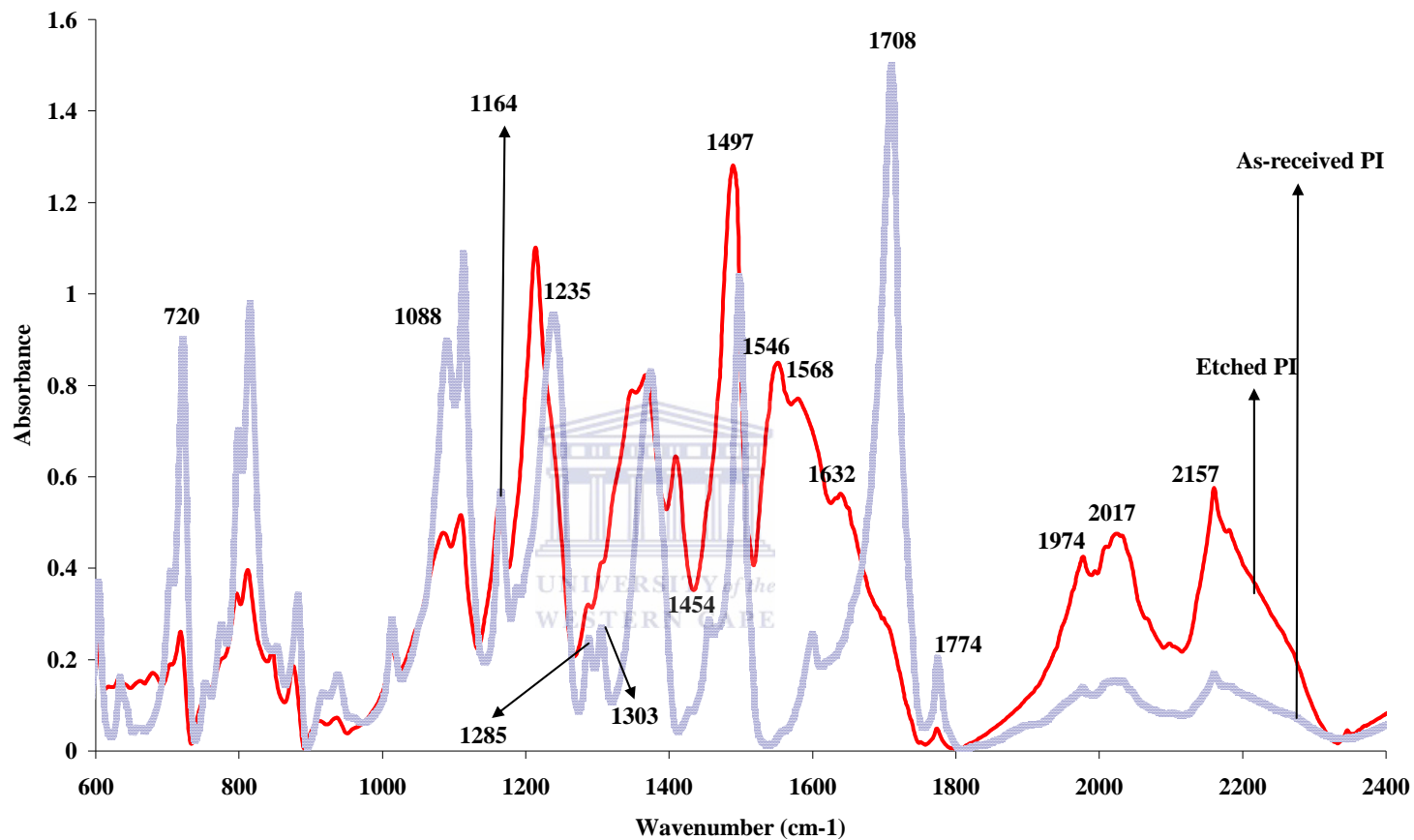


Figure 4-11: FTIR of unirradiated polyimide and 10 minutes 0.4 M NaOH etched unirradiated polyimide



The etching of polyimide in 0.4 M NaOH solution is presented in figure 4.10 for the 10 minutes etching time. It can be observed that some new absorption bands emerged after etching the polyimide samples. These bands are; 1400  $\text{cm}^{-1}$ , 1546  $\text{cm}^{-1}$ , 1575  $\text{cm}^{-1}$  and 1633  $\text{cm}^{-1}$ . The absorption band intensity at 1708  $\text{cm}^{-1}$  was completely eliminated while absorption at 1774  $\text{cm}^{-1}$  showed a reduced intensity. The effect of NaOH on the imide-amide ring of the polyimide appeared significant hence could result in ring opening and formation of polyamates structure. In effect, the availability of metal for ion exchange capacity could be enhanced since the affected bands constitute the polyimide backbone structure. The results agreed with the account of Yi *et al.*, (2004). Their work reported a superimposition of the amide I (1650  $\text{cm}^{-1}$ ) and the amide II bonds located at 1550  $\text{cm}^{-1}$  due to a broad spread of absorption bands at 1500 - 1700  $\text{cm}^{-1}$  after surface treatment of polyimide with 0.5 M KOH solution.



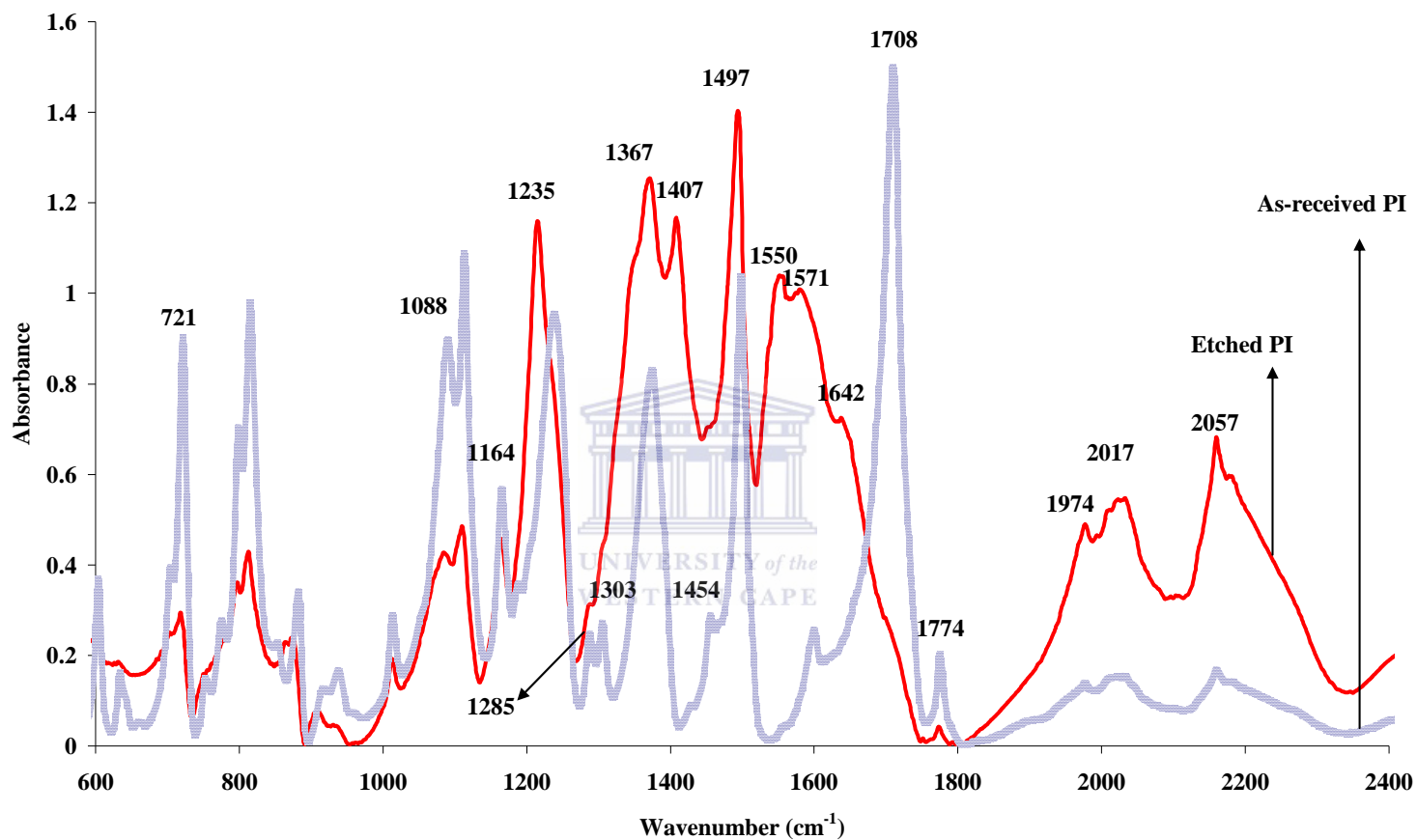


Figure 4-12: FTIR of unirradiated polyimide and 20 minutes 0.4 M NaOH etched unirradiated polyimide

After 20 minutes of etching unirradiated polyimide sample, it can be seen that the following absorption bands were reduced  $721\text{ cm}^{-1}$  and  $1774\text{ cm}^{-1}$ . This was also noticed for the 10 minutes treated polyimide sample. These bands are the imide deformation and cyclic imide bending respectively. The absorption bands located at  $1400\text{ cm}^{-1}$ ,  $1546\text{ cm}^{-1}$ ,  $1575\text{ cm}^{-1}$  and  $1633\text{ cm}^{-1}$  are still obvious but not with the intensity noticed for the 10 minutes etched sample. This suggests a continuous effect of the etchants on the polyimide backbone and the cyclic ring in the polyimide structure.



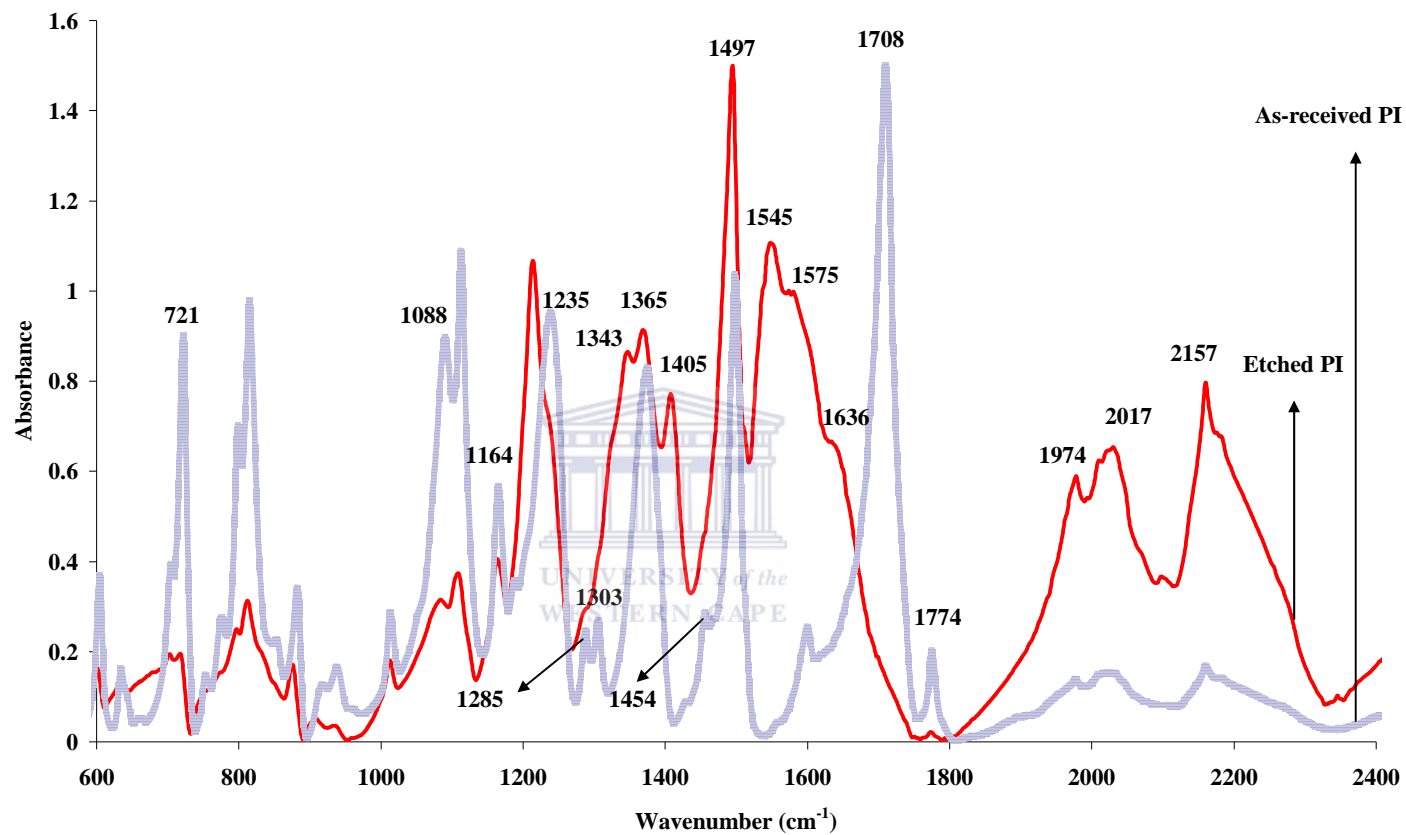


Figure 4-13: FTIR of unirradiated polyimide and 30 minutes 0.4 M NaOH etched unirradiated polyimide

Figure 4.12 represent the 30 minutes etched polyimide sample. It can be seen from the IR spectra that the characteristic absorption bands intensities have been significantly reduced. The bands at  $721\text{ cm}^{-1}$ ,  $1164$  and  $1088\text{ cm}^{-1}$  appeared reduced while there was complete elimination of absorption bands at  $1285\text{ cm}^{-1}$ ,  $1454\text{ cm}^{-1}$ ,  $1708\text{ cm}^{-1}$  and  $1303\text{ cm}^{-1}$ . The band at  $1774\text{ cm}^{-1}$  can be seen but at a more reduced intensity. The 30 minutes etching of the unirradiated polyimide can be seen to undergo significant molecular rearrangement due to the elimination and emergence of new bands. The IR study from fig. 4.12 can suggest that the treatment of the polyimide sample in 0.4 M NaOH has resulted in the creation of new functionality where the backbone structure of the polyimide altered.



#### ***4.4.3 FTIR of unirradiated polyimide etched with 0.4M NaOH dissolved in 13 % NaOCl solution***

A mixture of 0.4 M NaOH and 13 % NaOCl solution was prepared according to the procedure in section 3.2.1.4. The unirradiated polyimide samples were etched in the solution 5, 10, 20 or 30 minutes.



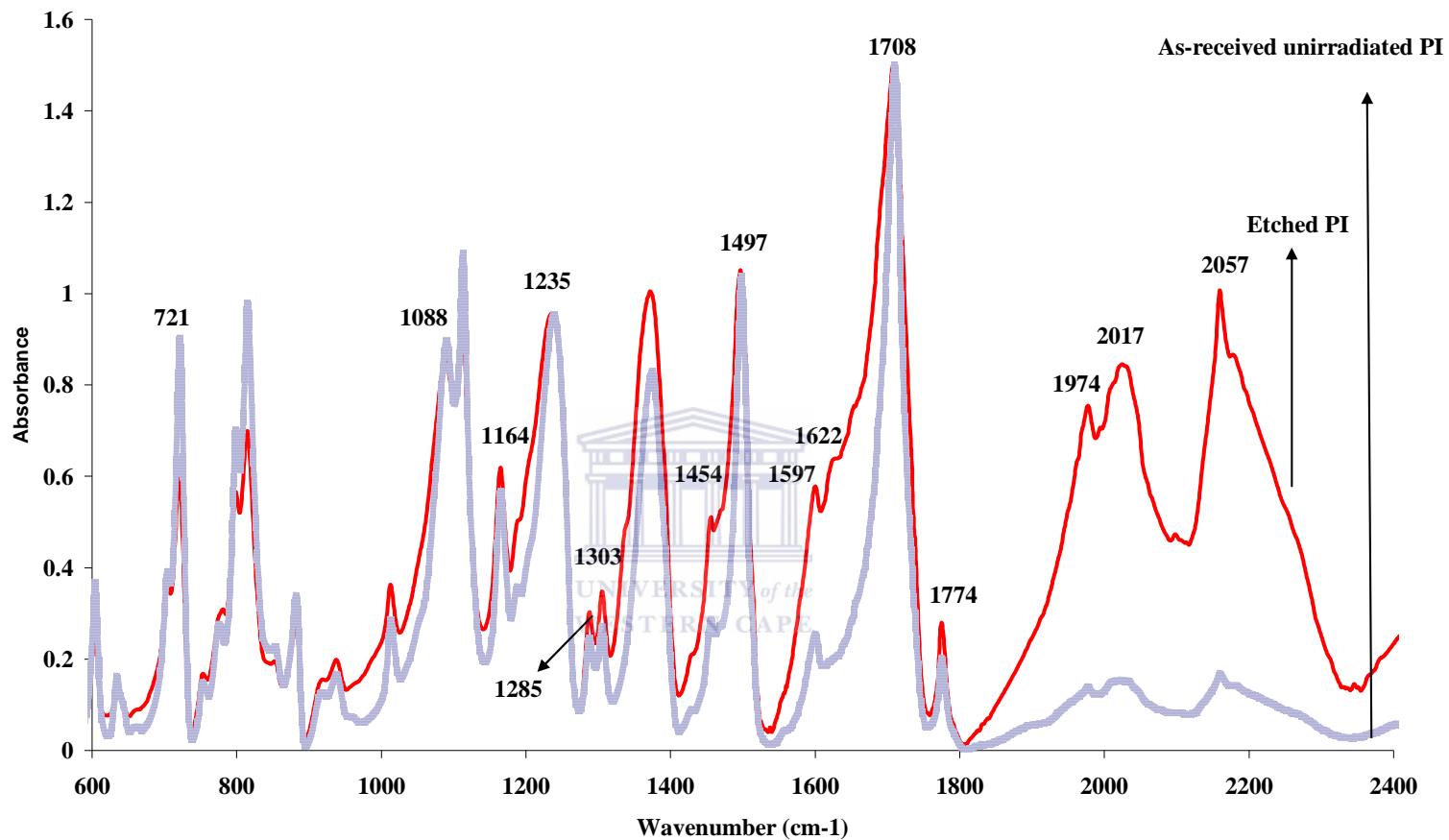


Figure 4-14: FTIR of unirradiated polyimide and 20 minutes 0.4 M NaOH/13 % NaOCl etched unirradiated polyimide

Figure 4.13 represents the polyimide film etched with 0.4M NaOH dissolved in 13 % NaOCl solution. This spectra is for the 20 minutes etching time. The absorption band appeared similar for the unirradiated and the etched polyimide sample except for a bump peak which appeared around  $1622\text{ cm}^{-1}$  and the increased absorption intensities noticed at  $2017\text{ cm}^{-1}$  and  $2057\text{ cm}^{-1}$ . The relative stability of the spectrum of the etched polyimide with the as-received polyimide sample can be attributed to the fact that the mixture of NaOH/NaOCl did not result in any significant change in the polyimide functionality after etching.

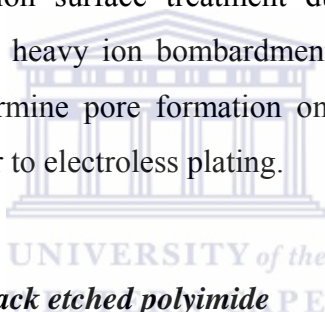




## 4.5 SURFACE TREATMENT OF IRRADIATED POLYIMIDE FILM

### 4.5.1 Introduction

This section will discuss the results of irradiated polyimide samples after etching in NaOCl and mixture of NaOH/NaOCl solutions. The procedures and conditions of etching have been discussed in section 4.5 and 4.6. The aim of this section is to understand if etching of irradiated polyimide would enhance the surface changes after etching and to make a comparison with the unirradiated polyimide samples and literatures. The samples of PI for heavy ion bombardment was performed in Russia and due to time constraint on the project, only alkaline chemical etching was done after the heavy ion irradiation surface treatment due to the non-availability of accelerator in SA to perform heavy ion bombardment. A detailed analysis such as cross-sectional study to determine pore formation on polyimide surface of etched irradiated PI is necessary prior to electroless plating.



### 4.5.2 Characterisation of track etched polyimide PE

The depth profile of track etched polyimide film (after etching with NaOCl, NaOH or NaOH/NaOCl solutions) is important for the application polyimide in gas separation. This section will present the characterisation of the etched polyimide films using the FTIR, SEM and hydrogen diffusion techniques. After etching in alkaline solutions, the samples were characterised using FTIR to examine any variance in absorption band intensity due to the difference in etching time. The surface morphology of the irradiated samples was studied by SEM in other to investigate surface roughness and pores distribution and shapes before and after etching. The pore depth profile on the polyimide samples after etching was studied using the hydrogen diffusion measurement.

#### 4.5.2.1 Visual inspection

The track etched polyimide samples were subjected to visual inspection. Polyimide film colour and texture were examined. A colour change from amber to yellow was observed after etching of the irradiated polyimide samples compared to the unetched samples. The colour change was similar for NaOCl and NaOH solutions track etched polyimide samples. It was noticed that after 30 minutes of etching, colour change of the track etched polyimide film was more intense which suggest strong chemical interaction between the etchants and the polyimide samples. The surface textures of the samples were observed to become coarse as a function of etching time.

#### 4.6 MORPHOLOGICAL STUDY BY SCANNING ELECTRON MICROSCOPY (SEM) OF IRRADIATED POLYIMIDE ETCHED WITH 13 % NaOCl AND 0.4M NaOH/13 % NaOCl SOLUTIONS.

This section will present the SEM results (Fig. 4.14 and Fig 4.16) of the track etched polyimide film. The etchings of the irradiated polyimide samples were limited to the use of NaOH/NaOCl and NaOCl solutions. These etchants were selected since etching rate depends on the etching temperature and active chlorine concentration of the etchants (Sudowe *et al.*, 2001). The surface morphology of the track etched polyimide film was studied to determine the depth profile through pores formation, pore distribution and pore sizes after the samples were etched. The etching of the samples was performed in NaOH and NaOCl solutions under same conditions as previously discussed in section 3. The average pores diameter (Fig. 4.15) of the track etched polyimide samples was measured as ( $\sim 0.43 \mu\text{m}$ ) for 0.4 M NaOH/13 % NaOCl solution and ( $0.51 \mu\text{m}$ ) for 13 % NaOCl solution. The similarity of pore sizes after etching the polyimide samples in different solutions further confirms the FTIR results where the absorption spectra as seen in Fig 4.19 – Fig. 4.22. The SEM morphological results for the track etched polyimide samples after etching with NaOH/ NaOCl solutions are presented below. The overall effect of etching of irradiated polyimide surface was studied using the SEM technique. The samples were etched for 10, 15,

20, 30, 40 or 60 minutes. The pore size, pore distribution and surface roughness of the polyimide samples after etching were imaged and carefully examined.



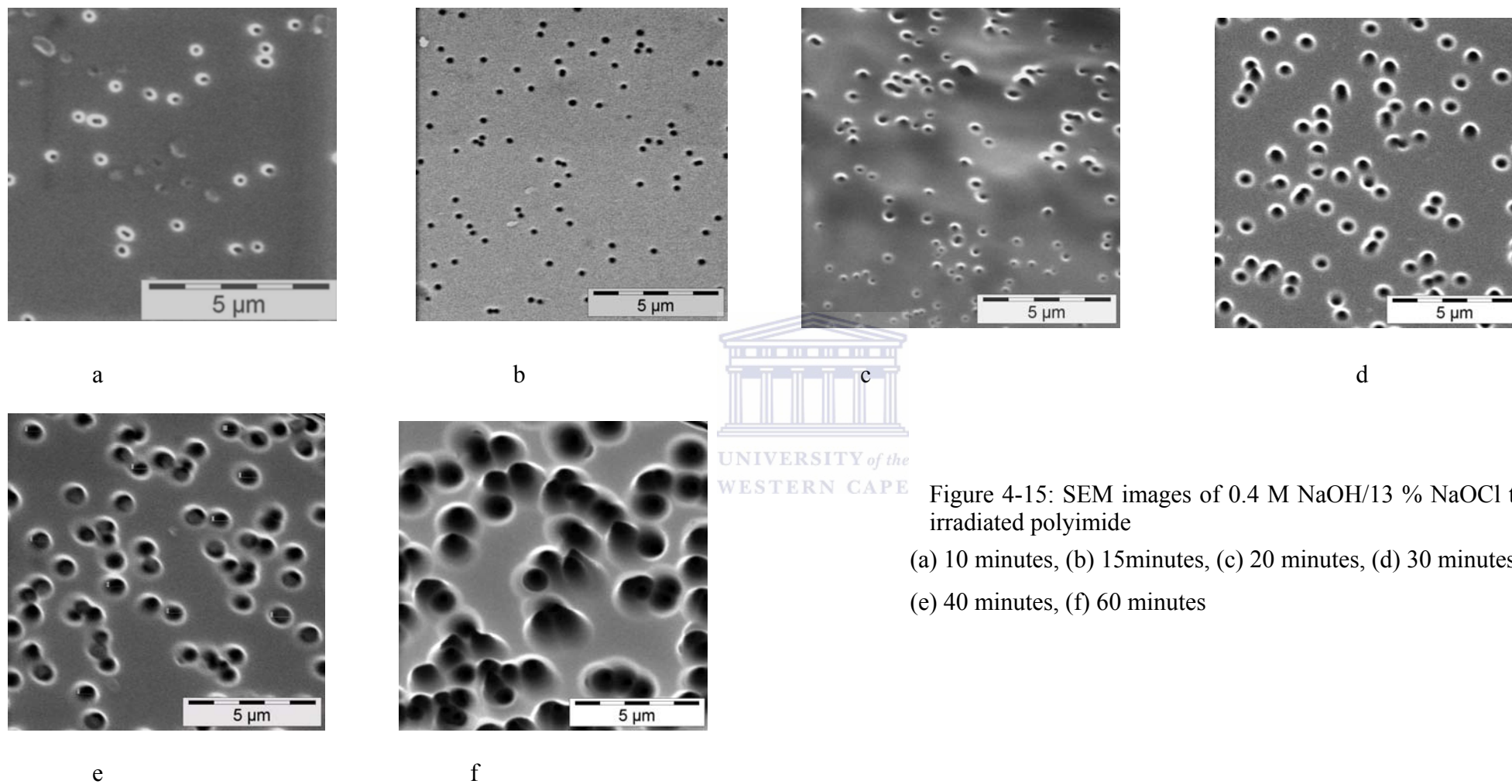


Figure 4-15: SEM images of 0.4 M NaOH/13 % NaOCl track etched irradiated polyimide

(a) 10 minutes, (b) 15 minutes, (c) 20 minutes, (d) 30 minutes,  
(e) 40 minutes, (f) 60 minutes

The SEM surface morphology was obtained at 10,000x magnification so as to image the surface of the polyimide samples and investigate the pore sizes and determine the surface roughening effects due to etching time.

Fig. 4.14 (a) - (f) represents the SEM analysis of the irradiated polyimide samples etched with 0.4M NaOH dissolved in 13 % NaOCl solution. The etching of the samples indicated the creation of pores on the polyimide surface. The pores appeared circular and dispersed according to fig. 4.14 (a) - (c) when shorter etching time was used (10 - 30 minutes). An increase in the etching time showed pore walls being destroyed and pores becoming enlarged at longer etching time of 60 minutes as observed in fig. 4.14 (d) - 4.14 (f). The pores of the etched film appeared conical in shape as observed in the surface after longer etching time. Also, the SEMs of polyimide surface samples indicated an increase in the film surface roughness with an increase in etching time. It was observed that the pore increased after the 20 minutes etching time. The pore size distribution was calculated and confirmed from the SEM images using the arbitrary measurement technique. The pore density from of the polyimide samples (Fig. 4.14d – 4.14f) agreed with the study of Mitrofanov *et al.*, (2006). A significant improvement from the result obtained in this work is the use of lower etching temperature (50 °C), lower concentration of etchant (0.4 M NaOH) and reduced time of etching (60 minutes). Mitrofanov *et al.*, (2006), reported the treatment of polyimide film at 80 °C. In the work of Mu *et al.*, (2010), higher concentration of 2.5 M NaOH was employed for 12 hours. According to Schiedt (2007), 5 M NaOH was used to etch polyimide film at 60 °C and 13 % NaOCl solutions at 55 °C for an average of approximately 4 hours treatment time. By using low temperature, lower etchant concentration and shorter time, this study successfully demonstrates that the depth profile and size of the pore formation can be controlled according to the results obtained from the SEM and pore size distribution reported.

#### 4.6.1 The pore size distribution of track etched polyimide using 0.4 M NaOH/ 13 % NaOCl mixture and 13 % NaOCl solutions

The graph below represents the pore radii measurement of tracked etched membrane. The pores were measure for each polyimide samples and compared for the two differently track etched polyimide film. This was to compare the effect of rate of etching as a function of time on the pore size of the track etched samples.

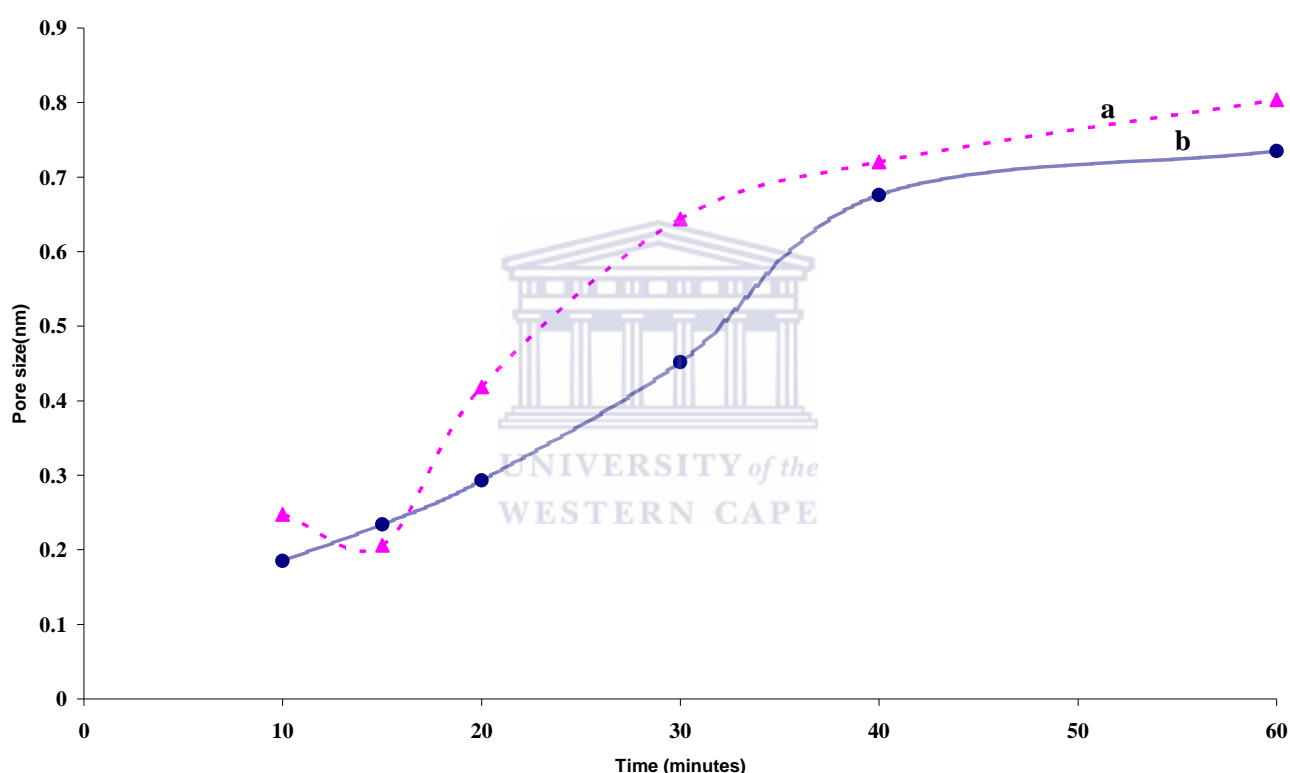


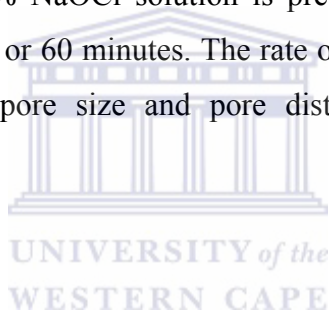
Figure 4-16: Graph with the compared pore size of track etched polyimide with (a) 13 % NaOCl and (b) 0.4M NaOH/13 % NaOCl

The pore size measurement graphs are presented in Fig. 4.15 to show the relationship of pore diameter as a function of the etching time. The graph represents track etched polyimide samples of NaOH/NaOCl solution and NaOCl solution. From the graph obtained in Fig 4.15, there is a linear relationship between etching time and pore radii. It was observed that the longer the etching time, the larger the pore radii. For

NaOH/NaOCl track etched polyimide, the pore diameter was measured as 0.19  $\mu\text{m}$  and 0.73  $\mu\text{m}$  as smallest and largest pore radii respectively. As for the NaOCl track etched polyimide film, pore radii were 0.25  $\mu\text{m}$  and 0.80  $\mu\text{m}$  as the smallest and largest pore diameter. This increase in pore suggests that chemical etchants are more readily available to act on the tracks bombarded with heavy ion after a prolonged time thereby creating more pores (Mitrofanov *et al.*, 2006).

#### **4.7 SCANNING ELECTRON MORPHOLOGICAL STUDY FOR NaOCl TRACK ETCHED POLYIMIDE SAMPLES**

In the SEM images below (Fig. 4.16), the morphological study of the track etched polyimide samples with 13 % NaOCl solution is presented. The etching time was varied from 10, 15, 20, 30 40 or 60 minutes. The rate of NaOCl etching as a function of surface pore formation, pore size and pore distribution were examined and discussed.



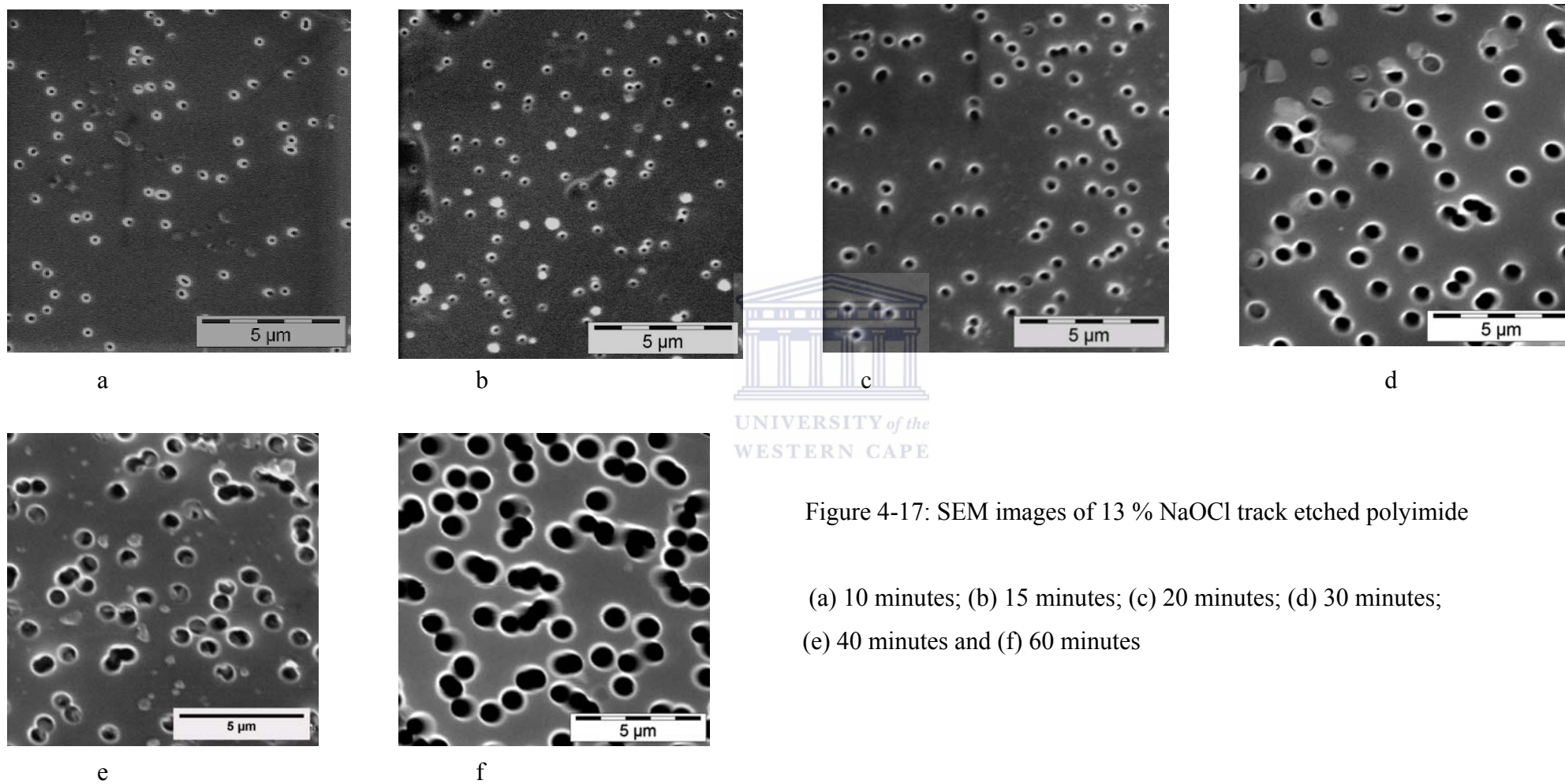
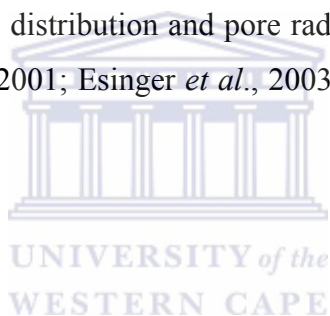


Figure 4-17: SEM images of 13 % NaOCl track etched polyimide

(a) 10 minutes; (b) 15 minutes; (c) 20 minutes; (d) 30 minutes;  
(e) 40 minutes and (f) 60 minutes



Fig 4.16 represent track etched polyimide using 13 % NaOCl solution between 10 – 60 minutes etching time. From the SEM images above, it was observed that the pores are well ordered, randomly distributed and there was a progressive increase in pore formation on the polyimide surface as a function of etching time. Also, the time of etching was seen to have destroyed the pore walls thereby increasing the pore diameter after etching for 60 minutes as seen in Fig. 4.16f. In Fig. 4.16d which represented track etched polyimide sample after 30 minutes, it was observed that the process of pore formation was probably the function of chemical reactivity between the polyimide surface and etchants to reveal the ion track areas. The pores showed circular shapes and the pore diameter graph in Fig. 4.15 showed that the pore diameter increased as a function of etching time. The rate of pore formation could have been due to the thickness of the polyimide film according to Esinger (2007). The overall effect of pore formation, pore distribution and pore radii after irradiation agreed with other reports (Sudowe *et al.*, 2001; Esinger *et al.*, 2003; Esinger 2007; Esinger *et al.*, 2010).



#### 4.7.1 Hydrogen diffusion measurement of 0.4 M NaOH/13 % NaOCl track etched polyimide sample

The hydrogen diffusion measurement was performed on track polyimide sample etched with NaOH/NaOCl solution. This result is to investigate the effect of pore radii on the permeation of hydrogen gas. The graphs below represent a compared hydrogen permeation study of different track etched polyimide samples at different time. The diffusion test was performed in the home-grown hydrogen diffusion reactor unit.

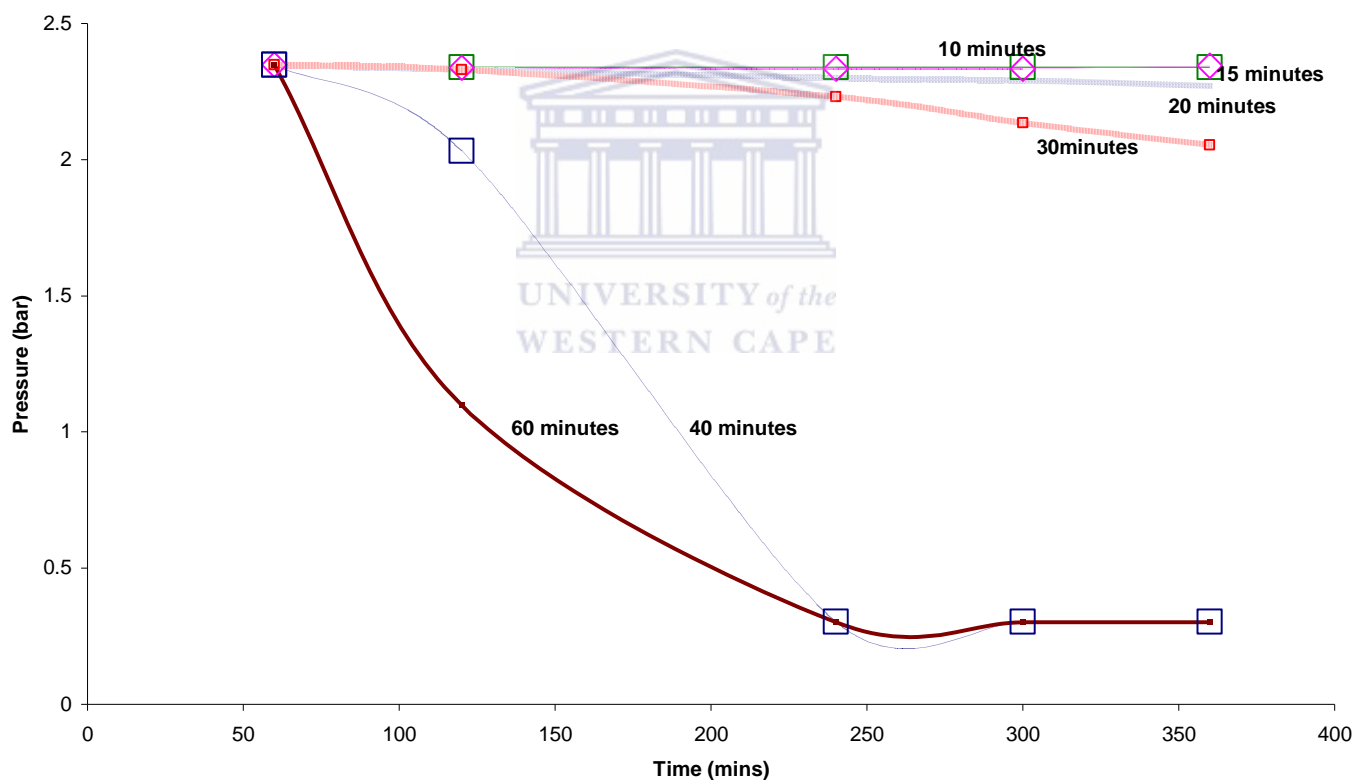
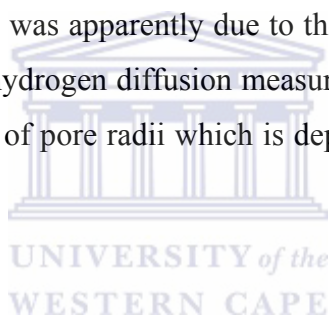


Figure 4-18: Hydrogen diffusion test for 0.4 M NaOH/13 % NaOCl track etched polyimide

Fig. 4.17 showed the rate of hydrogen gas permeation across the track etched polyimide surface after etching for 10, 15, 20, 30, 40 and 60 minutes in NaOH/NaOCl

solution. The diffusion measurement was performed for about 7 hours as a function of pressure drop for each sample. From the result above, the rate of diffusion of hydrogen was relatively stable until after the 30 minutes etched sample. The diffusion of hydrogen for the 10 minutes and 15 minutes sample was identical and relatively stable for almost 4 hours with pressure drop values 2.348 bar to 2.344 bar. This was expected since the etching time was minimal hence formation of pore diameter was small for any fast rate of hydrogen diffusion. As from the 20 minutes etching time, the rate of diffusion can be seen to occur gradually than the 10 and 15 minutes since the pore radii have increased while the corresponding pressure drop value was 2.27 bar after about 3 hours of diffusion measurement. The diffusion rate after 30 minute was relatively steady as pressure as indicated in the pressure drop value of 2.054 bar. For the 40 and 60 minutes etched samples, there was fast hydrogen diffusion kinetic with a sharp drop in pressure. This was apparently due to the large pore radii after etching above 40 minutes. From the hydrogen diffusion measurement, it was obvious that the rate of diffusion is a function of pore radii which is dependent on the time of etching of polyimide samples.



The graphs below represent the hydrogen diffusion measurement of 13 % NaOCl track etched polyimide.

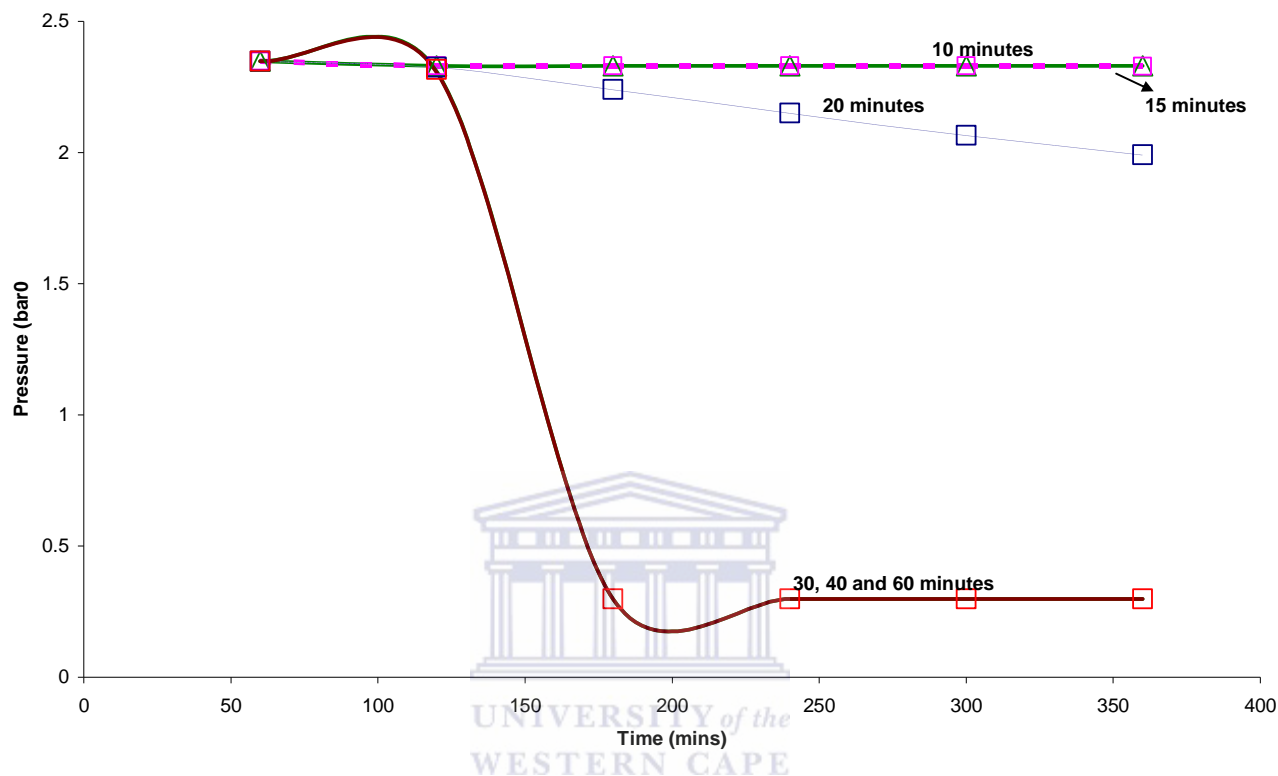


Figure 4-19: Hydrogen diffusion test for 13 % NaOCl track etched polyimide

In Fig. 4.18, the hydrogen diffusion analysis graphs of track etched polyimide samples for 10, 15, 20, 30, 40 and 60 minutes. From the result above, the 10 and 15 minutes track etched polyimide samples indicated identical diffusion rate. The pressure values dropped from 2.350 bar to 2.329 bar after about 6 hours of diffusion measurement. It could be seen that hydrogen diffusion across 10 and 15 minutes track etched samples did not show significant difference unlike the 20 minutes track etched polyimide film. As for the 20 minutes track etched sample, a steady rate of diffusion was observed while 1.991 bar was recorded as the pressure drop after about 6 hours. After 30 minutes of etching, the rate of diffusion increased which indicated the effect of pore radii on gas permeation across track etched polyimide surface.

#### ***4.7.2 FTIR spectra of irradiated polyimide etched with 0.4M NaOH dissolved in 13 % NaOCl solution***

The FTIR spectra will be presented for the irradiated polyimide etched with 0.4 M NaOH dissolved in 13 % NaOCl solution. The FTIR results presented represent a comparison of spectra for the unirradiated polyimide film and the irradiated polyimide etched between 10 minutes and 60 minutes. The first section of the IR spectra will focus on the deformation of the imide ring which is located at  $720\text{ cm}^{-1}$  while second section of the FTIR covered from  $2000\text{ cm}^{-1}$  to  $1200\text{ cm}^{-1}$  where other functional groups (table 4.1) of interest in the polyimide structure are present.



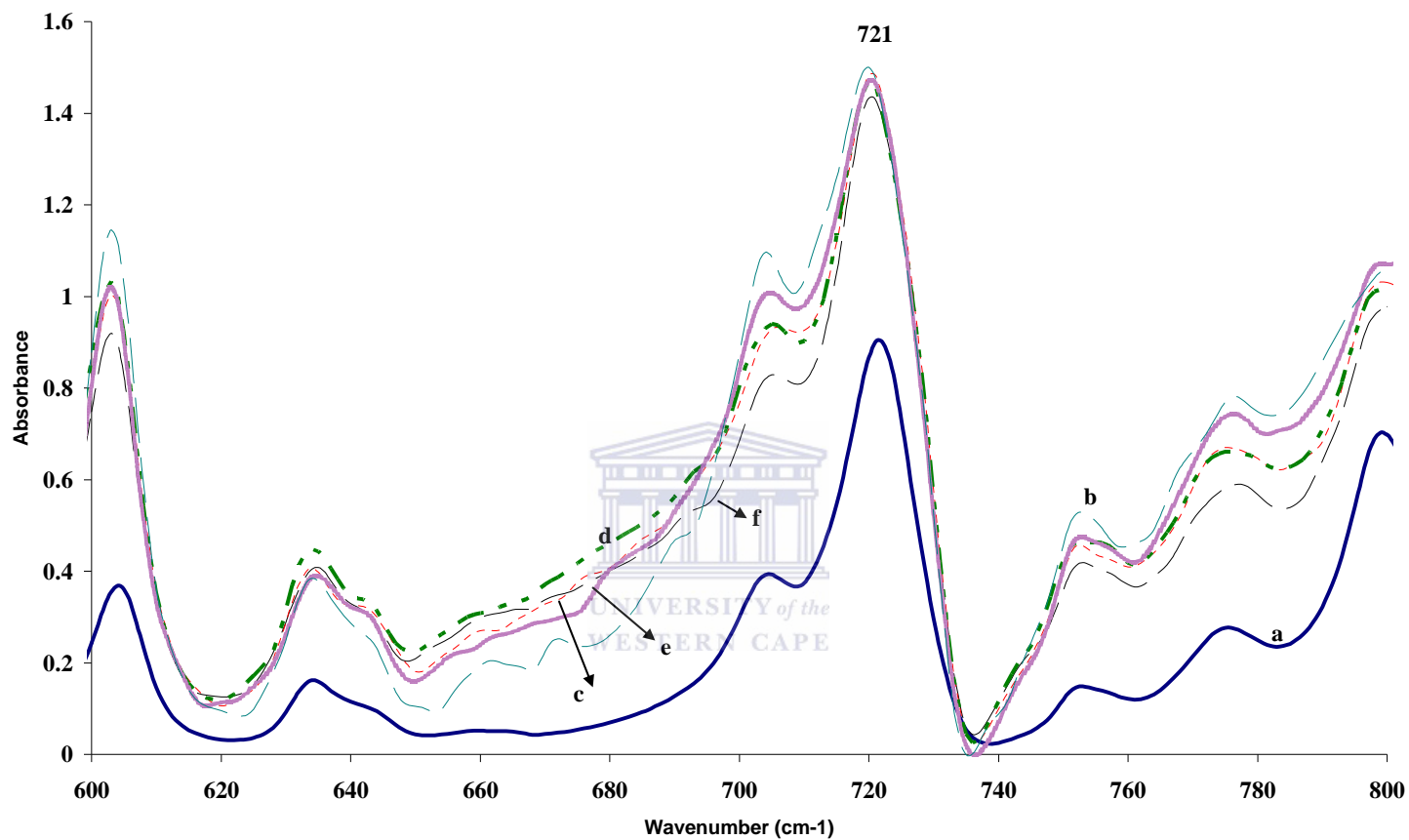


Figure 4-20: Compared FTIR (800-600cm<sup>-1</sup>) spectra of irradiated polyimide etched with 0.4M NaOH/13 % NaOCl solution (a) As-received polyimide, (b) 10 minutes etched, (c) 20 minutes etched, (d) 30 minutes etched, (e) 40 minutes etched and (f) 60 minutes etched.

The spectra of irradiated polyimide spectra are compared in figure 4.19 after etching in 0.4 M NaOH/NaOCl solution. Almost all of the absorption bands for the functional groups increased in intensity compared to the unirradiated sample shown in figure 4.19a. The absorption bands at 720  $\text{cm}^{-1}$  represents the imide deformation bonds and could be seen to increase in absorbance intensity with an increase in time of exposure to the etching solution with peak maximum at 40 minutes treatment time. The increase in the absorption band intensity of the imide deformation bonds as seen from this spectra indicated that the imide deformation bond was not affected by the chemical etchant. Although no direct correlation can be deduced from the absorption intensity and etching time, increase in absorption intensity of these spectra could strengthened the imidization but there is no literature report that has indicated the influence of this absorption band on polyimide reactivity.



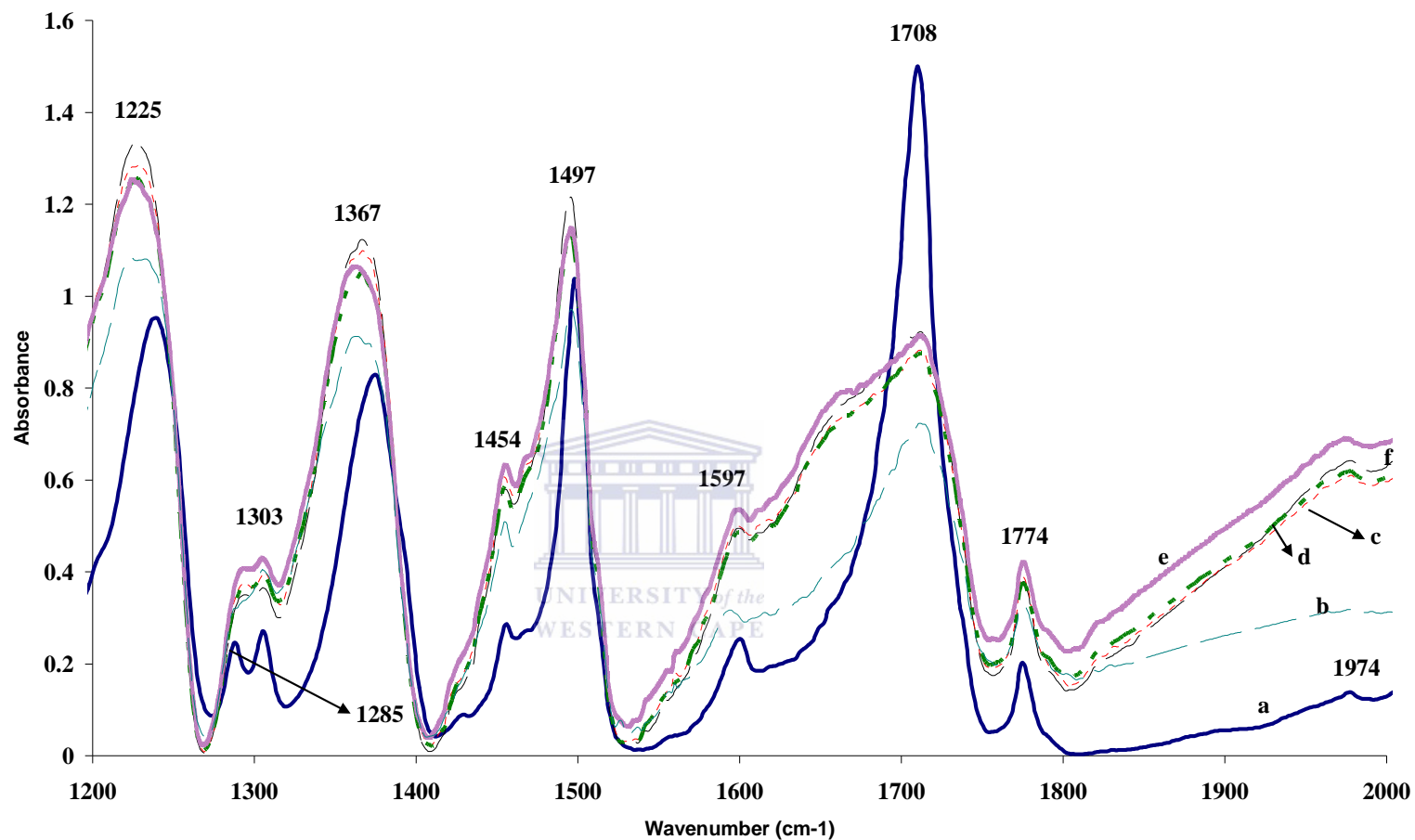


Figure 4-21: Compared FTIR (2000-1200cm-1) spectra of irradiated polyimide etched with 0.4M NaOH/13 % NaOCl solution (a) As-received polyimide, (b) 10 minutes etched, (c) 20 minutes etched, (d) 30 minutes etched, (e) 40 minutes etched and (f) 60 minutes etched.



The IR spectra range  $2000\text{ cm}^{-1}$  –  $1200\text{ cm}^{-1}$  in Fig. 4.20 represents the compared spectra of irradiated polyimide after etching with NaOH/NaOCl solution. It can be observed that the intensity of the imide structures represented by bands at  $1303\text{ cm}^{-1}$  and  $1775\text{ cm}^{-1}$  increased while the peak assigned to imide functional groups at  $1710\text{ cm}^{-1}$  is reduced. The region of  $1650\text{ cm}^{-1}$  (amide 1) and  $1550\text{ cm}^{-1}$  (amide 2), showed broad and reduced intensity compared with the original polyimide structure and agreed with the study of Yi Li *et al.*, (2004) and Mathakari *et al.*, (2009). The broad spectrum observed in  $1650\text{ cm}^{-1}$  (amide 1) and  $1550\text{ cm}^{-1}$  (amide 2) regions has been suggested to result in the formation of polyamate of sodium metal due to the conversion of imide to amide after alkaline hydrolysis. These regions have been reported to serve as ‘cation-exchange’ areas for the alkaline hydrolysed polyimide structure where a cation such as  $\text{Pd}^{2+}$  can substitute during reaction with the sodium polyamates. The ease of cationic exchange could also result from the electropositivity of metals and preferential displacement in a stronger cationic solution bath. Several studies from literature suggested this could be due to the presence of the C=O functional group in the polyimide backbone structure (Yi Li *et al.*, 2004; Mathakari *et al.*, 2009).

At  $1598\text{ cm}^{-1}$ , complete elimination of peak was observed after etching of polyimide structure. The observed peak disappearance at  $1303\text{ cm}^{-1}$  and  $1285\text{ cm}^{-1}$  of imide stretching can be observed for the etched film. An interesting absorption peak could be noticed at  $1708\text{ cm}^{-1}$  with reduced absorbance intensities. These reductions of bands intensities agreed with the work of Yi Li *et al.*, (2004) where they used 0.5 M KOH to etched polyimide at  $50\text{ }^{\circ}\text{C}$  for 20 minutes. They observed a reduction in intensity after polyimide treatment and concluded that this is due to the conversion of imide to amide and superimposition of the amide rings. The tight packing of the imide structure along the backbone of polyimide structure after etching in alkaline solutions could have been responsible for the reduction in absorbance intensity.

#### ***4.7.3 FTIR spectra of irradiated polyimide etched with 13 % NaOCl solution***

The FTIR results for the NaOCl track etched polyimide are presented in this section. The etching procedures have been discussed in previous sections.



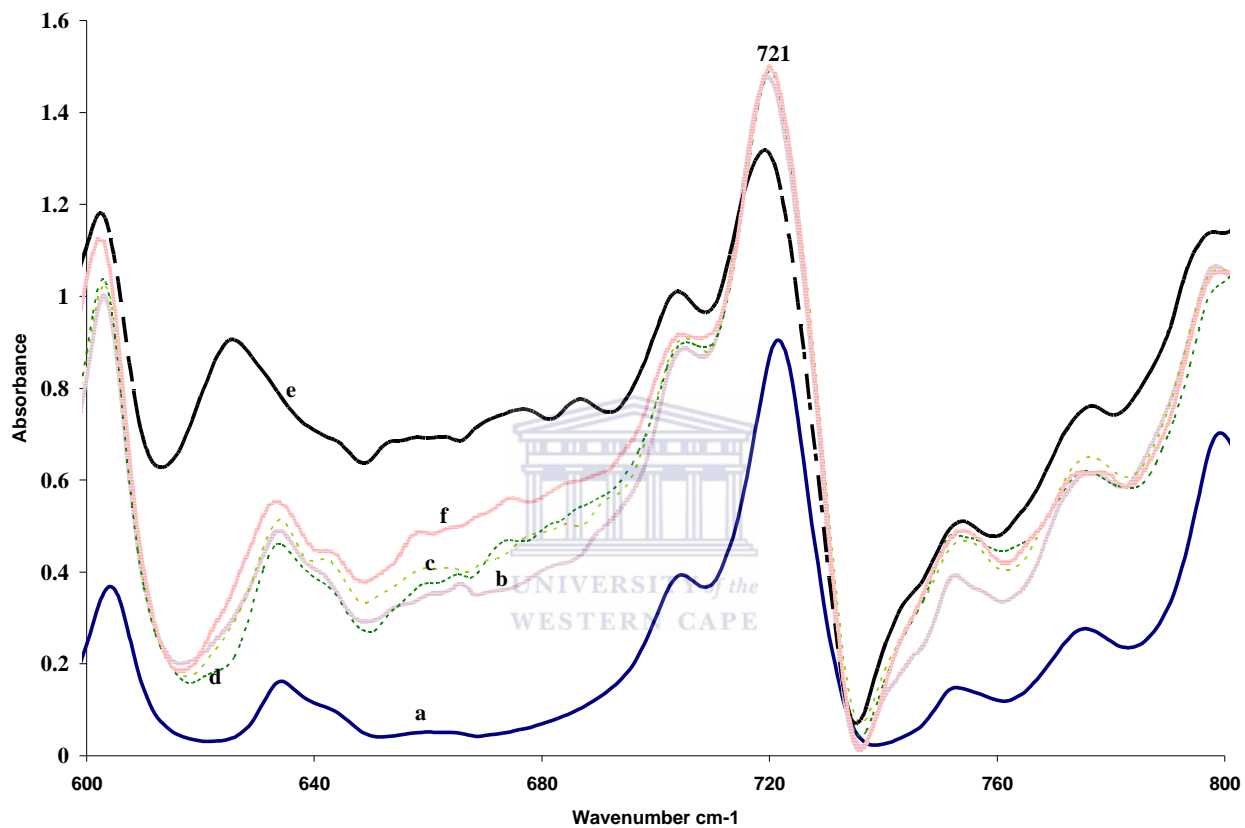


Figure 4.21 Comparison FTIR (800-600  $\text{cm}^{-1}$ ) spectra of irradiated polyimide sample etched with 13 % NaOCl solution; a (As-received polyimide), b (10 minutes), c (20 minutes), d (30 minutes), e (40 minutes) and f (60 minutes).

Figure 4.21 represents the compared spectra of irradiated polyimide etched with 13 % NaOCl solution. The spectra above cover the imide deformation band which is located at  $720\text{ cm}^{-1}$ . The characteristics absorption intensity appeared reduced for all irradiated etched samples. It can be observed from Fig. 4.21e which represent the etching time of 60 minutes appeared reduced and this suggest that the deformation of the polyimide functional groups at  $720\text{ cm}^{-1}$  can be degraded over prolonged time with some few bumps of absorption intensity peaks observed between  $640\text{ cm}^{-1}$  and  $680\text{ cm}^{-1}$ . In literature, there has not been any report of these functional groups in the polyimide structure for these absorption peaks probably because they do not constitute the main chain structures of the polyimide units.



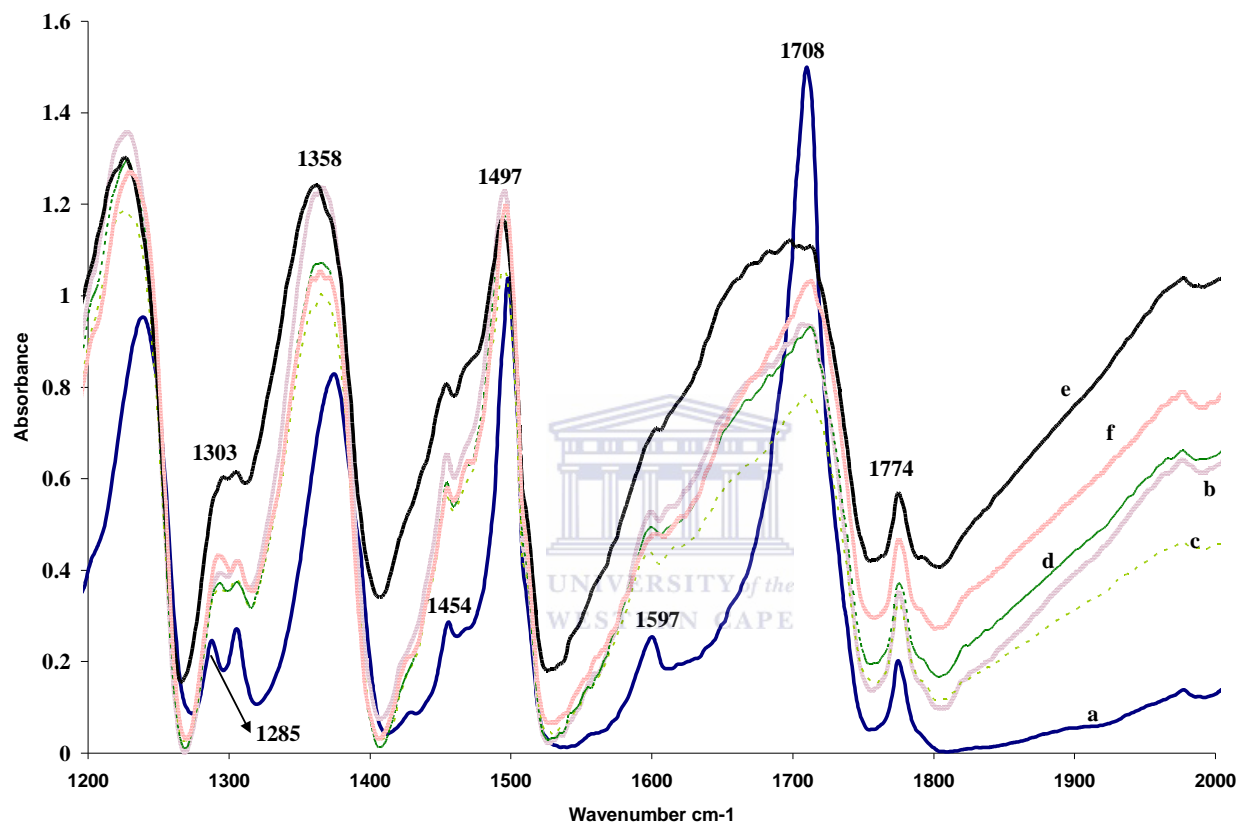
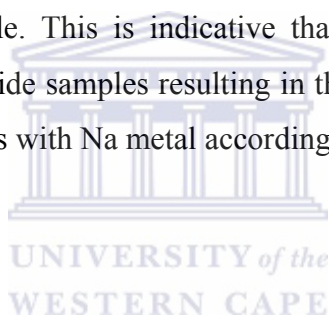


Figure 4. 22 Comparison FTIR ( $2000-1200\text{ cm}^{-1}$ ) spectra of irradiated polyimide sample etched with NaOCl solution; a (As-received polyimide), b (10 minutes), c (20 minutes), d (30 minutes), e (40 minutes) and f (60 minutes).

Figure 4.22 represent the compared spectra of etched irradiated polyimide with 13 % NaOCl solution for 10 or 20 or 30 or 40 or 60 minutes. From the spectra above, it was observed that the peak at  $1285\text{ cm}^{-1}$  completely disappeared after the sample was etched for 60 minutes. This disappearance could be as a result of the opening of the ketone-amide groups thereby making this unit available for metal exchange mechanism. The other peak affected by this surface treatment is the imide ring stretch located at  $1708\text{ cm}^{-1}$ . All the samples showed reduction in the band intensity at  $1708\text{ cm}^{-1}$  with the 60 minutes showing a broad spread of peaks relative to samples. The broad spectrum could be attributed to the degree of distortion of the back bone structure of the polyimide after 60 minutes. The other samples which were treated at lower time appeared to main relative sharp peaks suggesting that the tight chain packing were relatively stable. This is indicative that both solutions can promote identical effect on the polyimide samples resulting in the formation of polyamates by exchange of carboxylic groups with Na metal according to Yi Li *et al.*, (2004).



## CHAPTER 5

### 5.0 RESULTS AND DISCUSSION OF PALLADIUM MODIFIED POLYIMIDE

#### 5.1 CHARACTERIZATION OF PALLADIUM MODIFIED UNIRRADIATED POLYIMIDE

This chapter will focus on the characterisation results of palladium on modified unirradiated polyimide film. Palladium electroless plating was deposited on unirradiated polyimide (Kapton®) because the irradiated polyimide samples could not be afforded due to cost and time constraint. In this section, the results for palladium modified unirradiated polyimide will be presented and discussed. The unirradiated polyimide film (Kapton®) was modified with palladium (see section 3.4) after the polyimide samples have been etched with in separate solutions of NaOH and NaOCl as specified in sections 3.3.1.2 – 3.3.1.4. The palladium modified unirradiated polyimide samples were characterised using, SEM, TEM, TGA, XRD and the peel test. These characterisation techniques were used to determine the surface morphological structure using SEM and TEM analytical techniques. The crystalline structure of the palladium modified samples was investigated with XRD technique (refer to section 3.5.3) while thermal stability of the modified polyimide was measured by TGA analysis as discussed in section 3.5.5. The adhesive strength of palladium on treated polyimide surface was investigated by a peel test section 3.5.6 for the experimental details.

#### 5.2 MORPHOLOGICAL (SEM) STUDY OF UNIRRADIATED PALLADIUM MODIFIED ETCHED POLYIMIDE

The use of electroless deposition of metal on a substrate is considered to be a cheap, simple technique and enhances uniformity of metal films on supports (Li *et al.*, 1998).

Prior to the plating of polyimide with palladium, the surface of the polyimide film was etched to promote adhesion by increasing surface roughness and creating ‘active sites’ along the polyimide for palladium metal exchange. Fig. 5.1 shows SEM micrograph of NaOH etched polyimide, Fig. 5.2 shows SEM micrograph of NaOCl etched polyimide samples and Fig. 5.3 represents the SEM micrograph of NaOCl/NaOH etched polyimide. All the etched polyimide samples were plated with palladium by electroless deposition for 10 minutes according to the experimental approach set out in Fig 3.1 and the etching time for the samples was between 5 minutes to 30 minutes.

**5.2.1 The SEM images below represent NaOH etched polyimide film modified with palladium.**

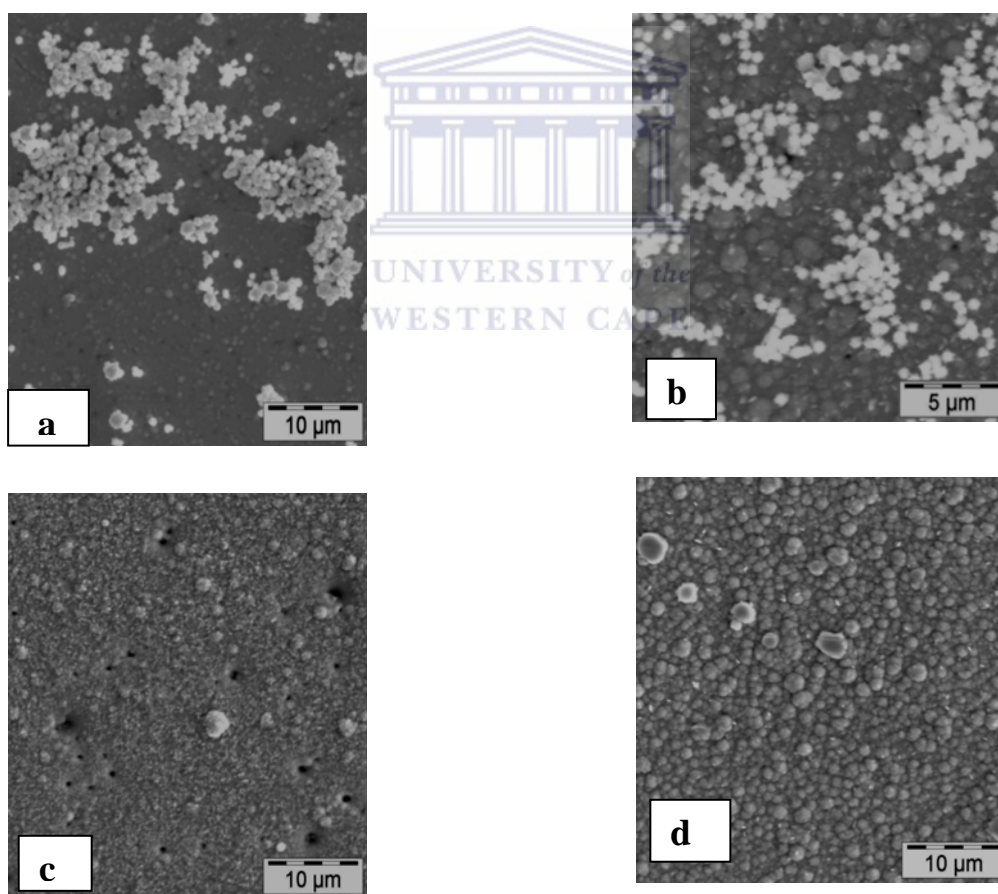


Figure 5-1: SEM micrograph of palladium modified unirradiated polyimide etched with 0.4 M NaOH (a) 5 minutes, (b) 10 minutes, (c) 20 minutes, (d) 30 minutes.



Figure 5.1 (a) – (d) represent the SEM palladium plated unirradiated polyimide after etching in 0.4 M NaOH solution. From the SEM images above, palladium metal particles can be seen to show disperse spherical particles in Fig. 5.1 (a) for 5 minutes palladium modified polyimide. In Fig. 5.1 (b), Fig 5.1 (c) and Fig. 5.1 (d) which represent the 10, 20 and 30 minutes etched polyimide samples; the dense layer of palladium particles structure appeared to increase with the surface etching time. In Fig. 5.1 (c), the rate of nucleation appears prevalent while Fig. 5.1 (d) shows increase in the growth of the palladium particles. The dense metal layer can increase the palladium-polyimide interlocking matrix through depth profile of palladium with the available active in the polyimide structure after etching thereby increasing adhesion strength of polyimide film. The palladium particles particle growth seems to occur via the ‘Stranski-Krastonov’ principle (Baskaran *et al.*, 2011) which is the layer-by-layer growth before agglomeration of particles as observed in Fig. 5.1 (b) and 5.1 (c) to form dense metal layer. Although electroless plating was employed to deposit palladium as a uniform layer on polyimide, a variance in the FTIR results as explained in section 4.4.2 could be responsible for the layer-by-layer growth since the available active sites after etching is accomplished as a function of etching time of the polyimide surface.

**5.2.2 The SEM micrograph result images are presented for 0.4 M NaOH/13 % NaOCl etched unirradiated polyimide film modified with palladium.**

The time was varied from 5 minutes to 30 minutes. As reported in the previous section, palladium electroless deposition was kept constant for all samples.

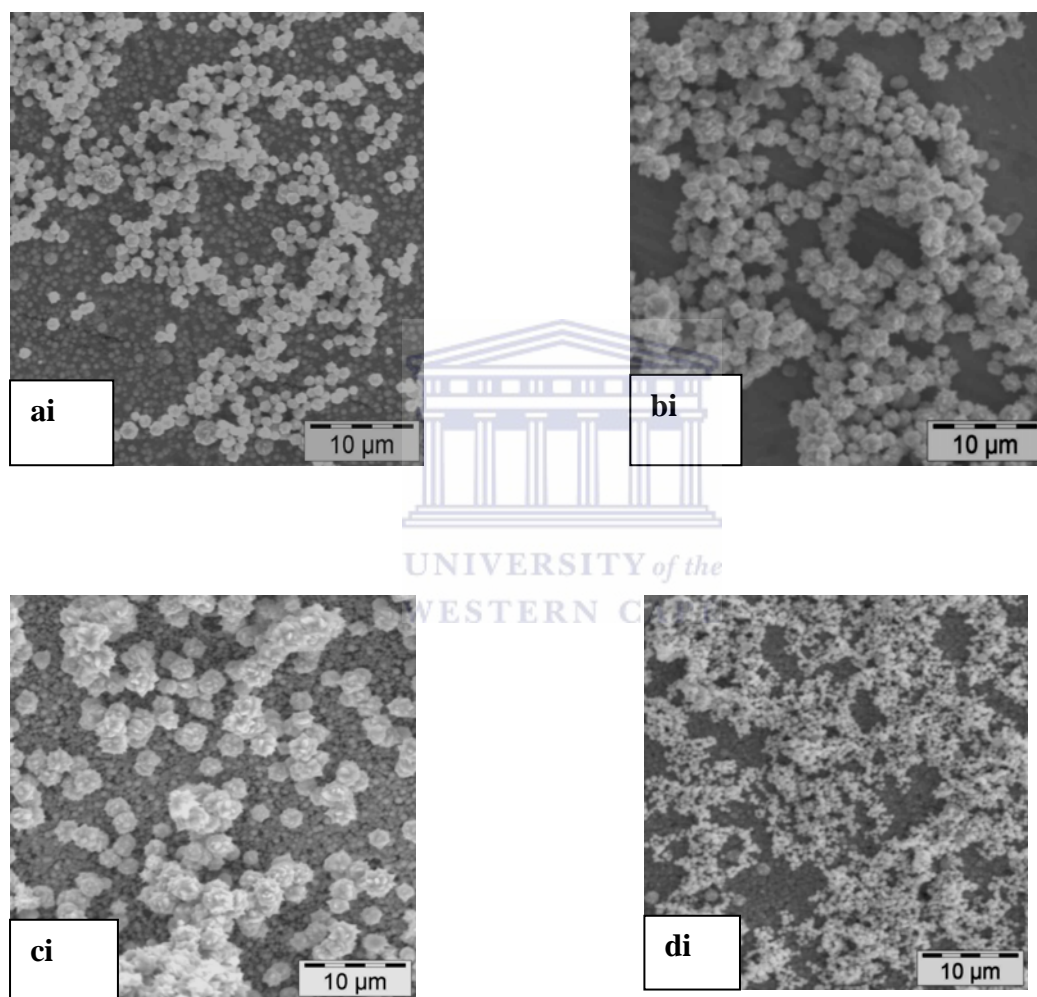


Figure 5-2: SEM micrograph of palladium modified unirradiated polyimide etched with 0.4 M NaOH/ 13 % NaOCl (ai) 5 minutes, (bi) 10 minutes, (ci) 20 minutes, (di) 30 minutes.

Fig. 5.2 (ai) – Fig. 5.2 (di) represents the unirradiated polyimide etched with a mixture of 0.4 M NaOH/13 % NaOCl solution from 5 minutes - 30 minutes. It was observed Fig. 5.2 (ai) – Fig. 5.2 (di) that the palladium particles formed on polyimide surface appeared as spherical clusters and not uniformly distributed over the surface of the polyimide membrane. Palladium particles can be seen to be sparsely distributed across the polyimide surface Fig. 5.2 (ai), instead under layer of particles can be noticed as seen in Fig 5.2 (ai) and Fig 5.2 (ci). These palladium particles can be seen to increase size in Fig. 5.2 (bi) which could due to increase in layer growth as a result of the continuous plating. In Fig 5.2 (ci), a new form of ‘under-layer’ growth of palladium particles was noticed while in Fig. 5.2 (di), palladium particles were observed to form a ‘mesh-like’ layer over the polyimide surface. Agglomeration of the palladium cluster particles can be seen to increase across the etching time Fig. 5.2 (bi) – Fig. 5.2 (di) and appeared in a ‘mesh-like’ structure with smaller particle sizes Fig. 5.2 (di). From the SEM images Fig. 5.2 (ai) – Fig.5.2 (di), the loosely packed palladium particle could be responsible for the poor adhesion of palladium particles and possible penetration of palladium particles into polyimide surface even though the FTIR result as discussed in section 4.4.3 showed the effect of etching solution as a function of time on polyimide surface. The poor adhesion as confirmed by the peel test could be due to poor depth profile of unirradiated polyimide surface hence binding strength between palladium particles and polyimide surface is low. This may also be responsible for the poor penetration of palladium metal into the polyimide matrix after electroless deposition.

5.2.3 The SEM micrograph of unirradiated polyimide film samples was etched in 13 % NaOCl and modified with palladium plating by electroless deposition.

Palladium electroless plating time on the etched polyimide film was kept constant for all samples.

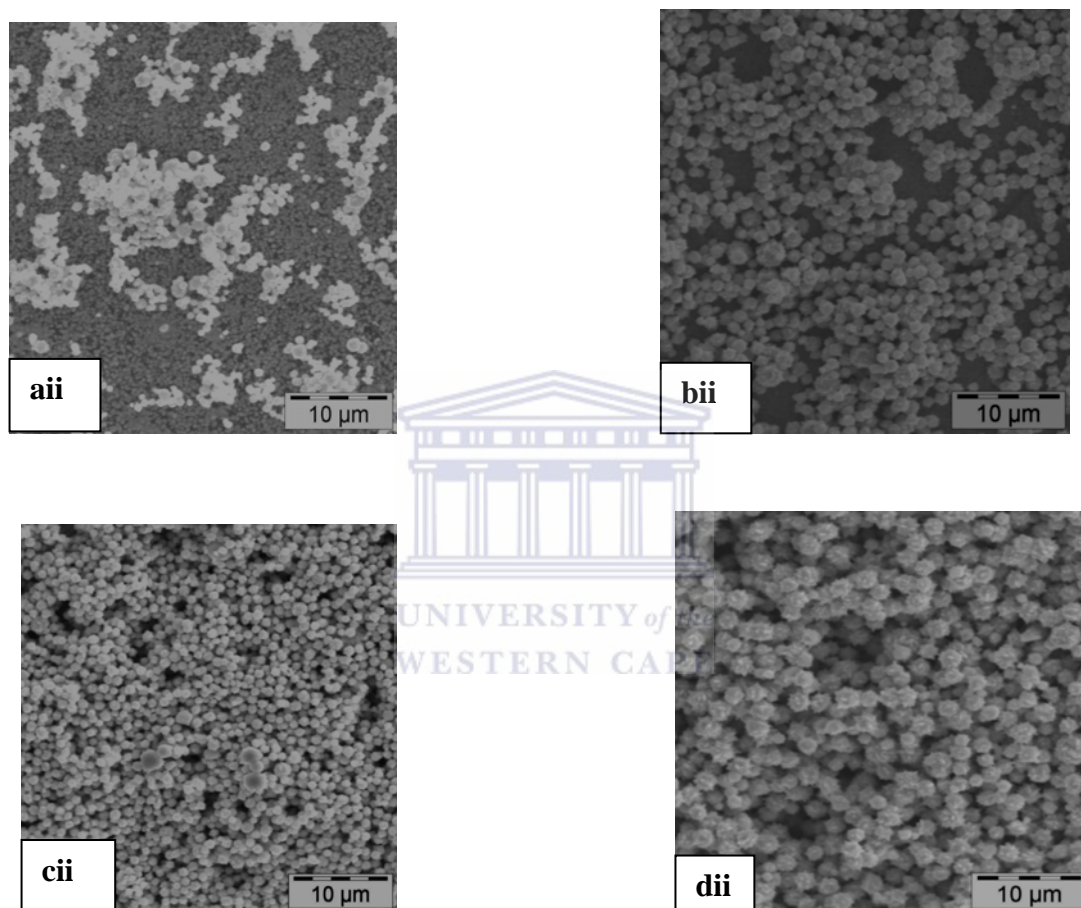
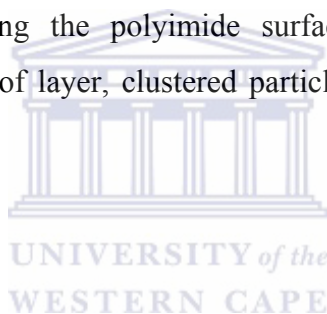


Figure 5-3: SEM micrograph of palladium modified unirradiated polyimide etched with 13 % NaOCl (aii) 5 minutes, (bii) 10 minutes, (cii) 20 minutes, (dii) 30 minutes

The palladium modified unirradiated polyimide samples were etched with 13 % NaOCl solution Fig. 5.3 (aii) – Fig. 5.3 (dii). SEM images indicated a spherical and well-ordered palladium particle arrangement over the polyimide surface which was confirmed by the XRD as discussed in Fig 5.7. The under-layer observed in Fig 5.3 (aii) resulted in ‘robust’ palladium particle agglomeration and tight packing of the palladium particles Fig. 5.3 (bii) – Fig. 5.3 (dii). These particles can be seen to increase in size with uniform spread over the polyimide surface Fig 5.4 (cii) and Fig. 5.4 (dii). Sodium hypochlorite solution is a strong etchant due to the chlorine content as confirmed with the FTIR result in section 4.4.3 (Trautmann *et al.*, 1999; Schiedt, 2007) and since the time of surface functionalization of polyimide is the only variable parameter in this case, it can be inferred that the palladium particle agglomeration grains is increased with increase in the polyimide surface treatment. It is also evident that palladium nucleation was initiated as seen in Fig. 5.3 (aii) and the particle growth occurred thereafter leading to the increase in grain sizes. The individual grain size of the palladium particles was 0.5  $\mu\text{m}$  (Fig. 5.3 (cii)) and the particle size for Fig 5.3 (dii) was 1.6  $\mu\text{m}$ . This result is found to be in agreement with the work of Yeung *et al.*, (1999) where palladium is plated on vycor support and the electroless microstructure investigated. According to Yeung *et al.*, (1999), metal film can show similar grain size and microstructure under similar initial plating rate.

### 5.3 MORPHOLOGICAL STUDY: TEM MICROGRAPH OF PALLADIUM MODIFIED UNIRRADIATED POLYIMIDE

Figure 5.4 – 5.6 represents the cross-section TEM micrograph results of unirradiated polyimide etched with 13 % NaOCl, 0.4 M NaOH and a mixture of 0.4 M NaOH/13 % NaOCl solutions. The TEM analysis is performed on polyimide modified with palladium to investigate the depth profile of the palladium particles and distribution of palladium particle on the polyimide surface. A visual study of the TEM images suggests the darker regions represent the presence of palladium particles while the lighter region is the polyimide support according to Shuxiang *et al.*, (2010). The palladium nanoparticles dispersion varies from uniform particle distribution to sparse and agglomeration which resulted in the formation of palladium clusters. Palladium penetration is observed along the polyimide surface suggest a distribution of palladium in ordered stretch of layer, clustered particles and thin film of palladium after electroless plating.



5.3.1 TEM micrograph results are presented for 0.4 M NaOH etched unirradiated polyimide film modified with palladium.

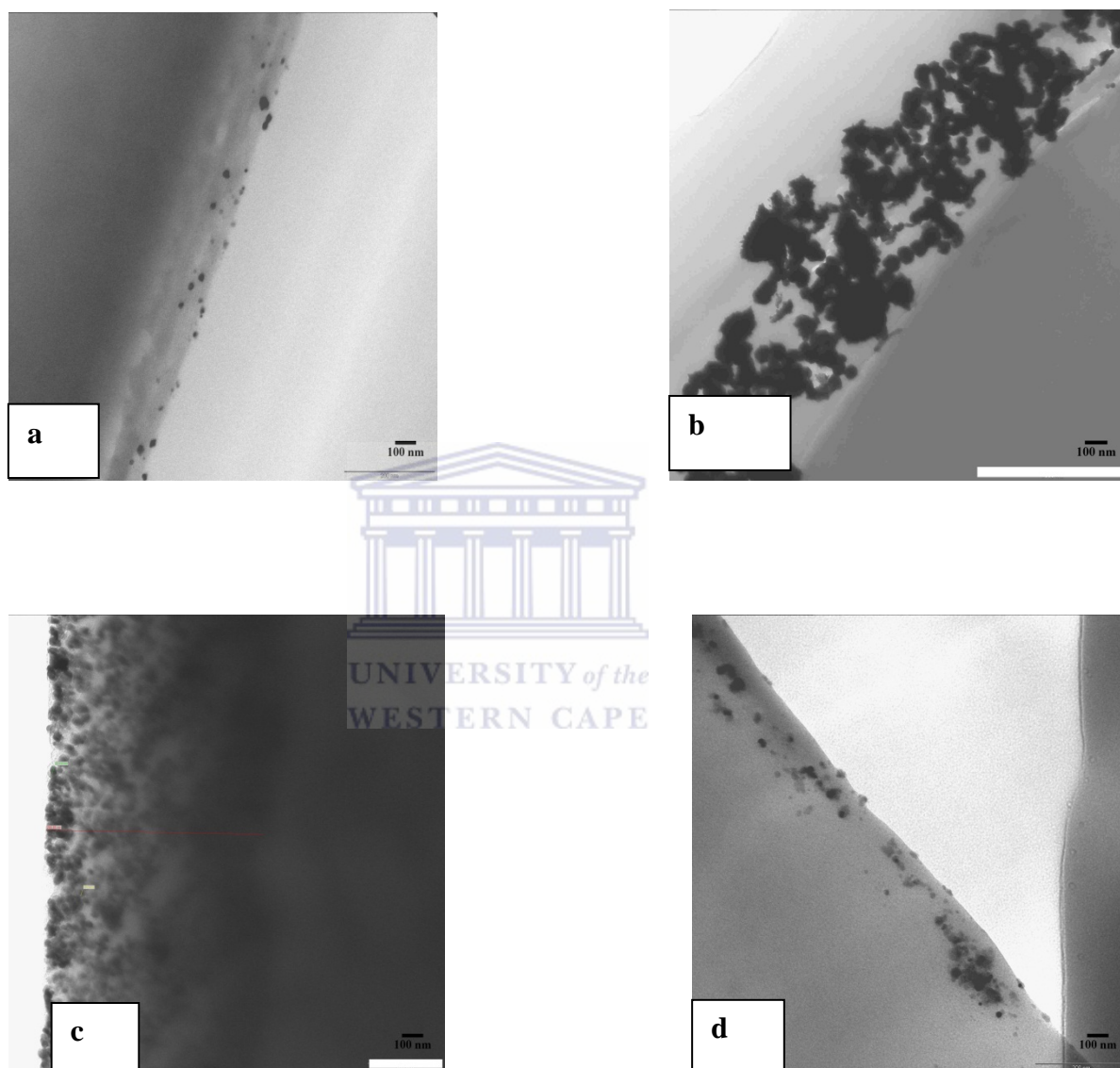


Figure 5-4: Cross-section of TEM micrograph of palladium modified unirradiated polyimide etched with 0.4 M NaOH (a) 5minutes, (b) 10 minutes, (c) 20 minutes, (d) 30 minutes

In Fig.5.4 (a) – Fig. 5.4 (d), TEM micrograph of palladium plated polyimide etched with 0.4 M NaOH shows isolated or scattered palladium particles from Fig. 5.4 (a) and clustered or agglomerated palladium particles along the polyimide surface as seen in Fig. 5.4 (b). In Fig. 5.4 (c), there is a homogenous penetration and dispersion of palladium metal particles into polyimide matrix. The chemical interaction between NaOH and the carboxyl units of the polyimide could have favour the palladium dispersion into the polyimide matrix (Yi Li *et al.*, 2004). The FTIR results in sections 4.4.3 can be related to palladium dispersion as seen in the significant change in the absorption intensity especially within the carbonyl functional group regions of the polyimide structure. A comparison of Fig 5.4 (c) with the SEM study Fig. 5.1 (c) seems to agree and the SEM result showed uniform ‘nucleated’ layer of palladium before the growth of the particles in Fig. 5.1 (d).





5.3.2 TEM cross-section micrograph of 0.4 M NaOH/13 % NaOCl etched unirradiated polyimide film modified with palladium

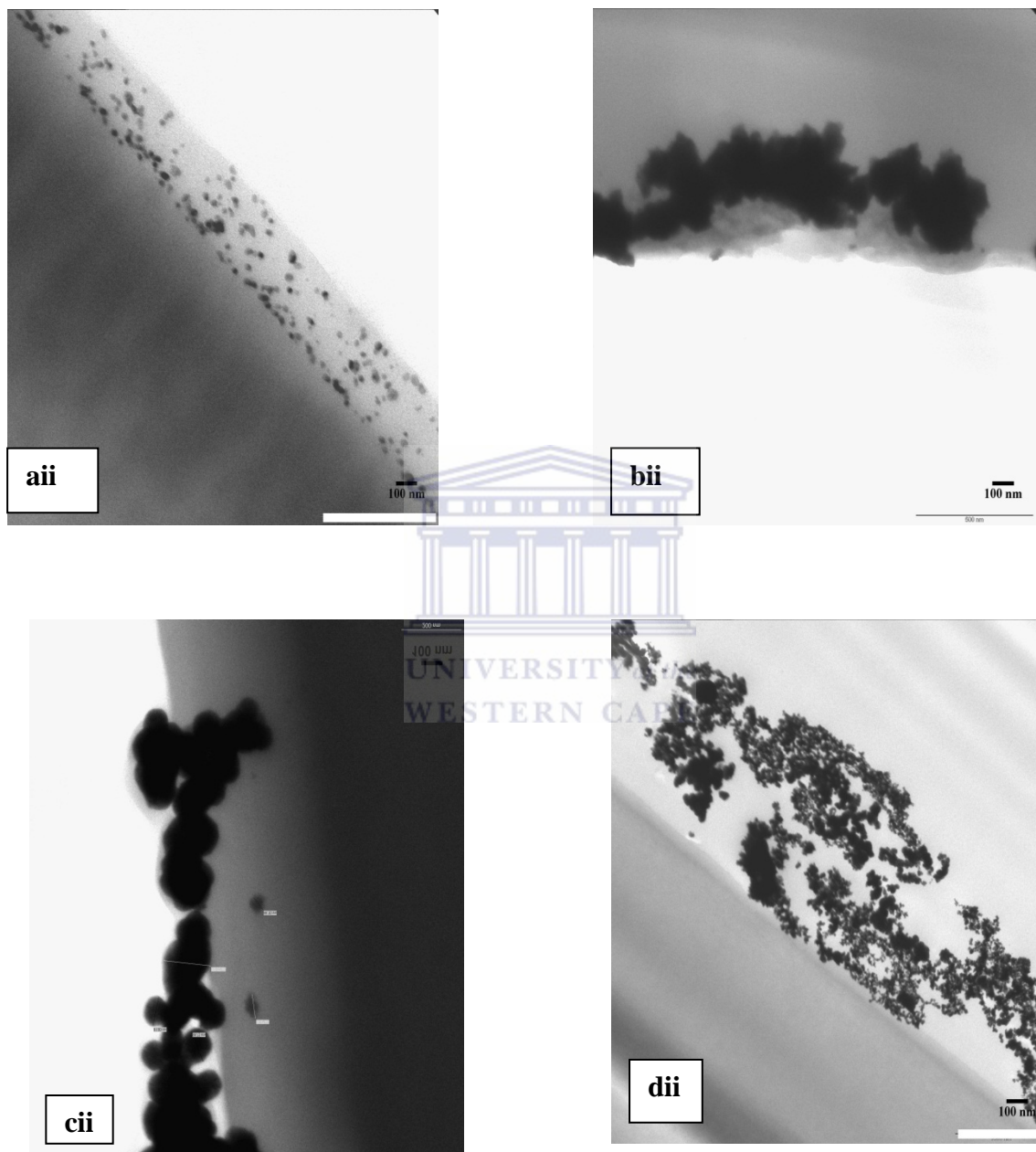


Figure 5-5: Cross-section of TEM micrograph of palladium modified unirradiated polyimide etched with 0.4 M NaOH dissolved in 13 % NaOCl (a) 5 minutes, (b) 10 minutes, (c) 20 minutes, (d) 30 minutes.

Cross section micrograph of TEM shown in Fig. 5.5 (aii) – Fig 5.5 (cii), palladium particles are seen to be arranged along the surface of the polyimide with each particles in a ‘speck-like’ form and distant apart in a pattern in the polyimide film Fig 5.5 (aii). In other cases Fig. 5.5 (bii) – Fig. 5.5 (dii), the palladium particles appeared to have agglomerated to form a thick film layer and with irregular penetration and embedding into the polyimide matrix. The effective rate and differences of palladium dispersion into the polyimide matrix can be due to the rate of etching time. Another possible reason for the significant rate of palladium dispersion could be due to the chemical interaction between the carboxyl unit of polyimide and NaOH solution (Yoda *et al.*, 2004).



5.3.3 *The TEM cross-section analysis of 13 % NaOCl etched unirradiated polyimide film modified with palladium.*

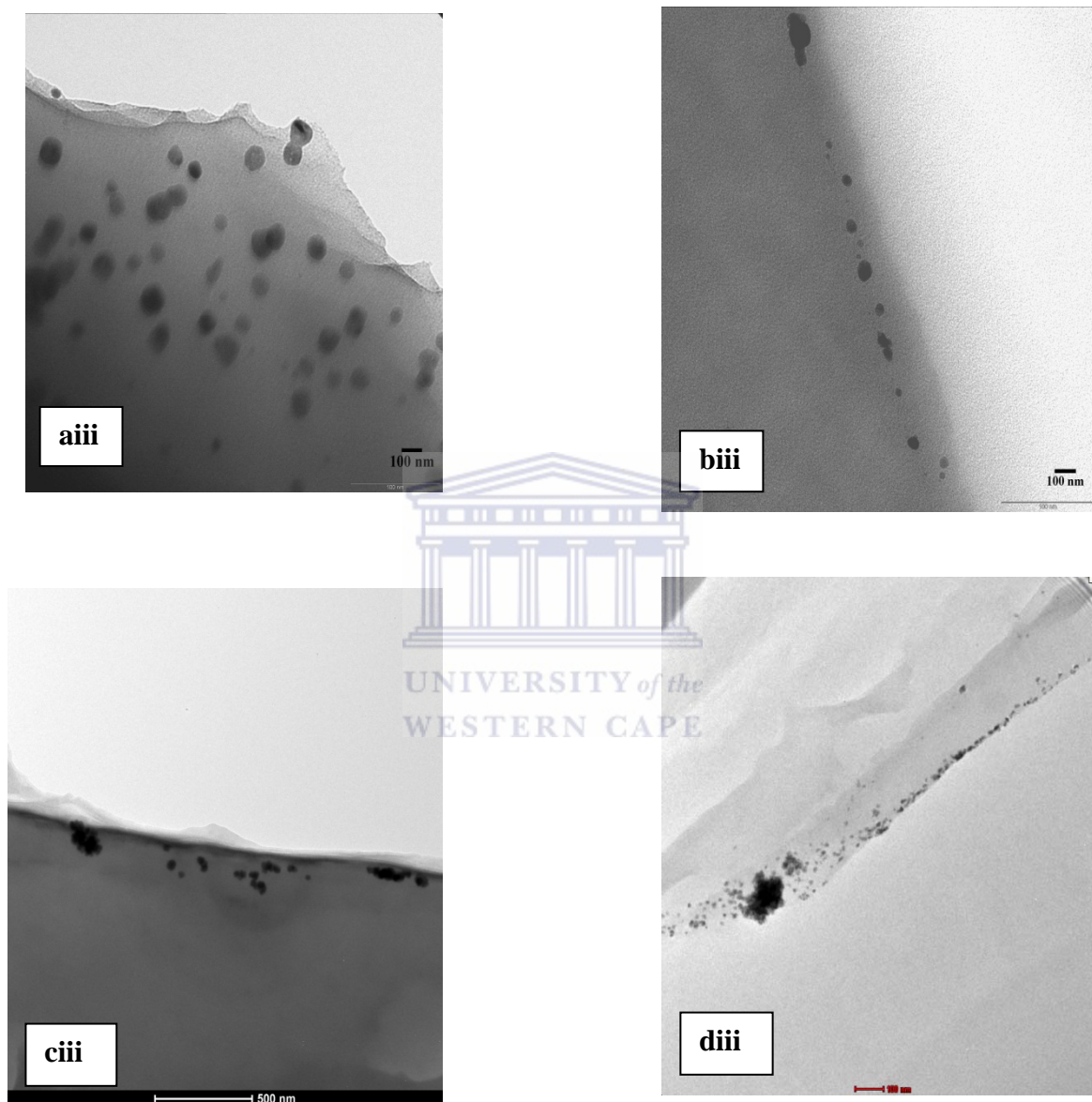


Figure 5-6: Cross-section of TEM micrograph of palladium modified unirradiated polyimide etched with 13 % NaOCl (a) 5 minutes, (b) 10 minutes, (c) 20 minutes, (d) 30 minutes

The TEM result from Fig. 5.6 for NaOCl etched polyimide modified with palladium showed palladium particles randomly distributed into the polyimide matrix (Fig. 5.6 aiii), while stretch of palladium particles was observed on the polyimide surface as in Fig. 5.6 (biii), (ciii) and (diii) along with the formation of clusters or aggregated particles. This pattern of metal distribution has been previously reported by [Marin and Serruys, (1995); Yoda *et al.*, (2004)]. In the case of palladium particle penetration into polyimide being studied, the difference in the particle sizes and distribution could be due to the effect of etching time and the absence of depth profile which may have promoted the penetration of palladium into the polyimide matrix.

#### 5.4 PEEL STRENGTH MEASUREMENT ON PALLADIUM-POLYIMIDE LAMINATES

The image below represents the peel test technique to study the adhesion strength of palladium on unirradiated and irradiated polyimide surface.

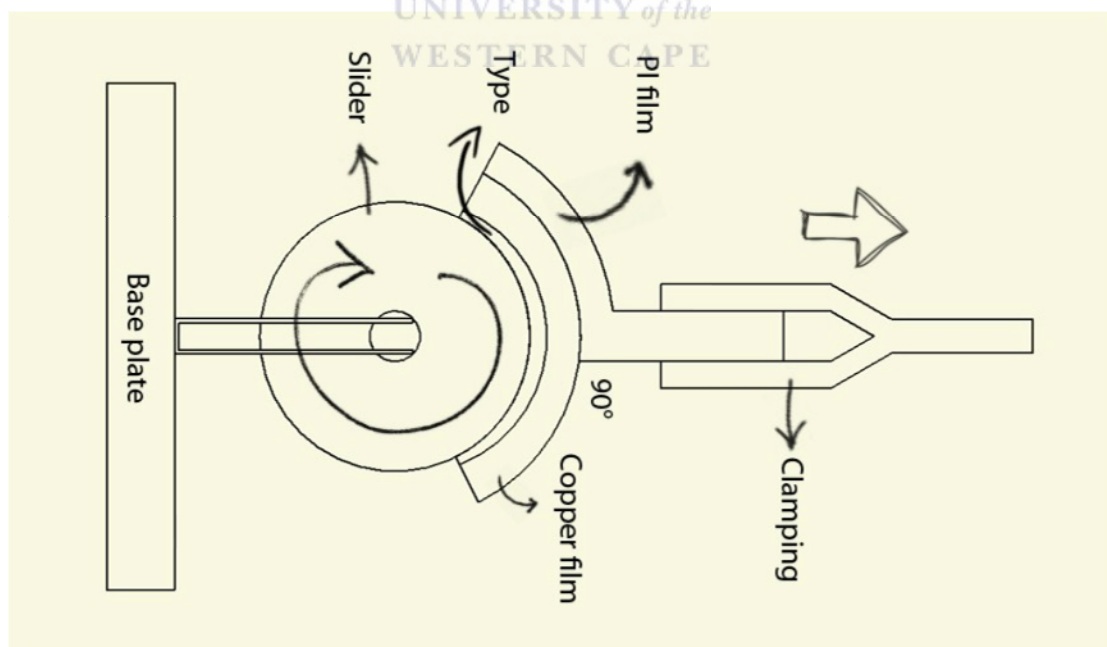


Figure 5-7: Schematic of Peel test measurement technique.

The peel strength was performed for 20 min etched unirradiated polyimide and track etched polyimide with electroless deposited palladium. Details of the sample preparation and instrumental set-up conditions have been highlighted in sections 3.6 and 3.6.1 respectively. It was found that as we are predict peel strength of palladium on unirradiated polyimide showed poor adhesion and equivalent to  $0.27 \pm 0.05$  N/mm. Unlike the irradiated polyimide film which showed peel strength value of  $1.36 \pm 0.07$  N/mm for the surfaces depth relief with cylindrical pores and for conical pores, the peel strength value was  $1.38 \pm 0.09$  N/mm. The influence of depth relief morphology study after peel strength analysis of palladium modified polyimide surfaces suggest that the creation of depth profile after etching irradiated polyimide increased the adhesion of palladium on polyimide surface. The peel strength of irradiated polyimide modified with palladium was investigated after exposing the palladium plated polyimide membrane to high temperature environment. The sample was treated at 250 °C in hydrogen atmosphere within 120 hours. It was observed that the value of peel strength decreased significantly. The cylindrical and conical pores peel strength values was measured as  $1.04 \pm 0.12$  N/mm and  $0.98 \pm 0.14$  respectively, while the unirradiated polyimide plated with palladium completely loose adhesion between palladium films and Polyimide support.

## **5.5 XRD RESULTS OF PALLADIUM MODIFIED POLYIMIDE AFTER ETCHING IN 13 % NaOCl SOLUTION**

X-ray diffraction (XRD) result of palladium modified polyimide will be presented and discussed. The palladium modified polyimide (Kapton®) as presented in Fig. 5.8 below represent the unirradiated polyimide etched in 13 % NaOCl solution prior to palladium deposition. A detail of the etching time has been discussed in section 3.3.1.1. Palladium plating time of the etched polyimide was kept constant at 10 minutes for all samples. The plating procedure has been discussed in section 3.4.

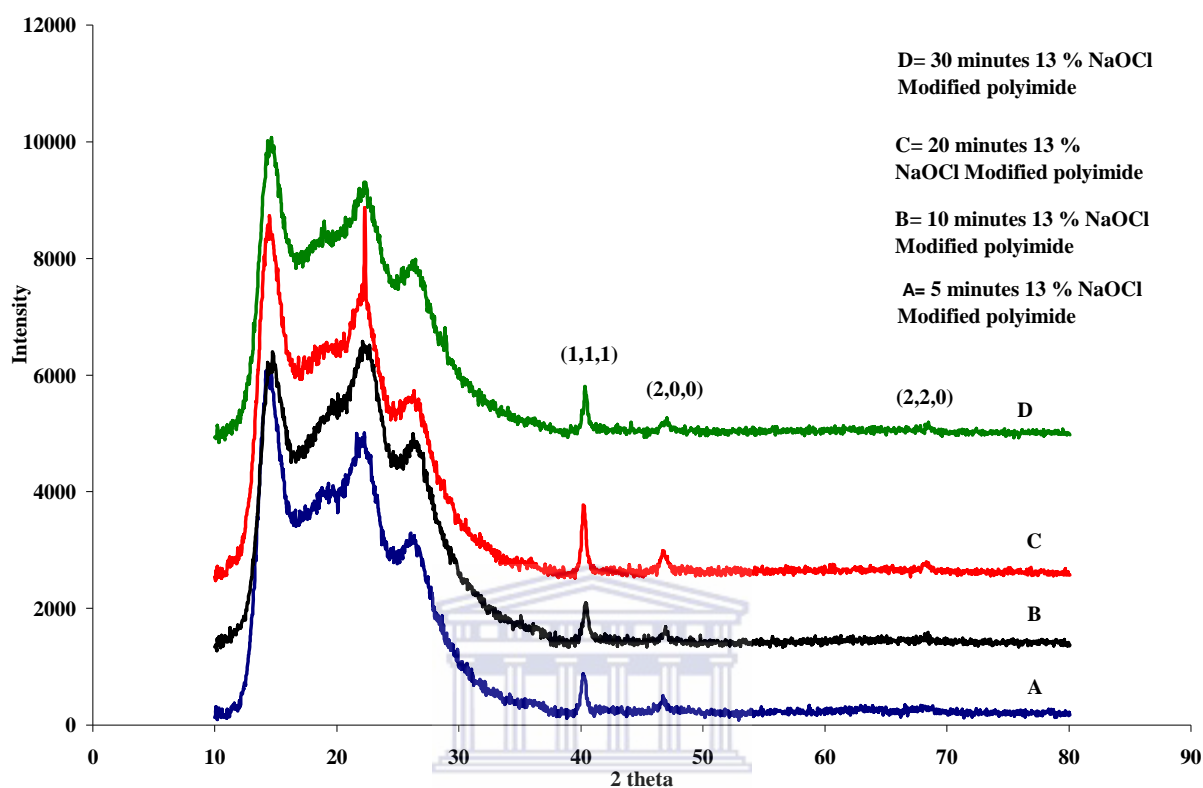


Figure 5-8: XRD of palladium plated polyimide etched with 13 % NaOCl solution (a) 5 minutes, (b) 10 minutes, (c) 20 minutes and (d) 30 minutes.

Figure 5.8 (a) – (d) represents the X-ray diffraction measurement of unirradiated polyimide samples that have been etched with 13% NaOCl solution for 5 – 30 minutes and then plated with palladium metal. The palladium plating of the polyimide samples was performed by electroless deposition for 10 minutes. From the XRD result, characteristic diffraction peaks which can be indexed for the presence of palladium in the polymer matrix were observed at  $40^\circ$  and  $48^\circ$  and  $68^\circ$   $2\theta$ . These diffraction peaks have been assigned to (1,1,1), (2,0,0) and (2,2,0) planes for the  $40^\circ$ ,  $48^\circ$  and  $68^\circ$   $2\theta$  peaks respectively (Ke *et al.*, 2007). It can be observed from Figure 5.8 that palladium diffraction peaks appeared for all etched and electroless plated polyimide samples at the  $40^\circ$  which is the (1,1,1) plane. The peak was common to all etched polyimide samples. In the case of 10 minutes etching with NaOCl polyimide,

no peak was visible whereas peaks of Pd started to emerge for the 20 minutes etched polyimide (2,2,0) plane peaks starts to emerge for the 20 minutes etched polyimide. This seems to suggest the preference of palladium to orientate in the (1,1,1) planes compared with other planes. The preference of palladium in the (1,1,1) could have been as a result of the overall effect of etching of the polyimide samples as confirmed by the FTIR results in Fig. 4.5 – Fig. 4.8. In the result, the etching appeared to be relatively similar for all the NaOCl etched unirradiated polyimide except for the 30 minutes (Fig. 4.8). Also, the distinct peaks at  $48^\circ$  and  $68^\circ$   $2\theta$  for the polyimide etched for 20 minutes imply deeper deposition of palladium into the polyimide matrix due to availability of active sites after etching as was confirmed by FTIR in Fig. 4.7.

## 5.6 XRD RESULTS OF POLYIMIDE PLATED WITH PALLADIUM AFTER ETCHING WITH 0.4 M NaOH SOLUTION

In Fig 5.9 below, the XRD results are presented of the palladium modified polyimide that was etched with 0.4 M NaOH solution (see section 3.3.1.2).

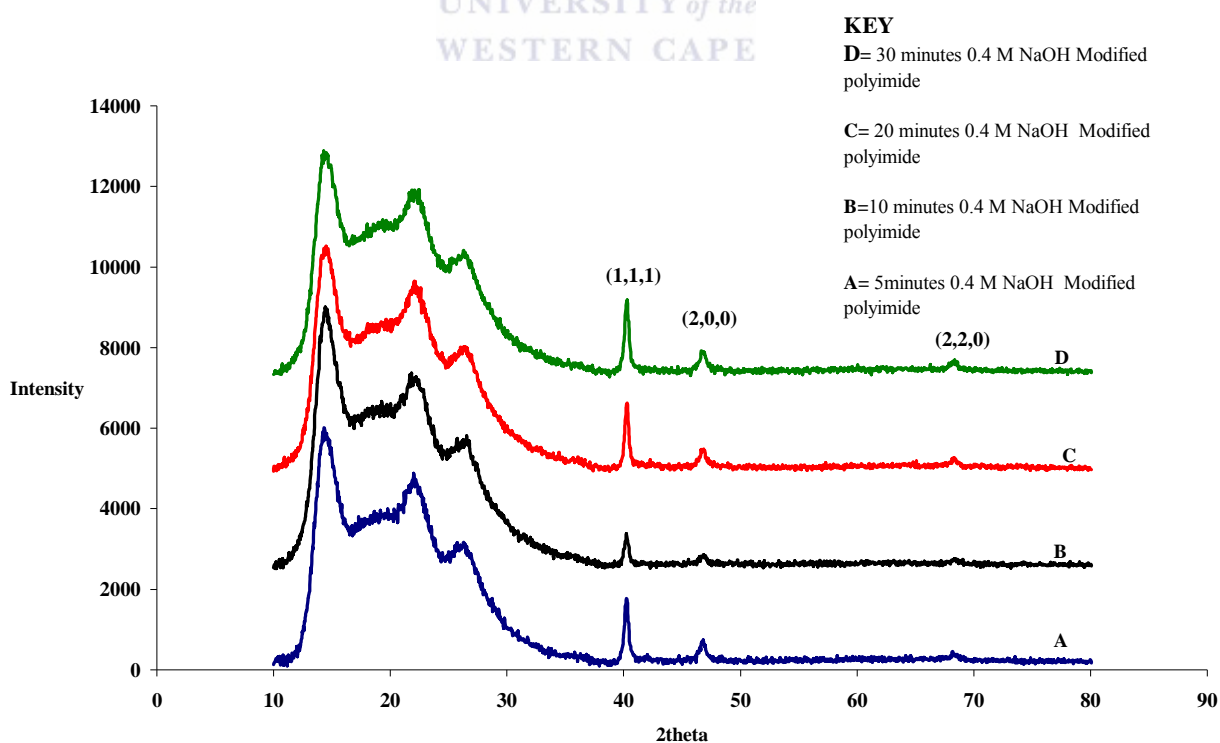


Figure 5-9: XRD of palladium modified polyimide after etching with 0.4 M NaOH solution for (a) 5 minutes, (b) 10 minutes, (c) 20 minutes and (d) 30 minutes

In the case of Fig. 5.9 (a) – (d) above, the XRD result for Pd plated polyimide film that had firstly been etched with 0.4 M NaOH solution showed a similar trend of palladium diffraction peaks at  $40^\circ$ ,  $48^\circ$  and  $68^\circ$   $2\theta$  as presented earlier in Fig. 5.8. Although three different etchants namely NaOCl, NaOH and 0.4M NaOH/13 % NaOCl solutions were used, the similarity of diffraction peaks observed after palladium plating of the variously etched polyimide samples did not agree with the FTIR analysis where different absorption peak intensity were observed for the various etchants. The similarity of the palladium deposition as confirmed by XRD result could be due to uniformity of palladium deposition by electroless deposition. Another reason that can be attributed to the similarity of diffraction peaks of palladium is the overall effect of either NaOCl or NaOH etching solution. These etchants have been reported to etch polymer surface in a similar way but with different surface roughening effects (Schiedt, 2007; Mitrofanov *et al.*, 2006). Although unirradiated polyimide was plated, the similarity of etching effect of NaOCl and NaOH/NaOCl was confirmed by the SEM morphological study as reported in section 4.6 and 4.7. From Fig. 5.1, 5.2 and 5.3, the time of etching seems not to translate to more palladium metal into the polymer matrix. This could be attributed to the fact that the commercial polyimide still maintains a degree of rigidity in its structure even after etching with either NaOCl or NaOH solutions. It has been suggested that multiple surface conditioning such as irradiation of polyimide surface with heavy ion prior to etching is more effective method to functionalise polyimide film surface (Esinger *et al.*, 2001; Mitrofanov *et al.*, 2006). This was confirmed with the IR study discussed earlier in Fig. 4.5 – Fig. 4.13. The single method surface conditioning has not been proven to be effective hence only etching method used for these polyimide samples could be responsible for the less availability of active sites for ion exchange during palladium electroless plating. In the work of Schiedt, (2007), it was established that conical pores formation is promoted by NaOH solution results in conical shapes while NaOCl solution gave cylindrical shape of pores. The pore shapes could determine the effective penetration of metal into the polyimide matrix.



### 5.7 XRD RESULTS OF POLYIMIDE PLATED WITH PALLADIUM AFTER ETCHING WITH 0.4 M NaOH SOLUTION

In Fig 5.10, the XRD results are presented of the palladium modified polyimide that was etched with 0.4 M NaOH/NaOCl solution. The detail of the etching and plating procedures are discussed in section 3.3.1.4 and 3.4 respectively.

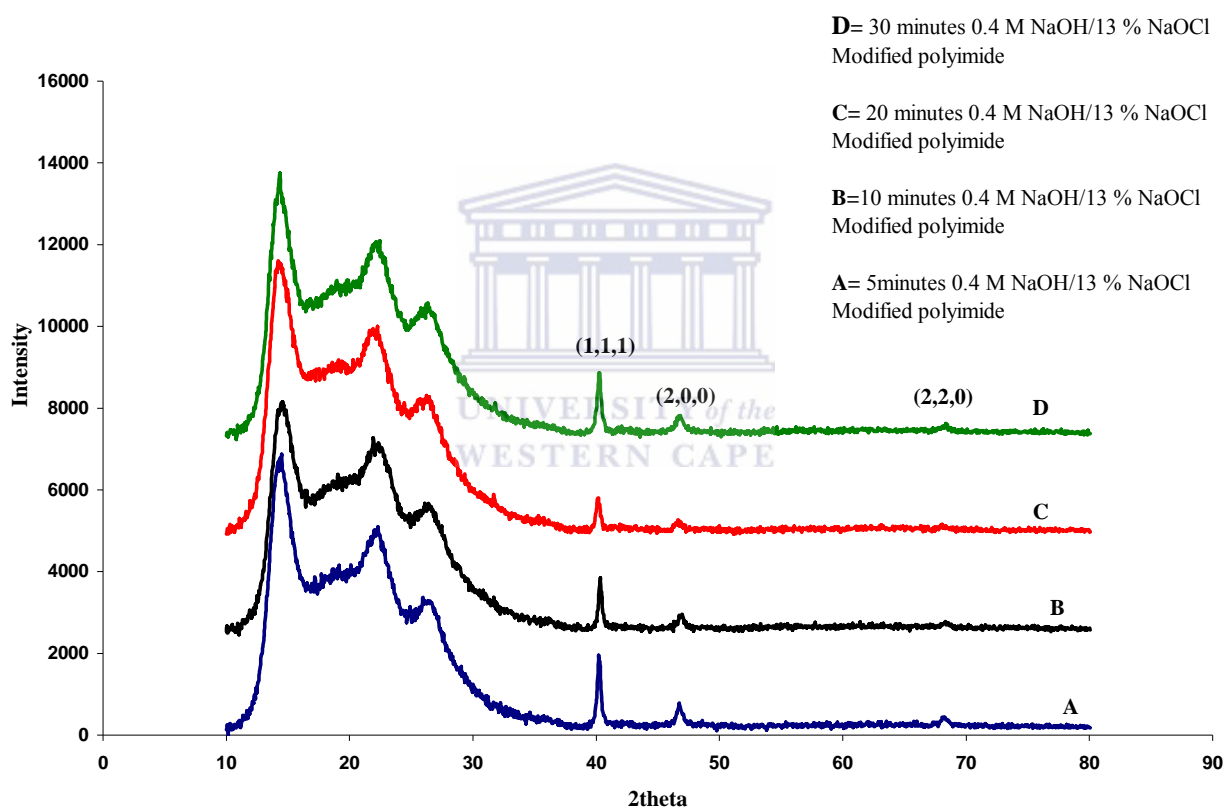


Figure 5-10: XRD of palladium modified polyimide after etching with 0.4 M NaOH solution for (a) 5 minutes, (b) 10 minutes, (c) 20 minutes and (d) 30 minutes

In Fig. 5.10, palladium metal particles could be seen for the NaOH etched polyimide film. From the XRD result above, the diffraction peaks at (1,1,1) plane appeared to reduce as a function of the etching time with the 20 minutes etched polyimide showing the minimum diffraction intensity. The (1,1,1) plane could be seen to have

increased after the 20 minutes etched sample. Along the (2,0,0) and (2,2,0) planes, the diffraction peaks did not show such intensity as the (1,1,1). This could suggest that palladium particles preferred the (1,1,1) plane compared to the (2,0,0) or (2,2,0) planes. Although the FTIR result in section 4.4.2 showed significant change in absorption intensity as a function of etching time, the emergence of these bonds did not imply that palladium uptake by the etched polyimide sample. This could probably be due to non-availability of active sites in the polyimide units when etched with NaOH and as such do not favour metal exchange during plating. The SEM result in Fig. 5.1 showed particles of palladium in layered form (Fig. 5.1c) seem to suggest that only surface coverage of palladium occurred without penetration into the polyimide matrix as expected.



## CHAPTER 6

### 6.0 CONCLUSIONS AND RECOMMENDATIONS

The scientific goal of this project was to develop simple and effective methodological approach for surface modification of polyimide film that will meet practical application as a composite membrane structure for hydrogen separation and purification. The requirements for a successful composite palladium-polyimide film include; high thermal stability above 400°C, exhibit good adhesion of palladium film on polyimide surface and high permeability in hydrogen atmosphere. These targets have been highlighted in the hypothesis and the aims/objectives of this project (sections 1.6 and 1.7). In considering these targets, unirradiated and irradiated polyimide films were etched with alkaline (NaOH, NaOCl and NaOH/NaOCl) solutions as a pathway to functionalise and create depth profile by pore formation on the polyimide surface prior to palladium plating. A successful composition of the alkaline solution was developed for the etching process at low temperature (less than 70 °C) and concentration. The alkaline etching of irradiated polyimide at low temperature proved successful for the control of depth profile of polyimide surface in relatively stable conditions of etching process. Of the available deposition techniques, electroless plating was considered for the plating of modified polyimide surface as a result of its simplicity, ease of film deposition control, film uniformity and economic costs. The composite palladium-polyimide film was investigated by peel test to determine the adhesion properties of the palladium on the polyimide surface.

In addressing the hypothesis (section 1.7), the following approaches were applied; the commercial (as-received), etched unirradiated and irradiated and palladium modified polyimide samples were characterised by Scanning Electron Microscopy (SEM), Transmission Electron Microscopy (TEM), Fourier Transformed Infra-Red (FTIR), X-ray Diffraction (XRD), Thermo-gravimetric Analysis (TGA) and hydrogen

diffusion measurement were applied to study the effects of etching as a function time and composition of etching solution.

The following results based on the characterisation of the unirradiated, irradiated and palladium-polyimide composite film, and conclusions are presented as follows:

1. Method for identification of functional groups present in both unirradiated and irradiated polyimide film by FTIR technique showed the presence of characteristics absorption bands in commercial (as-received) polyimide film. After etching of the unirradiated polyimide in alkaline (NaOH, NaOCl and NaOH/NaOCl) solutions at varying time, the effect of etching as a function of time showed the emergence of some characteristic absorption bands after etching with NaOH. In other FTIR results, characteristic absorption bands were destroyed as observed in the unirradiated polyimide etched with NaOH/NaOCl mixture while the NaOCl etched unirradiated polyimide showed reduction in absorption intensity after successive increase in etching time. From the experimental data, the 20 minutes is the most suitable etching time for both unirradiated and irradiated PI as seen in the FTIR results. The affected characteristic absorption bands lie along the polyimide backbone structure and have been identified to facilitate ion exchange mechanism by substitution of Na with Pd during electroless plating according to literature. By the surface modification of polyimide and using alkaline etching method, the difference in absorption band intensities as observed from the FTIR results, and due to the use of different etching solution suggested a preferential chemical interaction between the polyimide units and the etching solutions. The FTIR analytical technique was deeply employed in this study in other to understand the chemical relationship between the polyimide bond units (both side chains and backbone structures) and the chemical etchants.

2. Method for “depth profile” surface modification of irradiated polyimide using alkaline (NaOH/NaOCl and NaOCl) solution was developed. Overall effect of etching time and solution was confirmed by FTIR analysis as well as the SEM surface morphology study. The surface of treated and irradiated polyimide showed different

pores sizes and pore distribution as a function of etching time and etching solution. NaOCl and NaOH/NaOCl solutions were used to etch the irradiated polyimide. The preference of these two solutions was based on the effect of chlorine concentration during etching. The results from the FTIR and SEM studies agreed with other results found in literature for high temperature (70 °C – 80 °C) pores formation treatment in irradiated polyimide (Mitrofanov *et al.*, 2006; Esinger *et al.*, 2003; Esinger *et al.*, 2010) and also further confirmed that the amount of active chlorine concentration in etchants determine the rate of etching, size and shape of pores formed after etching (Sudowe *et al.*, 2001).

3. Method of palladium electroless plating on unirradiated polyimide surface was successfully adapted. Comparison of methods for surface activation by acceleration of unirradiated polyimide in process palladium electroless plating layers was deeply studied. Na<sub>2</sub>EDTA, NaOH and HCl solutions were applied to determine the effective acceleration solution prior to electroless deposition. During electroless plating of surface, removal by stripping of Sn from the seeded surface is important as well as to enhance uniformity of palladium on polyimide surface. The three accelerated solutions were applied and palladium film deposited via electroless technique. Polyimide surface accelerated with Na<sub>2</sub>EDTA showed better palladium film coverage and uniformity of the composite palladium-polyimide film. The palladium layer on polyimide film formed agglomerated particles which allowed to obtain continuous palladium films. The process of growing palladium film at different time of etching the polyimide was observed in the SEM study and palladium film deposition was optimized. It was found that for the creation of continuous palladium film on the surface of polyimide after alkaline treatment, electroless process must not be more than 20 minutes time.

The TEM morphology study to determine palladium film penetration into the polyimide matrix of palladium modified polyimide composite film was studied. The rate of palladium penetration for the NaOH etched polyimide surface indicated that the NaOH etched polyimide with excellent particle distribution and penetration into

the polyimide matrix after etching for 20 minutes for the unirradiated PI. In other cases (NaOCl and NaOH/NaOCl), disperse palladium particle with marginal penetration were observed. The availability of active sites as a result of ring opening during etching could have been a possible reason especially as noted for the alkaline etched polyimide sample. In the XRD analysis of palladium film on the surface of polyimide has shown the following; palladium occupied the (1,1,1) diffraction plane and was observed for all samples. Other planes occupied by the palladium metal are (2,2,0) and (2,0,0) which was not obvious as seen for the (1,1,1) plane. The (1,1,1) plane has been reported as the face cubic centre for palladium and with the highest sorption site for hydrogen due to the large surface available for hydrogen uptake. The preference of palladium to occupy this plane could be relative to the ease of atom arrangement at this plane or palladium metal stability property in this diffraction plane.

4. Analysis of thermal stability of palladium-polyimide composite film showed improved thermal properties for the palladium modified polyimide film above 450 °C. The commercial polyimide film was stable up to 350 °C. The thermal property observed to be relatively stable for all palladium modified sample. This suggested that palladium metal due to its high lattice expansion property increased the polyimide thermal property of the composite film.

5. Method of adhesion palladium on polyimide surface by peel test for this study was performed on the palladium modified unirradiated and irradiated polyimide composite films. The peel test for the palladium modified unirradiated polyimide composite film showed poor adhesion ( $0.27 \pm 0.05$  N/mm) of the palladium film layer on the unirradiated polyimide surface whereas the palladium modified irradiated polyimide composite showed good adhesion ( $1.36 \pm 0.07$  N/mm) of the palladium layer on the polyimide surface. The effects of heavy ion bombardment of polyimide and alkaline etching showed good palladium adhesion after plating on irradiated polyimide surface. The irradiated palladium modified polyimide was treated at 250 °C in hydrogen atmosphere over 120 hours and the peel strength decreased significantly.

6. The hallmark of this project was the design and assemblage of hydrogen diffusion reactor unit. The hydrogen diffusion test performed for alkaline etched unirradiated and irradiated polyimide samples. As for the alkaline etched unirradiated polyimide, the rate of hydrogen diffusion measurement at room temperature (25 °C) showed low hydrogen permeation with minimal decrease in pressure of 0.07 bar after 10 hours. At higher temperature of 250 °C and 325 °C, the diffusion rate was measured by pressure drop was 0.12 bar and 0.17 bar respectively.

The alkaline etched irradiated polyimide showed a relatively steady rate of hydrogen diffusion till 20 minutes. The successive increase in the time of etching increased the pore size of the irradiated polyimide surface and the rate of hydrogen diffusion of the sample. The relative increase in the pore size with time of etching indicates that pore size of the irradiated polyimide surface can be controlled with time of etching.

Based on the analyses and conclusions of the study, the following recommendations regarding future research direction were made:

1. Although the multiple surface modification of polyimide by irradiation, followed by chemical etching is an effective technique to alter the polyimide backbone structure, the introduction of functional groups that can act as ion exchange sites during electroless plating should be further investigated especially by introduction of exchangeable metal into the polyimide units during synthesis. From the experimental data, only heavy ion bombarded polyimide showed effective surface etching process due to pore formations and well distributed surface roughening. A conclusive analysis to determine the most suitable pore shape is required since both NaOH and NaOCl etching give different pore shapes.

2. Following the successful pre-testing of the home built hydrogen diffusion unit for etched unirradiated and irradiated polyimide, test for hydrogen permeability should be performed on the palladium-polyimide composite films to determine the

efficiency of the films in hydrogen separation and purification in industrial application.





## CHAPTER 7

## 7.0 REFERENCES

1. Adhikari, S., Ferdando, S., *Hydrogen Membrane Separation Techniques. Ind Eng.Chem. Res* (2006). **45**: p. 875-881.
2. Akamatsu, K., Ikeda, S., Nawafune H., *Site selective direct silver metallization on surface-modified polyimide layers. Langmuir*, (2003). **19**: p. 10366-10371.
3. Alvarez, A.-M., Robertson, I. M., Birnbaum, H. K. , *Hydrogen Embrittlement of a Metastable Titanium Alloy. Article*, (2004): p. 1-34.
4. Amandusson, H., Ekedahl, L.G., Dannetun, H. , *Hydrogen permeation through surface modified Pd and Pd/Ag membranes. . Journal of Membrane Science.* , (2001). **193**: p. 35-47.
5. Antler, M., *The development and application of palladium contact materials. . Platinum Met. Rev.* , (1987). **31**( 1): p. 13.
6. Armor, J.N., *The multiple roles for catalysis in the production of H<sub>2</sub>. Applied. Catalysis. A*, (1999). **176**(2): p. 159.
7. Bhansali, S., Sood, D.K. , *A novel technique for fabrication of metallic structures on polyimide by selective electroless copper plating using ion implantation. Thin Solid Films* (1995). **270**: p. 489-492.
8. Brogden, D., *Method of Making a Thin Gas Diffusion Membrane. US Patent* (1970). **3,505,180**, .
9. Bryden, K.J., Ying, Y.J., *Nanostructured palladium-iron membranes for hydrogen separation and membrane hydrogenation reactions. Journal of Membrane Science*, (2002). **203**: p. 29-42.
10. Buxbaum, R., E., Kinney, A. B. , *Hydrogen transport through tubular membranes of palladium-coated tantalum and niobium. Ind.Eng.Chem.Res*, (1996). **35**: p. 530-537.
11. Chae, B., Bin Kim, S., Lee, W. S., Kim, S., Choi, W., Lee, B., Ree, M., Lee, H.K., Jung, C.J, *Surface morphology,molecular reorientation,and liquid*

- crystal alignment properties of rubbed nanofilms of a well-defined brush polyimide with a fully rodlike backbone. Macromolecules, (2002). 35: p. 10119-10130.*
12. Charbonnier, M., Romand, M. , *Polymer pretreatments for enhanced adhesion of metals deposited by the electroless process. International Journal of Adhesion & Adhesives (2003). 23 p. 277–285.*
  13. Checchetto, R., Bazzanella, N., Patton, B., Miotello, A. , *Palladium membranes prepared by r.f. magnetron sputtering for hydrogen purification. . Surface Coatings and Technology., (2004). 177-178: p. 73-79.*
  14. Cheng, Y.S., Yeung, K. L. , *Effects of electroless plating chemistry on the synthesis of palladium membranes. Journal of Membrane Science., (2001). 182: p. 195.*
  15. Cleeton, J.P.E., Bohn, C.D., Muller, C.R., Dennis, J.S., Scott, S.A. , *Clean hydrogen production and electricity from coal via chemical looping: identifying a suitable operating regime. International Journal of Hydrogen Energy, (2009). 34.*
  16. Collins, J.P., Way, J. D., *Preparation and Characterization of a Composite Palladium-Ceramic Membrane. Ind. Eng. Chem. Res. , (1993). 32: p. 3006-3013*
  17. Danziger, M., Voitius, W., *Surface modification of polyimide to improve its adhesion to deposited copper layer. Polyimides and Other High Temperature Polymers, (2003). 2: p. 315-329.*
  18. Darling., A.S., *Thermal and electrolytic palladium alloy diffusion cells: Complementary methods of obtaining ultra-pure hydrogen. Platinum Met. Rev. , (1963). 7 (4): p. 126.*
  19. Data, S.A.E., *Statistics and Analysis - Oil, Gas, Electricity. (2008).*
  20. David Hart, A.B., Chase, A.,Howes, J. , *Liquid Biofuels and Hydrogen from renewable resources in the UK to 2050. A technical analysis, (2003). 82.*
  21. Ding, Y., Bikson, B., Nelson, J.K., *Polyimide membranes derived from poly(amic) salt precursor polymers.Synthesis and characterization. Macromolecules, (2002). 35: p. 905-911.*

22. DOE, *Hydrogen posture plan: An intergrated research, developepment and demostration plan Executive summary*, (2006): p. 1-82.
23. Dunson, L., D., *Synthesis and characterization of thermosetting polyimide oligomers for microelelctronics packaging. Published Thesis*, (2000): p. 1-264.
24. Edlund D.J., O.B., *Hydrogen permeable metal membrane and method for producing the same. United State Patent Application Publication*, (2000). **6152995**: p. 1-9.
25. Edlund, D.J., *Hydrogen-permeable metal membrane and method for producing the smae. United States Patent* (2000). **6,152,995**.
26. Edwards, P.P., Kuznetsov, V. L., David, W. I. F., Brandon, N. P. , *Hydrogen and fuel cells: Towards a sustainable energy future. Energy Policy*, (2008). **36**: p. 4356-4362.
27. Ensinger, W., Vater, P., Happel, S., Sudowe, R., Brandt, R. , *Nuclear track microfilters:gas separation ability andbeta-radiation stability. Radiation Measurements*, (2003). **36**: p. 707-711.
28. Ensinger, W., Sudowe, R., Brandt, R.,Neumann, R., *Gas separation in nanoporous membranes formed by etching ion irradiated polymer foils. Radiation Physics and Chemistry*, (2010). **79**: p. 204-207.
29. Escand'on, L.S., Ord'õñez, S., Vega, A., D'iez F, V. , *Sulphur poisoning of palladium catalyts used for methane combustion: Effect of the support. Journal of Hazardous Materials* (2008). **153** p. 742–750.
30. Escoubes, M., Dolveck, J. Y., Davenas, J., Xu, X. L., Boiteux, G., *Ion beam modification of polyimide membranes for gas permeation. Nuclear Instruments and Mtehods in Physics Research B*, (1995). **105**: p. 10-133.
31. Esinger, W., *Formation of nanopore membrane and nanowire by high energy ion irradiation of polymer foils. Surface and Coatings Technology*, (2007). **201**: p. 8442-8447.
32. Ferain, E., Legras, E. , *Track-etch templates designed for micro and nanofabrication. Nuclear Instrument and Methods in Physics Research B* (2003). **208** p. 115-122.

33. Fleischmann, M., Pons, S., *Electrochemically induced nuclear fusion of deuterium. Journal of Electroanalytical. Chem.* , (1989). **261**(301).
34. Garg, M., Quamara, J. K., *FTIR analysis of high energy heavy ion irradiated kapton-H polyimide. Indian Journal of Pure and Applied Physics*, (2007). **45**: p. 563-568.
35. Gary J.S., M.R., *Hydrogen from coal gasification: An economic pathway to a sustainable energy future. International journal of Coal Geology*, (2006). **65**.
36. Gray, D., Tomlinson, G. , *Hydrogen from Coal. Mitretek Technical Paper MTR 2002-31*, (2001): p. 1-32.
37. Han, S.S., Im, S.S., Won, C.J., Lee, H.J., Choi, Y.K., Kim, S.Y., *Synthesis and characterisation of new polyimides containing ethylene linkages. European Polymer Journal*, (2007). **43**: p. 1541-1548.
38. Hassan, A., Ismail, A. F., Saidi, H., *Gas separation using polymeric membranes: The recent development and its future. Jabatan Kejuruteraan Polimer*, (1991): p. 1-9.
39. Hoontrakul P., P.R.A., *Surface reactivity of polyimide and its effects on adhesion to epoxy. Journal Adhesion Science Technology*, (2006). **20**(16): p. 1905-1928.
40. Howard, B.H., Killmeyer, R.P., Rothenberger, K.S., Cugini, A.V., Morreale, B.D., Enick, R.M., Bustamante, F. , *Hydrogen permeance of palladium–copper alloy membranes over a wide range of temperatures and pressures. Journal of Membrane Science*, (2004). **241**: p. 207-218.
41. Huang, Y., Dittmeyer, R., *Preparation of thin palladium membranes on a porous support with rough surface. Journal of Membrane Science*, (2007). **302**: p. 160-170.
42. Huiyuan, G., Lin, Y.S., Yongdan, L., Baoquan, Z. , *Chemical stability and its improvement of Palladium based metallic membrane. . Ind Eng Chem Res.*, (2004). **43**: p. 6920-6930.
43. Hurley, J.P., McCollor, D., P. , *Materials for gas separation and hydrogen separation membranes. Semi-Annual Report*, (1997): p. 1-9.

- 
44. Ilias, S., King, F. G., Fan, T-F., Roy, S., *Separation of Hydrogen Using Electroless Deposited Thin-Film Palladium-Ceramic Composite Membran. DOE/MT/93008-97/C0750 Advanced Coal-Fired Power Systems '96 Review Meeting*, (1996).
  45. J.-W. Snoeck, J. W., Froment, G., F., *Steam/CO<sub>2</sub> Reforming of Methane. Carbon Filament Formation by the Boudouard Reaction and Gasification by CO<sub>2</sub>, by H<sub>2</sub>, and by Steam: Kinetic Study. Industrial Engineering Chemical Research*, (2002). **41**: p. 4252-4265.
  46. Jaguste, D.N., Bhatia, S.K. , *Combined Surface and Viscous-Flow of Condensable Vapor in Porous-Media. Chemical Engineering Science*, (1995). **50**(2): p. 167-182.
  47. Janes, M., *Low temperature fast-neutron and gamma irradiation of Kapton polyimide films. Journal of Nuclear Materials*, (1997). **245**: p. 185-190.
  48. Jayaraman, V., Lin Y.S., Pakala, M., Lin, R.Y., *Fabrication of ultrathin metallic membranes on ceramic supports by sputter-deposition. Journal of Membrane Science*, (1995). **99**(1): p. 89-100.
  49. Jensen, B.J., Hergenrother, P.M., Nwokogu, G., *Polyimides with pendent ethynyl groups. Polymer*, (1993). **34**(3): p. 630-635.
  50. Jitendra, K.Q., Sharma, A., Garg, M., Prabha, T. , *Photoconduction investigations in 75 MeV oxygen ion irradiated kapton-H polyimide. Nuclear Instruments and Methods in Physics Research B*, (2007). **262**: p. 215–219.
  51. Johanna, I.L., Mann, M., K., Margolis, R. M., Milbrandt, A., *An analysis of hydrogen production from renewable electricity sources. Solar Energy*, (2007). **81**: p. 773-780.
  52. John, C., *Interpretation of infrared spectra, A practical approach. Encyclopedia of analytical chemistry*, (2000): p. 10815-10837.
  53. Jun, S.C., Lee, H. K., *Palladium and palladium alloy composite membrane prepared by metal-organic chemical vapour deposition method (cold wall). Journal of Membrane Science*, (2000). **176**: p. 121-130.

54. Jung, H.S., Kusakabe, K., Morooka, S., Kim, D. S., *Effects of co-existing hydrocarbons on hydrogen permeation through a palladium membrane. Journal of Membrane Science*, (2000). **170**: p. 53-60.
55. Kajiwara, M., Uemiya, S., Kojima, T., *Stability and hydrogen permeation behavior of supported platinum membranes in presence of hydrogen sulfide. International Journal of Hydrogen Energy* (1999) **24**: p. 839-844.
56. Kawaguchi, M., Ohtsubo, E., Tsuda, T., Tahara, S., Iida, K., *Polyimide film for metals laminates with good adhesion. United States patent* (2008). **2008299402A120081204**.
57. Kawakami, H., Nakajima, K., Nagaoka, S. , *Gas separation characteristics of isomeric polyimide membrane prepared under shear stress. . Journal of Membrane Science* (2003). **211**: p. 291–298.
58. Ke, Z., Huiyuan, G., Zebao, R., Yuesheng, L., Yongdan, L., *Preparation of thin palladium composite membrane and application to hydrogen/nitrogen separation. Chinese Journal of Chemical Engineering*, (2007). **15**(5): p. 643-647.
59. Keuler, J.N., Lorenzen, L., Sanderson, R.D., Prozesky, V., Przybylowicz, W.J., *Characterising palladium–silver and palladium–nickel alloy membranes using SEM, XRD and PIXE. Nuclear Instruments and Methods in Physics Research B* (1999). **158**: p. 678.
60. Keuler, J.N., Lorenzen, L., Miachon, S. , *Preparing and testing Pd films of thickness 1-2 micrometer with high selectivity and high hydrogen permeance. Separation Science and Technology*, (2002). **37**(2): p. 379–401.
61. Kikuchi, E., Nemoto, Y., Kajiwara, M. , *Steam reforming of methane in membrane reactors: comparison of electroless-plating and CVD membranes and catalyst packing modes. Catalysis Today*, (2000). **56**: p. 75–81.
62. Kilicarlan, S., Afyon, O. M., Dogan, M., *Preparation of palladium composite membrane on pore structure modified and non-modified supports by electroless plating procedure. Turk Journal of Chemistry*, (2008). **32**: p. 699-710.

- 
63. Kim, Y.H., Ahn, S. K. Kwon, S. K. , *Synthesis and Characterization of Novel Polyimides Containing Bulky Trimethylsilylphenyl Group*. *Bull. Korean Chem. Soc.*, (2001). **22**( 5).
64. Kinoshita M., M., Y., Naruse, Y., *Computer analysis on steady state separation characteristics of hydrogen isotope separation system by cryogenic distillation*. *Journal of Nuclear science and technology*, (1981). **18**(7): p. 525-539.
65. Klienert, A.G., G. Pan, X. , *Compatibility of H<sub>2</sub> transfer via Pd membrane with the rate of heterogeneous catalyzed stem reforming*. *Journal catalysis today*, (2005). **104**.
66. Lau, L.L., Xiong, Y., Hong, L., *Study on the structure and adhesion of copper thin films on chemically modified polyimide surfaces*. *Polyimides and other higher tempearature polymers*, (2003). **2**: p. 331-343.
67. Lee, H.K., Nam, E.S., Lee, H.K., *Methods for preparing composite membrane for separation of hydrogen gas*. *United States patent*, (2002): p. 1-5.
68. Lee, S., Tien, C.Y., Hsu, C.F., *FTIR analysis of plasma damage of kapton*. *Plasma and polymers*, **4**(2/3): p. 229-239.
69. Lewis, F.A., Kandasamy, K., McNicholl, R.-A., Tongs, X. Q., *Hydrogen pressure-hydrogen content and electrical resistance-hydrogen content relationships of palladium and palladium alloy-hydrogen systems*. *International Journal of Hydrogen Energy*, (1995). **20**( 5): p. 369-372.
70. Li, A., Liang, W., Hughes, R. , *Characterisation and permeation of palladium/stainless steel composite membranes*. *Journal of Membrane Science*, (1998). **149**: p. 259-268.
71. Li, A., Liang, W., Hughes, R., *Fabrication of defect-free Pd/Al<sub>2</sub>O<sub>3</sub> composite membranes for hydrogen separation*. *Thin Solid Films*, (1999). **350**: p. 106-112.
72. Li, A., Liang, W., Hughes, R., *Repair of a Pd/Al<sub>2</sub>O<sub>3</sub> composite membrane containing defects*. *Separation Science and Technology*, (1999). **15**: p. 113-119.

73. Li, A., Liang, W., Hughes, R. , *The effect of carbon monoxide and steam on the hydrogen permeability of a Pd/stainless steel membrane. Journal of Membrane Science* (2000). **165**: p. 135-141.
74. Li, A., Liang, W., Hughes, R., *Fabrication of dense palladium composite membranes for hydrogen separation. Catalysis Today*, (2000). **56** p. 45–51.
75. Li, H., Goldbach, A., Li, W., Xu, H., *On CH<sub>4</sub> decomposition during separation from H<sub>2</sub> mixture with thin Pd membranes. Journal of Membrane Science*, (2008). **324**: p. 95-101.
76. Li, L., Yan, G., Wua, J., Yu, X., Guo, Q., Kang, E. , *Electroless plating of copper on polyimide films modified by surface-initiated atom-transfer radical polymerization of 4-vinylpyridine. Applied Surface Science* (2008). **254**: p. 7331–7335.
77. Li, Y., Lu, Q., Qian, X., Zhu, Z., Yin, J., *Preparation of surface bound silver nanoparticle on polyimide by surface modification method and its application on electroless metal application. Applied surface science*, (2004). **233**: p. 299-306.
78. Li, Y., Chen, D., Lu, Q., Qian, X., Zhu, Z., Yin J. , *Selective electroless deposition of copper on polyimide surface by microcontact printing. Applied surface science*, (2005). **241**(3-4): p. 471-476
79. Li, Y.S., McCool, B. A. , *Nanostructured thin palladium-silver membrane: Effects of grains size on gas permeation properties. . Journal of Material Science*, (2001). **36** (13): p. 3221-3227.
80. Liang, W., Hughes, R., *The effect of diffusion direction on the permeation rate of hydrogen in palladium composite membranes. Chemical Engineering Journal*, (2005). **112**: p. 81-86.
81. Liberman, V., Malba, V., Berhardt, A. F., *A study of Anisotropy of spin cast and vapour deposited polyimide films using internal reflection techniques. Materials Resarch Society*, (1996): p. 1-10.
82. Lin, M.Y., Rei, H. M., *Separation of hydrogen from the gas mixture out of catalytic reformer by using supported palladium membrane. Separation and Purification Technology*, (2001). **25**: p. 87-95.



- 
83. Lin, M.Y., Rei, H. M., *Study on hydrogen production from methanol steam reforming in supported palladium membrane reactor. Catalysis Today*, (2001). **67**: p. 77-84.
84. Lin, S., Harada, M., Suzuki, Y., Hatano, H., *Hydrogen production from coal by separating carbon dioxide during gasification. Fuel*, (2002). **81**: p. 2079-2085.
85. Low, T., B., Widjojo, N., Chung, S., T., *Polyimide/polyethersulfone dual-layer hollow fiber membranes for hydrogen enrichment. Industrial Engineering Chemical Research*, (2010). **49**: p. 8778-8786.
86. Lu, G.Q., Diniz da Costa, J. C., Dukec, M., Giessler, S., Socolowe, R., Williams, R. H., Kreutze, T. , *Inorganic membranes for hydrogen production and purification: A critical review and perspective. Journal of Colloid and Interface Science* (2007). **314** p. 589–603.
87. Malek, K., Coppens, M.O. , *Knudsen self- and Fickian diffusion in rough nanoporous media. Journal of Chemical Physics*, (2003). **119**(5): p. 2801-2811.
88. Marin, N., Serruys, Y., *Diffusion of metals deposited on a polyimide film (Kapton) under and out of irradiation. Nuclear Instruments and Methods in Physics Research B*, (1995). **105**: p. 175-180.
89. Maryam, T.R., Tahereh, K., Ali, K., , *Application of membrane separation processes in petrochemical industry: a review. Desalination* (2009). **23**: p. 199-244.
90. Mathakari, N.L., Jadhav, V.S., Kanjilal, D., Bhoraskar, V.N., Dhole, S.D. , *Surface and structural changes in polyimide by 100 MeV Ag<sup>7+</sup> ion irradiation. Surface & Coatings Technology*, (2009). **203**: p. 2620–2624.
91. Matsui, S., Sato, H., Nakagawa, T, *Effects of low molecular weight photosensitizer and UV irradiation on gas permeability and selectivity of polyimide membrane. Journal of Membrane Science*, (1998). **141**: p. 31-43.
92. Maurizio, V., Rosalinda, I., Salvatore, P., Carmelo, S. , *Optimized bath for electroless deposition of palladium on amorphous alumina membranes. . Surface & Coatings Technology* (2006) **200**: p. 5800–5806.

93. Mei-Hui, T., Yin-Kai, L., Chi-Jung, C., Pei-Chun, C., Jui-Ming, Y., Wei-Ming, C., Shih-Liang, H., Sheng-Chung, N., *Polyimide modified with metal coupling agent for adhesion application*. *Thin Solid Films* (2009). **517**: p. 5333–5337.
94. Meyer, F., *Hydrogen selective properties of Cesium hydrogensulphate membranes*. **Published Thesis**, (2006).
95. Mishra, R., Tripathy, S. P., Dwivedi, K. K., Khathing D.T., *Spectroscopic and thermal studies of electron irradiated polyimide*. *Radiation Measurements*, (2003). **36**: p. 621-624.
96. Mitrofanov, A.V., Apel, Yu. P., Blonskaya, I. V., Orelovitch, O. L., *Diffraction filters based on polyimide and poly(ethylene naphthalate) track membranes*. *Technical physics*, (2006). **51**(9): p. 1229-1234.
97. Moore T., S.P., *Hydrogen from coal*. *International journal of coal geology*, (2006). **65**.
98. Naddaf, M., Balasubramanian, C., Alegaonkar, P.S., Bhoraskar, V.N., Mandle, A.B., Ganeshan, V., Bhoraskar, S.V., *Surface interaction of polyimide with oxygen ECR plasma*. *Nuclear Instruments and Methods in Physics Research B* (2004). **222** p. 135–144.
99. Nam, S.E., Lee, S. H., Lee, H. K., *Preparation of a palladium alloy composite membrane supported in a porous stainless steel by vacuum electrodeposition*. *Journal of Membrane Science*, (1999). **153**: p. 163-173.
100. Naotsugu, I., Tomomitsu, A., Takafumi, S., *Preparation of thin palladium composite membrane tube by CVD technique and its hydrogen perselectivity*. *Catalysis Today*, (2005). **104**.
101. Nathan, W.O., Nenoff, T. M., *Membranes for Hydrogen Separation*. *Chemical Reviews*, (2007). **107**(10): p. 34.
102. Nenoff T.M., S.R.J., *Membrane for Hydrogen Purification: An important step towards a Hydrogen-based economy*. *Material research science bulletin*, (2006). **31**: p. 735-744.

- 
103. Neyman E., D.J.G., Dillard D.A., *Plasma and silane surface modification of SiC/Si adhesion and durability for the epoxy-SiC system. The Journal of Adhesion*, (2006). **8**: p. 331-353.
104. Ng J.H.-G., D.M.P.Y., M Lamponi., Moffat B.G. McCarthy A. , Suyal H. , Walker A.C., Prior K.A., Hand D.P. , *A direct-writing approach to the micro-patterning of copper onto polyimide. Circuit World*, (2009). **352**(2): p. 3-17.
105. Noda K., S.O., *Hydrogen Separator and Process for Production thereof. United State Patent Application Publication*, (2006). **2006/0115643 A1**.
106. Norwicka, E., Dus, R., *Hydrogen dissociative adsorption on palladium hydride and titanium hydride surfaces: Evidence of weakly bound state of hydrogen adatoms. Alloys and Compounds*, (1997). **253-254**: p. 506-510.
107. Nurdan, D.S., Richard, O. C., *An alternative method for selective metal deposition onto flexible materials. Journal of Material Processing Technology*, (2008). **196**: p. 155-159.
108. Okazaki, J., Ikeda, T., Tanaka, D. A. P., Suzuki, T. M., Mizukami, F., *In situ high-temperature X-ray diffraction study of thin palladium /-alumina composite membranes and their hydrogen permeation properties. Journal of Membrane Science*, (2009). **335**: p. 126–132.
109. Paglieri, S.N., Way, J. D. , *Innovations in palladium membrane research. Separation and purification methods*, (2002). **31**(1): p. 1-170.
110. Pan, X.L., Stroh, N., Brunner, H., Xiong, G. X. Sheng, S. S., *Pd/Ceramic Hollow Fibers for H<sub>2</sub> Separation. . Separation and Purification Technology*, , (2003). **32**: p. 265-270.
111. Park, J.S., Li, K., Jin, F. L. , *Synthesis and characterisation of hyper-branched polyimides from 2,4,6-triaminopyrimidine and dianhydride system. Materials Chemistry and Physics*, (2008). **108**: p. 214-219.
112. Park, S.C., Yoon, S.S., Nam, J.D., *Surface characteristics and adhesive strengths of metal on O<sub>2</sub> ion beam treated polyimide substrate. Thin Solid Films*, (2008). **516**: p. 3028–3035.

- 
113. Peachey, N.M., Snow, R. C., Dye, R. C., *Composite Pd/Ta metal membranes for hydrogen separation. Journal of Membrane Science*, (1996). **111**: p. 123-133.
114. Powell E. C., Q.G.G., *Polymeric CO<sub>2</sub>/N<sub>2</sub> gas separation membranes for the capture of carbon dioxide from power plants flue gases. Journal of Membrane Science*, (2006). **279**: p. 1-49.
115. Quicker, P., Höllein, V., Dittmeyer, R. , *Catalytic dehydrogenation of hydrocarbons in palladium composite membrane reactors. Catalysis Today*, (2000). **56** p. 21-34.
116. Qureshi, A., Singh, N. L., Rakshit, A. K., Singh, F., Avasthi, D. K., *Swift heavy ion induced modification in polyimide films. Surface & Coatings Technology* (2007). **201** p. 8308-8311.
117. Ramachandranraghu, R., Menon, R.K. , *An Overview of Industrial uses of Hydrogen. International Journal of Hydrogen Energy*, (1998). **23**( 7): p. 593-598.
118. Ramos, M.D.M., *Theoretical study of metal-polyimide interfacial properties.*
119. Ree, M., Park, Y. H., Shin, T. J., Nunes T. L., Volkens W., *Self-adhesion of poly(4,4'-oxydiphenylene biphenyltetracarboximide) and its adhesion to substrates. Polymer*, (2000). **41**: p. 2105-2111.
120. Report, H., *Hydrogen from Coal programme. Research, Development and Demonstration plan.External draft review*, (2005).
121. Rezac, M.E., Sorensen, E. T., Beckham, H. W., *Transport properties of crosslinkable polyimide blends. Journal of Membrane Science*, (1997). **136** p. 249-259.
122. Ritter, J.A., Ebner, A. D. , *State-of-the-Art Adsorption and Membrane Separation Processes for Hydrogen Production in the Chemical and Petrochemical Industries. Separation Science Technology*, (2007). **42**(6): p. 1123-1193.
123. Roa, F., Way, D., *The effect of air exposure on palladium-copper composite membranes. Applied Surface Science*, (2005). **240**: p. 85-104.

124. Robertis, E., De., Abrantes, L. M., Motheo, A. J. , *The influence of experimental parameters on the structure, morphology and electrochemical behaviour of Pd-P thin films prepared by electroless deposition. Thin Solid Films* (2008) **516**: p. 6266-6276.
125. Robinson, I., Mabuza, M., Masetlana, R., Duval, J. A. G. Mwape, P., Perold, J. W., Köhler, M., Duval, J. A. G. , *SOUTH AFRICA'S MINERAL INDUSTRY. Department of Minerals and Energy: Republic of South Africa*, (2005/2006): p. 183.
126. Robinson I., D.J.A.G., Mwape P. Perold J.W., *South Africa's Mineral Industry*. (2006). **23rd revised edition**: p. 1-83.
127. Rothenberger, K.S.C., A. V., Howard, B. H., Killmeyer, R. P., Ciocco, M. V., Morreale, B. D., Enick, R. M., Bustamante, F., Mardilovich, I. P., Ma, Y. H., *High Pressure hydrogen permeance of porous stainless steel coated with thin palladium film via electroless plating. Journal of Membrane Science*, (2004). **244**(1-2): p. 55–68
128. Sakamoto, F., Kinari, Y., Chen, F. L., Sakamoto, Y., *Hydrogen permeation through Palladium alloy membranes in mixtures gases of 10% Nitrogen and Ammonia in the Hydrogen. International Journal of Hydrogen*, (1997). **22**(4): p. 369-375.
129. Sakintuna, B., Lamari-Darkrim, F., Hirscher, M., *Metal hydride for solid hydrogen storage: A review. International Journal of Hydrogen*, (2007). **32**: p. 1121-1140.
130. Schiedt, B., *Charaterisation and application of ion track-etched nanopores. Published Thesis*, (2007): p. 124.
131. Shao, C., Lu, N., Deng, Z., *DNA-assisted electroless deposition of highly dispersed palladium nanoparticles on glassy carbon surface: Preparation and electrocatalytic properties. Journal of Electroanalytical Chemistry*, (2009). **629**: p. 15–22.
132. Shao L., T.L.B., Chunga T-S., Greenberg A. R. , *Polymeric membranes for the hydrogen economy: Contemporary approaches and prospects for the future. Journal of Membrane Science*, (2009). **327**: p. 18-31.

- 
133. sheet, D.D., *Summary of Kapton. Article*, (2006): p. 1-5.
134. Shoko, E., McLellan, B., Dicks, A. L., Diniz da Costa, J. C. , *Hydrogen from coal: Production and utilisation technologies. International Journal of Coal Geology*, (2006). **65**: p. 213– 222.
135. Shuxiang, M., Dezheng, W., Yue, W., Zhanpeng, W., Xiaoping, Y., Wantai, Y., *Fabrication of Nickel oxide nanocomposite layer on a flexible polyimide substrate via ion exchange technique. Applied materials and interfaces*, (2010). **2**(1): p. 111-118.
136. Singh, B., Sheth, A. C., Dahotre, N. B., *Laser synthesis of palladium-alumina composite membranes for production of high purity hydrogen from gasification. Applied Surface Science*, (2006). **Article in press**: p. 8.
137. Sircar, S., Golden, T.C., *Purification of hydrogen by Pressure swing adsorption. Separation Science and Technology*, (2000). **35**(5): p. 667-687.
138. Sircar, S., *Pressure Swing Adsorption. Ind. Eng. Chem. Res.*, (2002). **41**: p. 1389-1392.
139. Southward R. E., S.D.M., *Reflective and electrically conductive surface silvered polyimide films and coatings prepared via unusual single-stage self-metallization techniques. Progress in organic coatings*, (2001). **41**: p. 99-119.
140. Steckenreiter, T., Esser, M., Fuess, H., Fuhrmann, J., Spohr, R., Trautmann, C. , *Solvent induced track sensitization. Role of amines. Nuclear Instruments and Methods in Physics Research B* (1996) **107**: p. 393-396.
141. Stephens, E.L., Myles, A., Thomas, R. R., *Kinetics of Alkaline Hydrolysis of a Polyimide Surface. Langmuir*, (2000). **16**: p. 4706-4710.
142. Stevens, K.J., Ingham, B., Toney, M. F., Brown, S. A., Lassesson, A., *Structure of palladium nanoclusters for hydrogen gas sensors. Current applied physics*, (2008). **8**: p. 443-446.
143. Stiegel G. J., R.M., *Hydrogen from coal gasification: An economical pathway to a sustainable energy future. International Journal of Coal Geology*, (2006). **65**: p. 173-190.

144. Sudowe, R., Vater, P., Ensinger, W., Vetyer, J., Penzhorn, R. D., Brandt, R., *Basic Research on Nuclear Track Microfilers for Gas Separation. Radiation Measurements* (1999). **31** p. 691-696.
145. Sudowe, R., Vater, P., Brandt, R., Vetyer, J., Ensinger, W., *Filter with <100nm radius pores for gas separation formed by high energy ion radiation of polymers Nuclear Instruments and Methods in Physics Research B* , (2001). **175-177**: p. 564-568.
146. Sungrok, K., Jyongsik, J., *A Highly Efficient Palladium Nanocatalyst Anchored on a Magnetically Functionalized Polymer-Nanotube Support. DOI* (2006) **10.1002.200602456**.
147. Suzuki, T., Yamada, Y., Tsujita, Y., *Gas transport properties of 6FDA-TAPOB hyperbranched polyimide membrane. Polymers*, (2004). **45**: p. 7167-7171.
148. Swanslger, W.A., Swisher, J. H., Darginis, J. P., Schoenfelder, C. W. , *Hydrogen Permeation in Palladium-Chromium Alloys. The Journal of Physical Chemistry* (1976). **80**(3): p. 1-5.
149. Takatani, H., Kobayashi, T., Kawano, M., Kobayashi, K., *Hydrogen separation membrane, hydrogen separation unit manufacturing method for hydrogen separation membrane. United State Patent Application Publication*, (2003). **2003/0233940 A1**.
150. Thoen, P.M., Roa, F., Way, J. D., *High flux palladium-copper composite membranes for hydrogen separation. Desalination*, (2006). **193**: p. 224-229.
151. Tian-Xiang, C., Shu-De, Y., Kun, W., Huan, W., Zhi-Bo, D., Di, C., *Structure Characterization of Modified Polyimide Films Irradiated by 2MeV Si Ions. Chinese Physical Letter*, (2009). **26**(2): p. 101-103.
152. Tina, M.N., Richard, J. S. , *Membranes for Hydrogen Purification: An important step towards a Hydrogen based economy. Materials Research Science Bulletin*, (2006). **31**: p. 735-744. .
153. Tran, T.D., Mori, S., Suzuki, M., *Characteristics of polyimide-based composite membranes fabricated by low-temperature plasma polymerization. Thin Solid Films*, (2008). **516**: p. 4384-4390.

- 
154. Trautmann, C., Bouffard, S., Spohr, R. , *Etching threshold for ion tracks in polyimide. Nuclear Instruments and Methods in Physics Research B* (1996). **116**: p. 429-433.
155. Trautmann, C., Bruchele, W., Spohr, R., Vetter, J., Angert, N., *Pore geometry of etched ion tracks in polyimide. Nuclear Instruments and Methods in Physics Research B*, (1996). **111**: p. 70-74.
156. Trautmann, C., Bruchler, W., Spohr, R., Vetter, J., Angert, N., *Pore geometry of etched ion track in polyimides. Nuclear Instruments and Methods in Physics Research B*, (1999). **111**: p. 70-74.
157. Tsutomu, N., Hiroki, S., Shigetoshi, M. , *The effect of ultraviolet light irradiation on gas permeability in polyimide membrane added sensitizer. Journal of Photopolymer Science and Technology* (1996). **9**(2 ): p. 363- 366.
158. Turner, J.A., *Sustainable Hydrogen Production. Science*, (2004). **305**: p. 971-974.
159. Uemiya, S., Matsuda, T., Kikuchi, E., *Hydrogen permeable palladium-silver alloy membrane supported on porous ceramics. Journal of Membrane Science*, (1991). **56**: p. 315-325.
160. Uemiya, S., Kato, W., Uyama, A., Kajiwara, M., Kojima, T., Kikuchi, E. , *Separation of Hydrogen from gas mixtures using supported platinum group metal membranes. . Separation Purification Technology*, (2001). **22-23**: p. 309-317.
161. Umegaki, T., Yan, J-M., Zhang, X-B., Shiyoama, H., Kuriyama, N., Xu, Q., *Boron and Nitrogen-based chemical Hydrogen storage materials. International Journal of Hydrogen Energy*, (2009). **34**: p. 2303-2311.
162. Unemoto, A., Kaimai, A., Sato, K., Otake, T., Yashiro, K., Mizusaki, J., Kawada, T., Tsuneki, T., Shirasaki, Y., Yasuda, I., *The effect of co-existing gases from the process of steam reforming reaction on hydrogen permeability of palladium alloy membrane at high temperatures. International Journal of Hydrogen energy*, (2007). **32**: p. 2881-2887.



- 
163. Wang, L., Cao, Y., Zhou, M., Liu, Q., Ding, X., Yuan, Q., *Gas transport properties of 6FDA-TMPDA/MOCA copolyimides. European Polymer Journal*, (2008). **44**: p. 225-232.
164. Warnecke, R., *Gasification of biomass: comparison of fixed bed and fluidized bed gasifier. Biomass and Bioenergy*, (2000). **18**: p. 489-497.
165. Williams, M., Nechaev, A.N., Lototskya, M.V., Yartys, V.A., Solberg, J.K., Denys, R.V., Pinedae, C., Li, Q., Linkov, V.M. , *Influence of aminosilane surface functionalization of rare earth hydride-forming alloys on palladium treatment by electroless deposition and hydrogen sorption kinetics of composite materials. Materials Chemistry and Physics* (2009). **115**: p. 136–141.
166. Wu Z., W.D., Qi S., Zhang T., Jin R., *Preparation of surface conductive and highly reflective silvered polyimide films by surface modification and in situ self-metallization technique. Thin Solid Films*, (2005). **493**: p. 179-184.
167. [www.platinum.matthey.com](http://www.platinum.matthey.com).
168. Xu, F.J., Zhao, J. P., Kang, E. T., Neoh K. G., *Surface functionalisation of polyimide films via chloromethylation and surface-initiated atom transfer radical polymerisation. Industrial Engineering Chemical*, (2007). **46**: p. 4866-4873.
169. Yamakawa, K., Ege, M., Ludescher, B., Hirscher, M., Kronmüller, H. , *Hydrogen permeability measurement through Pd, Ni and Fe membranes. Journal of Alloys and Compounds*, (2001). **321**: p. 17-23.
170. Ye, W., Li, Y., Yang, B., Chunming, W., *Comparative study of electroless deposited Pd/Ag films onto p-silicon (100)-activated seed layers of Ag and Pd. Journal of Solid Electrochemical*, (2007) **11**: p. 1347-1351.
171. Yeung, K.L., Christiansen, S. C., Varma, A. , *Palladium composite membranes by electroless plating technique relationships between plating kinetics, film microstructure and membrane performance. Journal of Membrane Science*, (1999). **159**: p. 107-122.

- 
172. Yu-Sheng, H., Wha-Tzong, W., Sheng-Chang, W., Kuen-Ru, C., *Chemical formation of palladium-free surface-nickelized polyimide film for flexible electronics. Thin film solid*, (2008). **516**: p. 4258–4266.
173. Yi L., Qinghua L., Xuefeng Q., Zikang Z., Jie Y., *Preparation of surface bound silver nanoparticles on polyimide by surface modification method and its application on electroless metal deposition. Applied Surface Science* (2004) **233** p. 299–306.
174. Yoda S., Atsushi H., Hiroyuki S., Yuko U., Kenji H., Tomoya T., and Katsuto O., *Preparation of a Platinum and Palladium/Polyimide Nanocomposite Film as a Precursor of Metal-Doped Carbon Molecular Sieve Membrane via Supercritical Impregnation. Chem. Mater.* (2004) **16** p. 2363-2368.
175. Zhang, C., Zhang, M., Cao, H., Zhang, Z., Wang, Z., Gao, L., Ding, M., *Synthesis and properties of a novel isomeric polyimide/SiO<sub>2</sub> hybrid material. Composites Science and Technology*, (2007). **67**: p. 380-389.
176. Zhang, Q.H., Dai, M., Ding, M. X., Chen, D. J., Gao, L. X., *Mechanical properties of BPDA-ODA polyimide fibres. European Polymer Journal*, (2004). **40**: p. 2487-2493.
177. Zhao, H.B., Xiong, G. X., Baron, G. V., *Preparation and characterization of palladium-based composite membranes by electroless plating and magnetron sputtering. Catalysis Today*, (2000). **56**: p. 89-96.
178. Zhao, H.-B.F., K. P., Gu, J.-H., Lia, A.-W., Stroh, N. Brunner, H., Xiong, G.-X., *Preparation of palladium composite membranes by modified electroless plating procedure. Journal of Membrane Science*, (1998). **142**: p. 147-157.
179. Zhongliang, S., Shanqiang, W., Jerzy, A. S., *Microstructure transformation of Pd membrane deposited on a porous Inconel substrate in hydrogen permeation at elevated temperature. Journal of membrane science*, (2006). **284**: p. 424-430.
180. Zhongliang, S., Shanqiang, W., Jerzy, A. S., Mustapha, R., *An observation of palladium membrane formation on a porous stainless steel substrate by electroless deposition. Journal of membrane science* (2006). **280**(1-2): p. 705-711.

181. Zhongmin, W., Venessa, L., Chan, S. L. , *Review of Alloy Membranes/Films for Hydrogen Separation or Purification. Journal of Rare Earth*, (2005). **23**: p. 611-617.
182. Züttel, A., *Materials for hydrogen storage review. Materials Today*, (2003): p. 24-33.



## Appendix 1

### APPENDIX 1 1: LIST OF COMPONENTS FOR THE HOME-GROWN HYDROGEN DIFFUSION REACTOR UNIT

<b>Gas supply accessories</b>	<b>GC1</b>	<b>Gas cylinder (H<sub>2</sub>)</b>	
	<b>V1</b>	<b>Pressure regulator / reducer output pressure &lt; 4 bar</b>	
<b>Fittings</b>	<b>J1</b>	<b>Union tee / DN 16</b>	
		<b>Clamps (3x)</b>	
		<b>Pfeiffer adapter, DN 16 ISO-Kf / 6 mm Swagelok</b>	<b>PF 141 522-X</b>
	<b>J2</b>	<b>SS Swagelok Tube Fitting, Union, 6 mm x 1/8 in. Tube UNIVERSITY OD of the</b>	<b>SS-6M0-6-2</b>
	<b>J3</b>	<b>SS Swagelok Tube Fitting, Union Cross, 1/8 in. Tube OD</b>	<b>SS-200-4</b>
	<b>J4</b>	<b>SS Swagelok Tube Fitting, Union Tee, 1/8 in. Tube OD</b>	<b>SS-200-3</b>
	<b>J5</b>		
	<b>J6</b>	<b>SS Swagelok Tube Fitting, Male Connector, 1/8 in. Tube OD x 1/4 in. Male NPT</b>	<b>SS-200-1-4</b>
	<b>J7</b>		

## *Appendix 1*

<b>J8</b>	<b>SS Swagelok Tube Fitting, Female Connector, 1/8 in. Tube OD x 1/4 in. Female NPT</b>	<b>SS-200-7-4</b>
<b>M1</b>	<b>Membrane block - male fitting SS Swagelok Tube Fitting, Male Connector, 1/8 in. Tube OD x 1/4 in. Male ISO Parallel Thread</b>	<b>SS-200-1-4RP</b>
<b>M2</b>	<b>Membrane block - female fitting SS Swagelok Tube Fitting, Female Connector, 1/8 in. Tube OD x 1/4 in. Female ISO Parallel (Gauge) Thread</b>	<b>SS-200-7-4RG</b>
<b>M3</b>	<b>Membrane block - gasket (10x) Copper Gasket for 1/4 in. ISO Parallel (Gauge) Thread (RG) Fittings</b>	<b>CU-4-RG-2</b>
<b>P1</b>	<b>SS tubing 6 mm OD</b>	<b>SS-T6M-S-1.5M-6ME</b>
<b>P2</b>	<b>SS tubing 1/8" OD</b>	<b>SS-T2-S-028-6ME</b>